Alma Mater Studiorum · Università di Bologna

Scuola di Scienze
Corso di Laurea Magistrale in Fisica del Sistema Terra

Daily temperature trends in Trentino Alto Adige over the last century

Relatore:
Prof. Michele Brunetti

Presentata da:
Antonello Angelo Squintu

Sessione III
Anno Accademico 2013/2014

” ...per la scienza

di un uomo saggio.”

(Z.B.)

ABSTRACT

Numerosi lavori apparsi sulla letteratura scientifica negli ultimi decenni hanno evidenziato come, dall'inizio del XX secolo, la temperatura media globale sia aumentata. Tale fenomeno si è fatto più evidente dagli anni '80, infatti ognuno degli ultimi tre decenni risulta più caldo dei precedenti. L'Europa e l'area mediterranea sono fra le regioni in cui il riscaldamento risulta più marcato, soprattutto per le temperature massime (dal 1951 sono cresciute di +0.39 °C per decennio) che hanno mostrato trend maggiori delle minime. Questo comportamento è stato osservato anche a scala nazionale (+0.25°C/dec per le massime e +0.20°C/dec per le minime). Accanto all'aumento dei valori medi è stato osservato un aumento (diminuzione) degli eventi di caldo (freddo) estremo, studiati attraverso la definizione di alcuni indici basati sui percentili delle distribuzioni. Resta aperto il dibattito su quali siano le cause delle variazioni negli eventi estremi: se le variazioni siano da attribuire unicamente ad un cambiamento nei valori medi, quindi ad uno shift rigido della distribuzione, o se parte del segnale sia dovuto ad una variazione nella forma della stessa, con un conseguente cambiamento nella variabilità. In questo contesto si inserisce la presente tesi con l'obiettivo di studiare l'andamento delle temperature giornaliere sul Trentino-Alto-Adige a partire dal 1926, ricercando cambiamenti nella media e negli eventi estremi in due fasce altimetriche. I valori medi delle temperature massime e minime hanno mostrato un evidente riscaldamento sull'intero periodo specialmente per le massime a bassa quota ($+0.13 \pm 0.03$ °C/dec), con valori più alti per la primavera ($+0.22 \pm 0.05$ °C/dec) e l'estate ($+0.17 \pm 0.05$ °C/dec). Questi trends sono maggiori dopo il 1980 e non significativi in precedenza. L'andamento del numero di giorni con temperature al di sopra e al di sotto delle soglie dei percentili più estremi (stimate sull'intero periodo) indica un chiaro aumento degli estremi caldi, con valori più alti per le massime ad alta quota (fino a +26.8% per il 99-esimo percentile) e una diminuzione degli estremi freddi (fino a -8.5% per il primo percentile delle minime a bassa quota). Inoltre, stimando anno per anno le soglie di un set di percentili e confrontando i loro trend con quelli della mediana, si è osservato, unicamente per le massime, un trend non uniforme verso temperature più alte, con i percentili più bassi (alti) caratterizzati da trend inferiori (superiori) rispetto a quello della mediana, suggerendo un allargamento della PDF.

ABSTRACT

In last decades several works appeared in scientific literature highlighted, since the beginning of 20th century, an increase of the mean global temperature. This phenomenon has been more evident since 1980's, effectively each of the last three decades has been warmer than the previous ones. Europe and mediterranean area showed to be among the regions with stronger warming trends, especially for maximum temperatures (since 1951 temperatures have increased with a trend of +0.39°C per decade, higher than what observed for minimum temperatures). This behaviour have been observed at Italian scale (+0.25°C/dec and +0.20°C/dec. for maximum and minimum temperatures respectively). Together with the increase of mean values it has been observed an increase (decrease) in the number of warm (cold) events. These have been studied through the definition of some indices based on distribution percentiles. Debate is still open on the causes determining changes in extreme events: whether they are due changes in the mean values (therefore linked to a rigid shift of the distribution) or if part of this signal is due to changes in the distribution shape (with consequent changes in variability). In this context this thesis is aimed at studying tendencies of daily temperatures in Trentino-Alto-Adige over the 1926-2013 period, searching for changes in the mean and in extreme events in two altitudinal bands. Average minimum and maximum temperatures have shown an evident warming trend over the whole period especially for maximum temperatures at low elevations ($+0.13 \pm 0.03$ °C/dec), with higher values for Spring ($+0.22 \pm 0.05$ °C/dec) and Summer ($+0.17 \pm 0.05$ °C/dec). These trends have higher values since 1980 and generally non-significant before. Trends in exceedance probabilities over and below more extreme percentile thresholds (estimated over the entire period) indicate a clear increase in warm extremes, with highest values for maximum temperatures at highest elevations (up to +26.8% for 99th percentile) and a decrease of cold extremes (down to -8.5% for 1st percentile of minimum temperature at low elevation). Furthermore, estimating year by year thresholds of a percentile set and comparing their tendencies with the median trend it has been observed, only for maximum temperatures, a non-uniform trend towards higher temperatures, where lower (higher) percentiles are characterized by lower (higher) trends than the median trend, suggesting a widening of the PDF.

Contents

Chapter 1

Global warming and statistical interpretation.

Occurring of extreme events and unusual cold or warm days stimulated attention of mass media and public opinion on climate issues. A large quantity of works published in last years pointed out how, during twentieth century, land surface air temperature (LSAT) underwent a significant increase that has become more evident since the 1970's.

1.1 Trends in the mean temperature

IPCC [2013] assessed that it is certain that Global Mean Surface Temperature has increased since 19th century and, furthermore, last decades appear to be warmer than the previous ones. In particular the first decade of 21st century has been the warmest since observations are available.

The average of air temperature over land has been observed to be affected by warming trends at different scales and over various time ranges. Calculation of trends depends on the considered periods due to natural variability. This happens in particular when trends are calculated over short periods so that the choosing of extremal years may affect the results. Trends might also be calculated not with linear behaviour in time but might be given by higher orders. Nevertheless linear trends are found to be nicely consistent with data and, furthermore, they may be treated and understood more easily.

Studies on temperature trends are performed analyzing recorded data from samples whose geographical coverage can vary from global to national or sub-national (regional) level. These changes has been observed especially since 1950 ([Vose et al., 2005], [Alexander et al., 2006], [Rohde et al., 2012], [Donat et al., 2013]). Estimated trends over the entire globe are displayed in figure 1.1.

Studies have found that, at global scale, the distribution shifts look to be larger for minimum temperatures [Alexander et al., 2006]. Vose et al. [2005] observed trend for minimum temperatures in the 1951-2004 period to be nearly 1.5 times the one

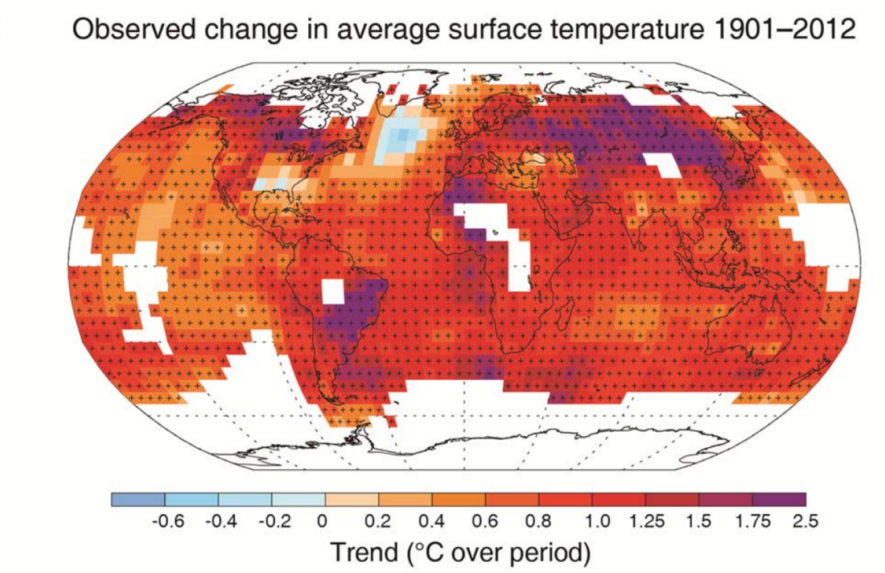

Figure 1.1. *Map of global observed trends in surface temperature over the 1901-2012 period. [IPCC, 2013]*

observed for maximum (0,204 vs. 0,141 °C/dec) (figure 1.2 (a)). Consequently diurnal temperature range (DTR) showed a significant decrease, evidence not found for the 1979-2004 period, where Vose et al. [2005] observed coherent trends for maximum and minimum temperature (see figure 1.2 (b)).

In order to deeper inspect warming climate features, analyses performed by great part of the studies look first of all at the entire series and then focus on single seasons. In these cases the year is divided into four periods composed as usual:

- SPRING: March, April and May;
- SUMMER: June, July and August;
- AUTUMN: September, October and November;
- WINTER: December, January and February.

An animated debate is taking place among scientific community whether climate changes are linked only to rigid shift in the mean or to changes in higher moments of the distributions, since variations in some of them may affect significantly tail probabilities ([Mearns et al., 1984],[Katz and Brown, 1992]) .

Some works have studied the role of possible increase of distribution width in the occurring of extreme events ([Schär et al., 2004],[Della-Marta et al., 2007]). Effect on extremes due to changes of distribution tails were modeled by some authors and compared to observed data. These analyses suggested the presence of changes in width

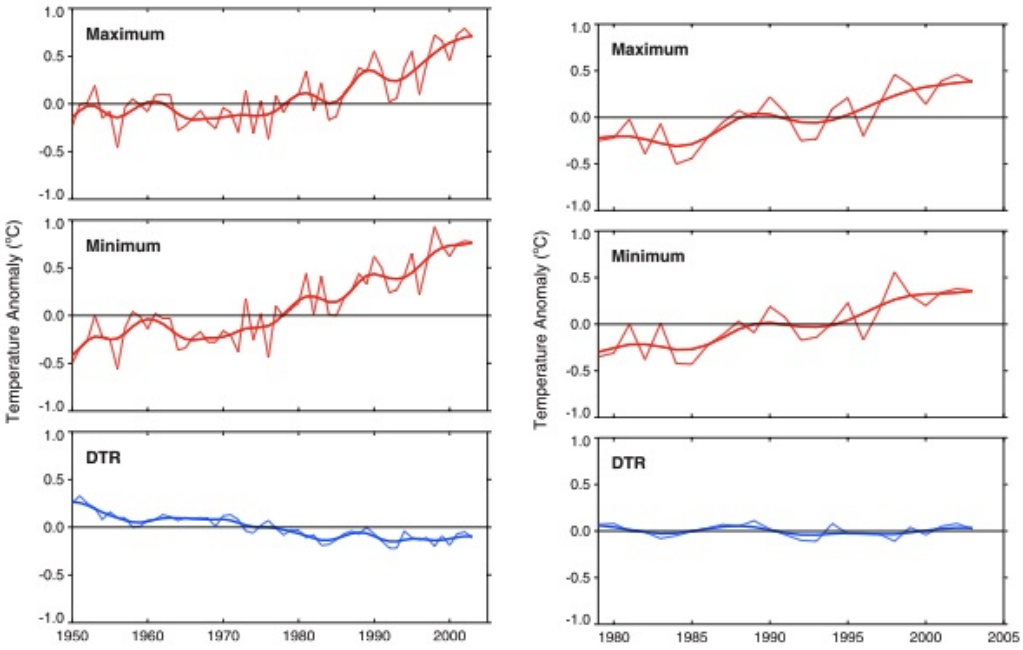

(a) (b)

Figure 1.2. *Observed trends for maximum, minimum temperatures and DTR for 1951-2004 (a) and 1979-2004 (b) periods. [Vose et al., 2005]*

and asymmetry of PDFs. Such changes in variability were effectively found, observing widening of the distribution during warming periods and narrowing during cooling periods ([Klein Tank and Können, 2003],[Klein Tank et al., 2002]).

On the other hand, as discussed forward in the text, a large number of studies assess that changes in higher moments of temperature distributions are not relevant when compared with the effects of changes in the mean.

Therefore scientific community still debates whether higher moments and their changes will still remain negligible or they will become dominant, even if in last decades there have not been evidences in such direction [Scherrer et al., 2005].

1.2 Distribution of anomalies and indices

Changing climate has been observed to be characterized also by the frequency increase of extremal events. Analytical treatment of these events may be afforded:

- fitting data with theoretical probability density functions and studying their evolution through time;
- analyzing the distributions of extremes through the Generalized Extreme Values (GEV) or Generalized Pareto Distribution(GPD);
- looking at particular indices that describe some features of the distributions, as the ones introduced by the CLIVAR (Research Programme on Climate Variability and Predictability) Expert Team on Climate Change Detection and Indices (ETCCDI).

First two methods try to describe with analytical tools the behaviours of available data. But some problems occur in these cases, since the choice of the parameter values and the selection of the shape of distributions (gaussian, skew-normal, etc.) are not univocally determined.

Providing an objective definition of extreme events and clear criteria to identify them is not simple, indeed. For these reasons, in great part of works, surveys on temperature series are effectuated through calculation of several kinds of indices that can relate to characteristics of temperatures themselves or to features of their probability distribution. In latter case more common indices are the median and various fixed or moving thresholds calculated looking at percentiles of the considered distributions. These indices have been defined by CLIVAR, in order to provide an indices set universally comparable.

Hereafter are some examples of CLIVAR indices (and their definition found on the ETCCDI web site) that will be mentioned in this text:

- FD, Number of frost days: Annual count of days when TN (daily minimum temperature) < 0°C;
- SU, Number of summer days: Annual count of days when TX (daily maximum temperature) > 25°C;
- TR, Number of tropical nights: Annual count of days when TN (daily minimum temperature) > 20°C.
- TN10p: percentage of days of the sub-sample having minimum temperature lower than the 10th percentile. That is: let TN_{ij} be the daily minimum temperature on day i in period j and let $TN_{in}10$ be the 10th percentile of that calendar day (calculated in a reference window of days before and after the selected date) . The percentage of days of the sub-sample is determined by all TN_{ij} that satisfy the condition: $TN_{ij} < TN_{in}10$. Same for maximum temperatures (TX) and for different values of the percentile (1, 2, 5, 20, etc.).

- TN90p: percentage of days of the sub-sample having minimum temperature higher than the 90th percentile. That is: let TN_{ij} be the daily minimum temperature on day i in period j and let $TN_{in}90$ be the 90th percentile of that calendar day (calculated in a reference window of days before and after the selected date) . The percentage of days of the sub-sample is determined by all TN_{ij} that satisfy the condition: $TN_{ij}>TN_{in}90$. Same for maximum temperatures (TX) and for different values of the percentile (99, 98, 95, 80, etc.).

Percentiles are important indicators in the analysis of changing in the behaviour of extreme values. Effectively they allow to individuate how a distribution shifts or modifies its shape. Following the definition provided above, value of the x^{th} percentile is empirically determined sorting data of a selected period in increasing order and individuating the temperature having x% of sample with lower values. For example, having a 5000-elements sorted data set, 5th percentile is that temperature which appears in the 250th position; this means that 5% of data have lower value than the considered one.

Percentiles may be object of two different analysis:

- estimating percentile thresholds year by year and studying their temporal behaviour;
- estimating percentile thresholds over a reference period and counting, for each year and for each season, the number of exceedances.

1.3 Evidences of strengthening extreme events at global scale

Coherently with evidences found for trends in the temperature mean, second half of twentieth century has shown to be the period with highest increase of warm extreme events and decrease of cool events.

Analyzing trends in the parameters of GPD, Brown et al. [2008] found that the only parameter that appears to change in time is parameter that describes the position of the distribution, that acts like the mean. This variation is more marked for minimum temperatures than maximum and in particular concerns cold tail of minimum temperature distributions. Analogous results were obtained by Nogaj et al. [2006] analyzing North Atlantic region. These results strengthen the hypothesis of variations in the mean to be dominant in global warming.

Frich et al. [2002], analyzing an intercontinental data set coming from Nothern Hemisphere and Australia, found a clear reduction of the number of frost days and an evident increase of the percentage of events above the 90th percentile of minimum temperatures (figure 1.3).

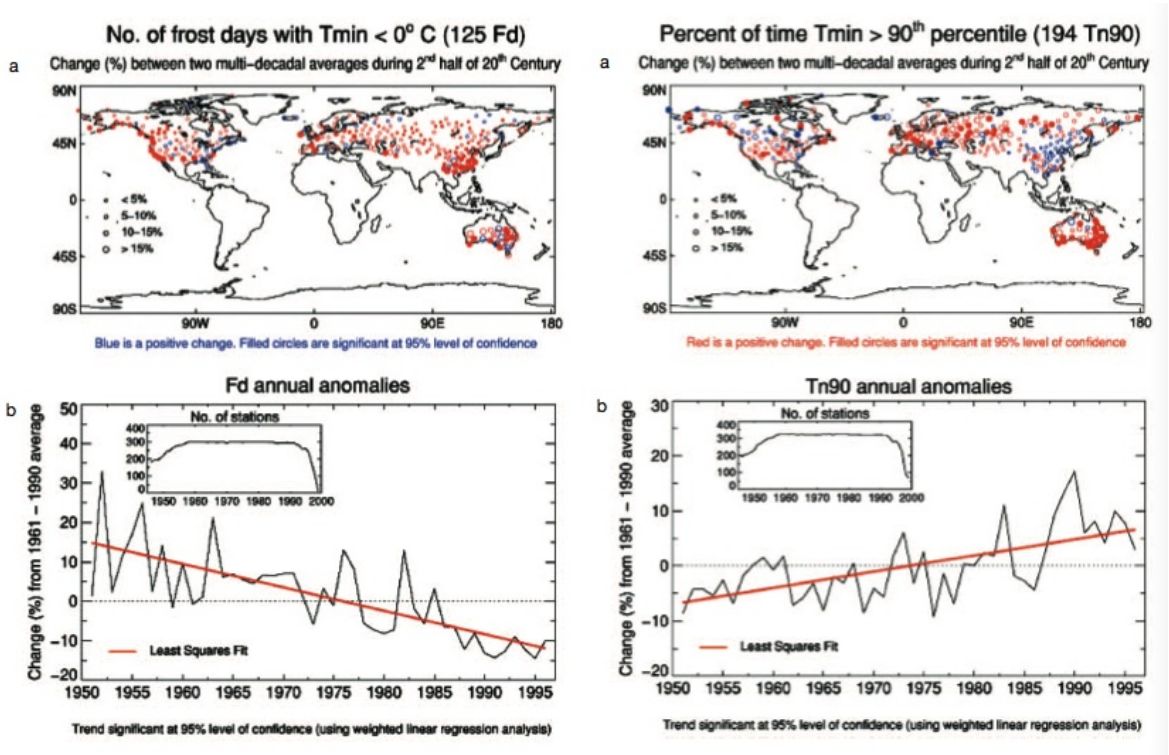

Figure 1.3. *Left: Number of frost days. Trend for each analyzed station (top) and annual percentage change (bottom). Right: Percentage of days with minimum temperature above the 90th percentile. Trends for each station (top) and annual percentage variation (bottom). In both bottom plots percentage are calculated with respect to the 1961-1990 period. [Frich et al., 2002]*

Donat and Alexander [2012] conjugated inspection on indices and threshold with an analysis on distribution moments. They looked for changes in distribution features separating global sample (anomaly temperatures calculated with respect to 1961-1990 period) into two data-sets, first one from 1951 to 1980 and second one from 1981 to 2010. Ranking and arranging in gaussian-like distribution these daily data sets, they found a clear shift toward higher temperatures in the probability density function. Plots in figure 1.4 allow to see how distributions of temperature shifted towards warmer values, both for minimum and maximum temperatures. On global sample (upper panels) mean of minimum temperatures increased by 0.8°C and maximum ones by 0.6°C, these variations were checked with a t-student test, demonstrating the significance of the results.

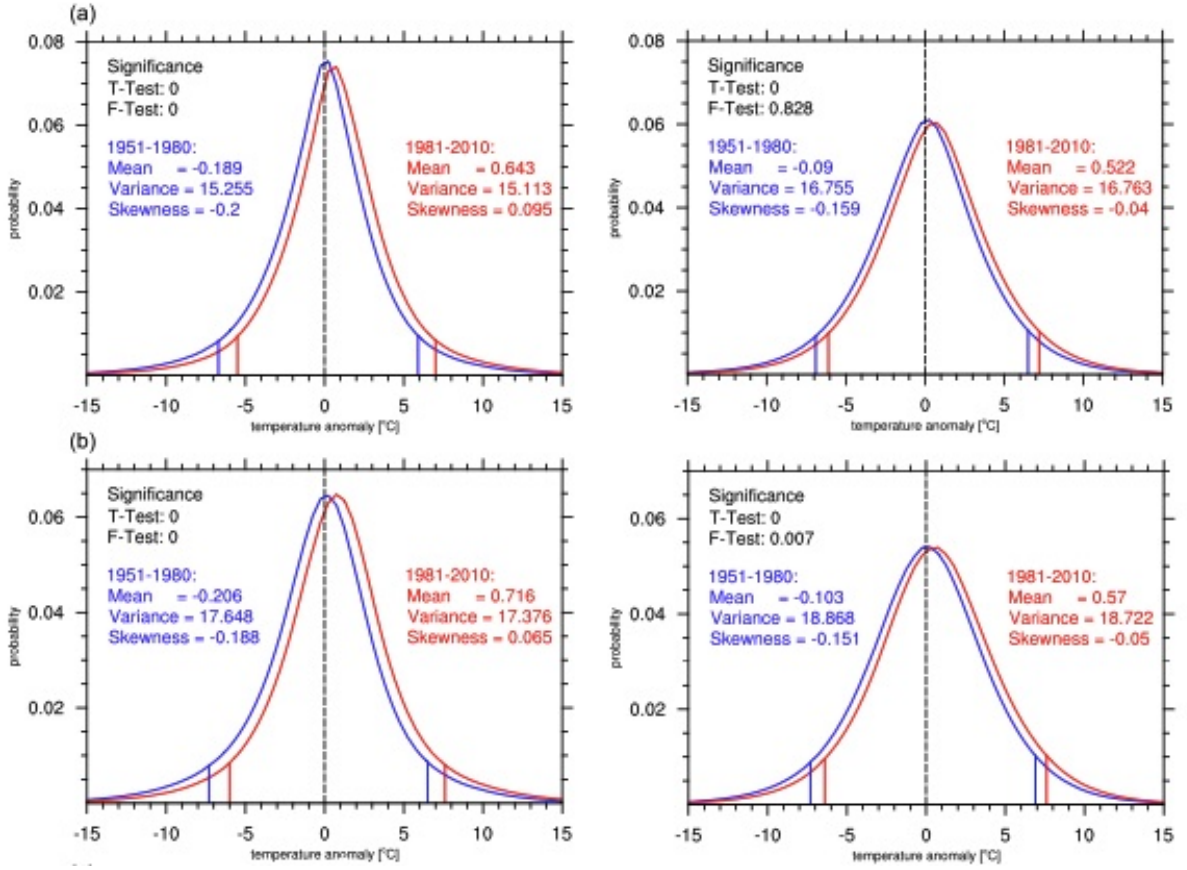

Figure 1.4. *Probability density functions of anomalies of daily temperatures for the 1951-1980 period (blue) and the 1981-2010 period(red). On the left column anomalies for minimum temperatures are displayed, on the right column same for maximum temperature. Upper plots refer to global sample, while lower ones are for northern hempisphere extratropical latitudes (more than 30°N). Vertical lines represent, for each distribution, 5th and 95th percentiles. [Donat and Alexander, 2012]*

In the same plots changes in position of percentiles are clear. There they appear to move to warmer values. Effectively lower threshold (5th percentile) of the older data-set for minimum (maximum) have become the 3.2nd (3rd) percentile, while upper percentile (95th percentile) have moved to 92.7th (93rd). This evidences were linked with the outcomes that for minimum temperatures (whose changes were more marked) number of events above older 95th percentile in 1981-2010 was greater by 40% than that observed for 1951-1980 period.

In spit of what found in some other studies, Donat and Alexander [2012] observed variations in higher moments. Variance showed different behaviours on the analyzed stations, but appeared to describe wider distribution in particular over tropical areas. Nonetheless variance gave very heterogeneous results that didn't allow the identification of a clear trend. On the other hand, in this study, outcomes have shown a clear variation in skewness to higher values, bringing asymmetry to warmer events.

Furthermore Donat and Alexander [2012] took same conclusions for different latitudinal bands. Distribution behaviour they found showed approximately same time evolution for the mean and skewness and heterogeneous outcomes for variance. In figure 1.4 distributions for northern extratropical band are displayed.

Alexander et al. [2006] and, more recently, Donat et al. [2013] analyzed behaviour in time of minimum and maximum global anomaly considering the number of events above or below defined thresholds in a gridded data set.

Alexander et al. [2006] analyzed separately global gridded data set for 1901-1950, 1951-1978 and 1979-2003 periods and found a pronounced warming especially in the last period. In particular, gathering second and third period, they found a large part of global surface involved by a larger warming in minimum temperatures than maximum ones, as already observed in other studies on global scale. In fact 74% of land area sampled showed a decrease in the number of cold nights, with a reduction of 20 days of these events since 1951. Similarly warm night have increased for 73% of considered land area surface, observing that in 2004 number of warm nights reached 25 days more than 1951.

Turning point of fluxes of events was found to be around mid 1970's. Effectively since 1979 every year has been above the long term average for warm nights, and since 1977 every year stood below the long term average for cold nights (see figure 1.5). Similar behaviours have been found for seasonal data set, where since 1985 (1988) spring showed to have a number of warm (cold) night higher (lower) than the long term average. This warming has been observed to be marked in particular over Asian regions.

Donat et al. [2013], looking in particular at minimum temperatures and at event below colder thresholds, found a decrease of cool nights. In figure 1.6 decrease of the number of cool nights in comparison with reference period (1961-1990) is clear. It can bee seen that frequency of cold nights decreased by 18 days, while warm nights have increased by 20 days since 1980 (figure 1.7).

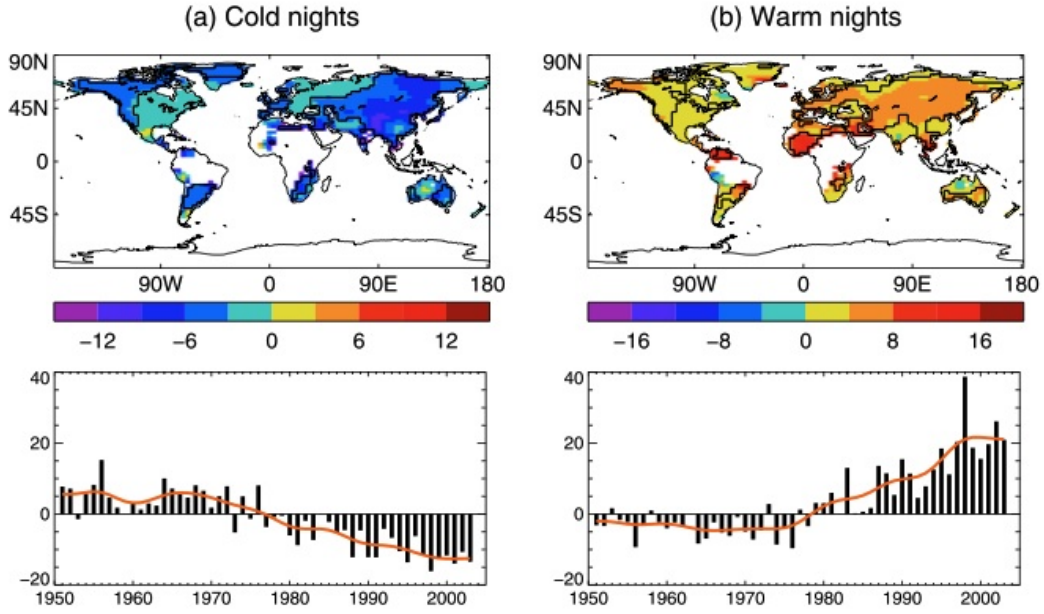

Figure 1.5. *Map of fluxes of events for cold and warm nights (top). Bottom panels: annual anomalies, with respect to 1961-1990 average, of number of days whose minimum temperature layed below 10th percentile (left) and above 90th percentile (right). [Alexander et al., 2006] .*

Simultaneously analyses on maximum temperatures revealed a decrease of cool days and growth of number of warm days, but showing a less marked intensity comparing to minimum temperatures (see figures 1.8, 1.9). Trends of maximum temperature showed at the same time a less homogenous spatial structure, since north-american east coast and south-american west coast revealed to have a slight cooling trend [Donat et al., 2013]. These local cooling trends resulted to be linked in particular to the decrease of maximum temperatures in summer season, in spite of decreasing of cold days observed over all land surface of the planet in other seasons (figure 1.10, 1.11). Studies on precipitation in those areas permitted to infer that this cooling was correlated with an increase of rainfall [Donat et al., 2013].

Trends for minimum and maximum temperatures flows of events were calculated fitting fluxes obtained over the entire sample (1901-2010) and over the last 60 years. In both cases trends in the second part of 20th century and first decade of 21st century have shown a higher value for minimum temperatures.

Donat et al. [2013] looked also at flows of events for seasonal data-sets. Maximum temperatures showed, coherently with the rest of the work, positive trends for almost all regions for every season. These trends appeared to be stronger during winter (DJF for northern hemisphere, JJA for southern hemisphere). Seasonal minimum temperatures average revealed warming trends too. Furthermore cool nights appeared to be less frequent in cold month for Asia, while Europe showed a decrease of cold night especially during spring and summer.

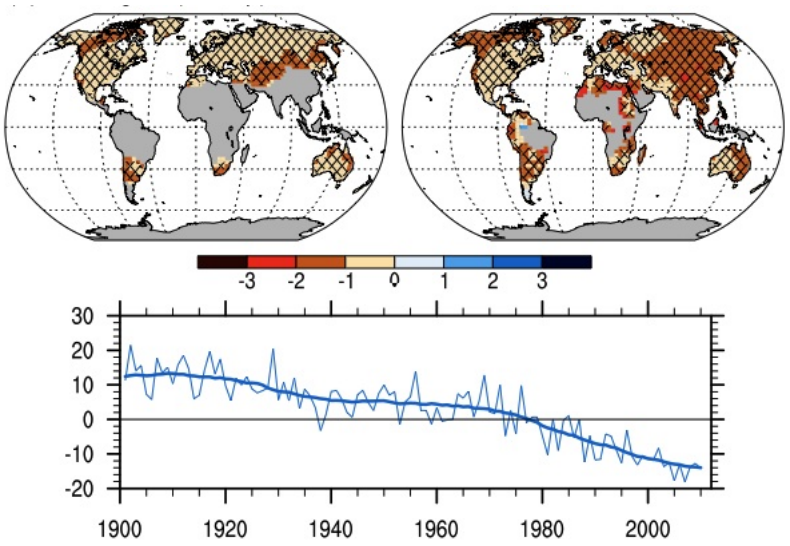

Figure 1.6. *Trends (in annual days per decade) of number of days whose minimum temperature stays below the 10th percentile of the entire data set. On top-right trends for 1901-2010 are displayed, while on the left same but for 1951-2010. On the bottom plot one may see the number of days (with respect to 1961-1990 mean) below the chosen threshold [Donat et al., 2013].*

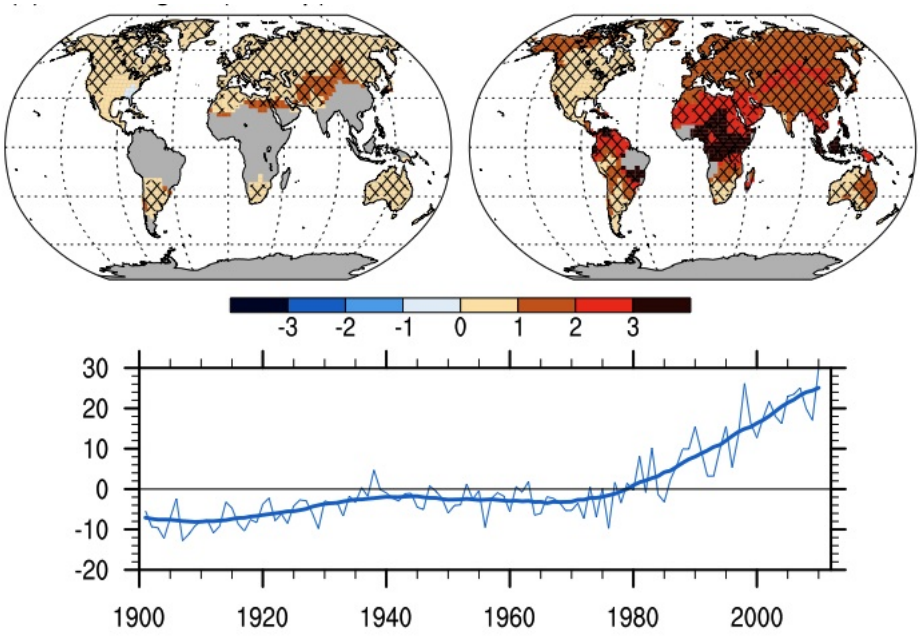

Figure 1.7. *Trends (in annual days per decade) of number of days whose minimum temperature stays above the 90th percentile of the entire data set. On top-right trends for 1901-2010 are displayed, while on the left same but for 1951-2010. On the bottom plot one may see the number of days (with respect to 1961-1990 mean) above the chosen threshold [Donat et al., 2013].*

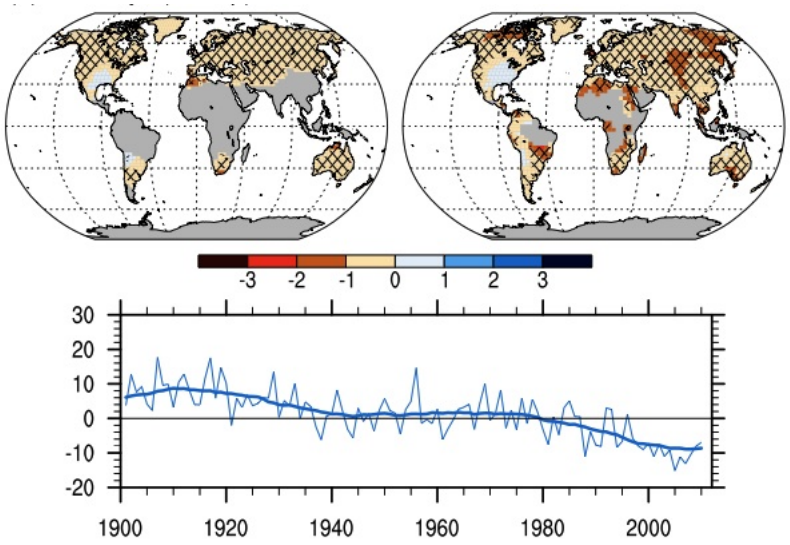

Figure 1.8. *Trends (in annual days per decade) of number of days whose maximum temperature stays below the 10th percentile. On top-right trends for 1901-2010 are displayed, while on the left same but for 1951-2010. On the bottom plot one may see the number of days (with respect to 1961-1990 mean) below the chosen threshold [Donat et al., 2013].*

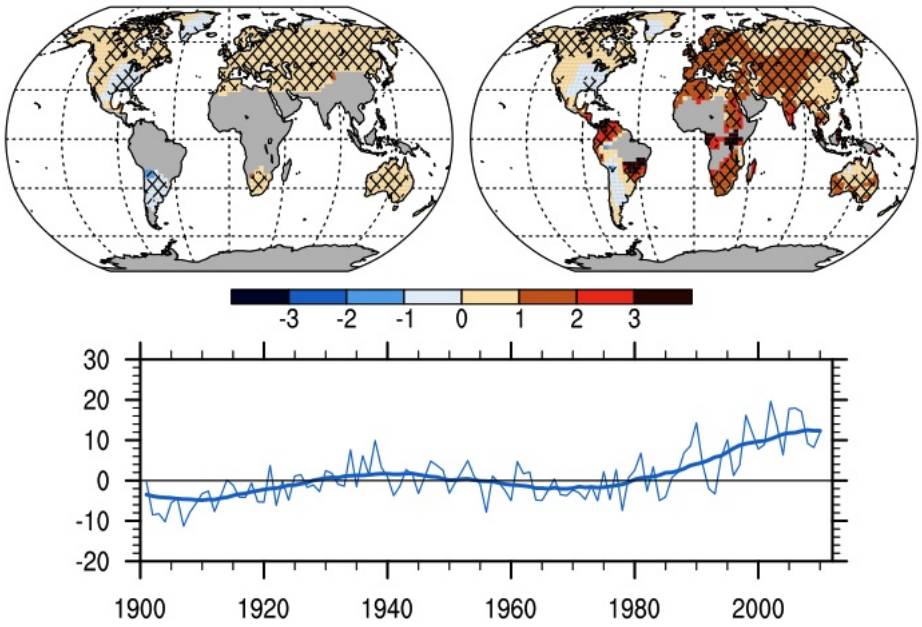

Figure 1.9. *Trends (in annual days per decade) of number of days whose maximum temperature stays above the 90th percentile. On top-right trends for 1901-2010 are displayed, while on the left same but for 1951-2010. On the bottom plot one may see the number of days (with respect to 1961-1990 mean) above the chosen threshold [Donat et al., 2013].*

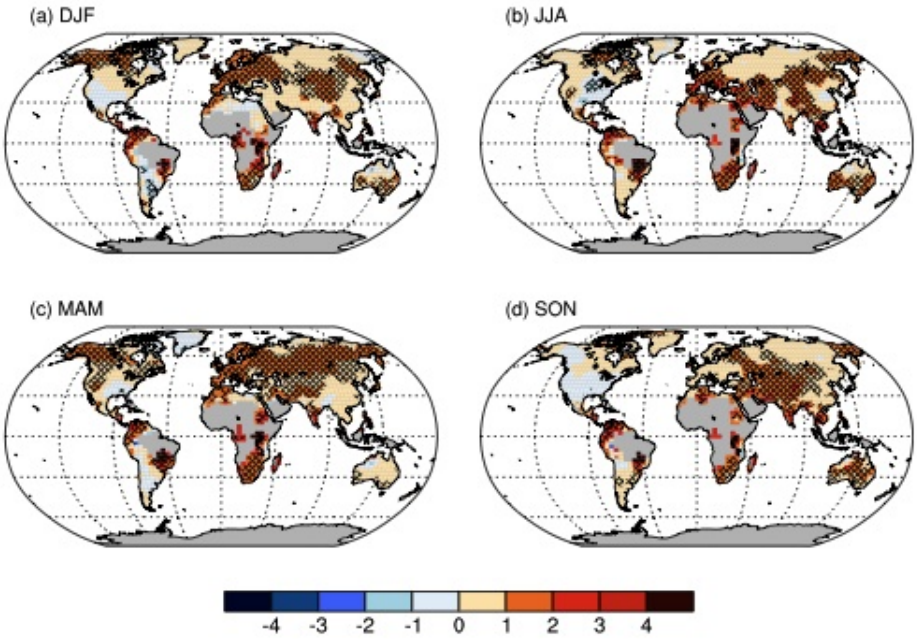

Figure 1.10. *Same as previous figures but lookin at each season separately for warm days (maximum temperatures above 90 percentile) [Donat et al., 2013].*

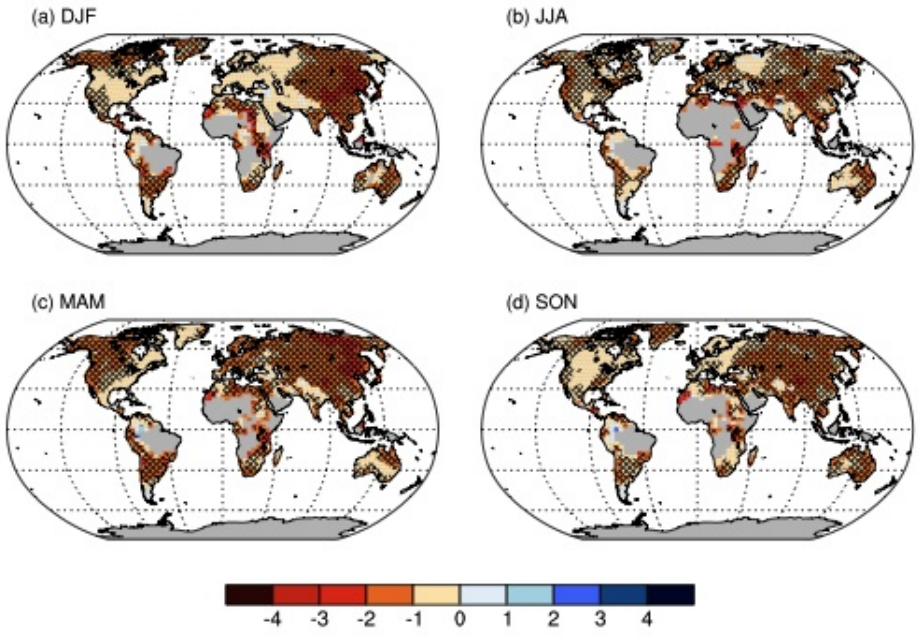

Figure 1.11. *Same as figure 1.10, but for cool nights (minimum temperatures below 10 percentile) [Donat et al., 2013].*

1.4 European warming climate trends

Increasing of frequency and duration of warm spells during early 21st century have aroused interest in focusing studies over Europe, that appears, together with Mediterranean Area to be more sensible to warming climate than other regions of the globe and where number of extreme events is predicted to increase in the near future ([Giorgi, 2006] [Ballester et al., 2010]).

Yan et al. [2002] studied absolute extreme temperatures (coldest and warmest) over Europe, finding a slight decrease of cold extremes since the end of 19th century and a significant increase of warm extreme events beginning from 1960, with a rate of approximately 10 % in a century. Analysis of seasonal data set revealed that yearly lowest temperature have increased since 18th century for all seasons but summer. In particular since 1961 annual lowest temperature underwent a strong warming, an example is the trend of 0.7° C per decade recorded in St Petersburg. At the same time highest seasonal temperatures showed to be stationary until 1960 and since then these ones have undergone a less marked warming than lowest ones, with a consistent reduction in seasonal temperature range. It was also noticed that variability concerned especially lowest winter records and highest summer records.

As far as fluxes of events through fixed threshold are concerned, analyses on European context were performed by Simolo et al. [2011] over the 1960-2010 period. Operating a Principal Component Analysis (see section 4.1) they individuated three zones: Alpine and Carpatian Region, Atlantic and Northern Sea, and searched for changes of distribution parameters in each region. Changes in temperature have shown to be mostly due to a rigid shift of the whole distribution. Unlike what found in previous works on global range, this shift has been observed to be more marked on maximum temperature rather than on minimum ones, especially over the Atlantic Region (see figure 1.12). In particular this area shows +0.39 $\pm$ 0.07 °C/decade(dec) for maximum temperatures and +0.37 $\pm$ 0.05 °C/dec for minimum ones, while Alpine-Carpatian has +0.36 $\pm$ 0.07 °C/dec and +0.39 $\pm$ 0.07 °C/dec and Northern Sea has +0.34 $\pm$ 0.09 °C/dec and +0.32 $\pm$ 0.08 °C/dec

Occurrence of extreme events and their exceedance probabilities were modelled linking them to shift in the mean of a skew-normal distribution (see equation 1.1) that best fitted available data.

$$f(z) = 2\phi(z)\Phi(\alpha z) \tag{1.1}$$

Where:

$$\phi(z) = \frac{1}{\sqrt{2\pi}} e^{-\frac{z^2}{2}} \tag{1.2}$$

$$\Phi(\alpha z) = \int_{-\infty}^{\alpha z} \phi(y)dy \tag{1.3}$$

In this model fluxes of events through thresholds located in $\bar{z}_p$ and $-\bar{z}_p$ are calculated as follows:

$$F_t(t) = \int_{-\infty}^{\bar{z}_p} dz f(z,t) \tag{1.4}$$

$$F_t(t) = \int_{1-\bar{z}_p}^{+\infty} dz f(z,t) \tag{1.5}$$

where p is a given probability threshold. Obtained fluxes are then larger through the warmer threshold and the ratio of flux of events in the warmer threshold respect to the colder one is described by an exponential law.

This model fitted nicely recorded data (figure 1.13), so that the hypothesis that conferred changes in extreme events to shift of the mean was backed up.

Comparison among european sub-regions revealed that in particular data about western Europe underwent warming for temperature indices. This happened both for lower and higher percentiles in record distributions. Moberg et al. [2006] looked at which regions in Europe had been affected by stronger warming. They found a more evident increasing of maximum temperatures (on yearly range) on southern Europe (Iberian Peninsula in particular). Looking at seasonal scale they also observed a more marked warming in summer records over central and western Europe for both maximum and minimum temperatures, with a significant change in summer daily maximum temperature range over Germany and Alpine region [Moberg et al., 2006] .

Moberg et al. [2006] made also studies on percentiles. They looked at linear trends over the 1901-2000 period for a data-set of European station west of 60°E. In particular they found no relevant differences between minimum and maximum trends (as confirmed by Makowski et al. [2008]) on the overall context, but some differences on certain percentiles over limited regions. Western Europe, especially Iberian Peninsula showed steeper warming for all indices. Looking at figure 1.14 one may see comparison for lower and upper percentiles (2nd, 5th, 10th and complementary). As already said, warming involves all indices for all seasons.

Focusing on winter trends of percentiles: relevant trends appear for maximum temperature upper percentiles (98th: 1.6 °C/100yr, 95th: 1.5°C/100yr), while minimum temperature show more marked trends for coldest tails rather than warmest tails. Looking at summer they found weaker changes, in particular the median revealed a trend of 0.8°C/100yr, less than what found for winter (1°C/100yr). In both season 10th and 90th percentiles showed to be highly correlated with the mean, suggesting a rigid shift of the distribution. Concentrating on particular areas of the continent, Moberg et al. [2006] observed significant increase in indices for winter (98th percentile of maximum temperatures and 2nd percentile of minimum ones) on Iberian Peninsula and southern Europe. While summer showed an increase over central and western Europe for 98th percentile of both minimum and maximum temperatures.

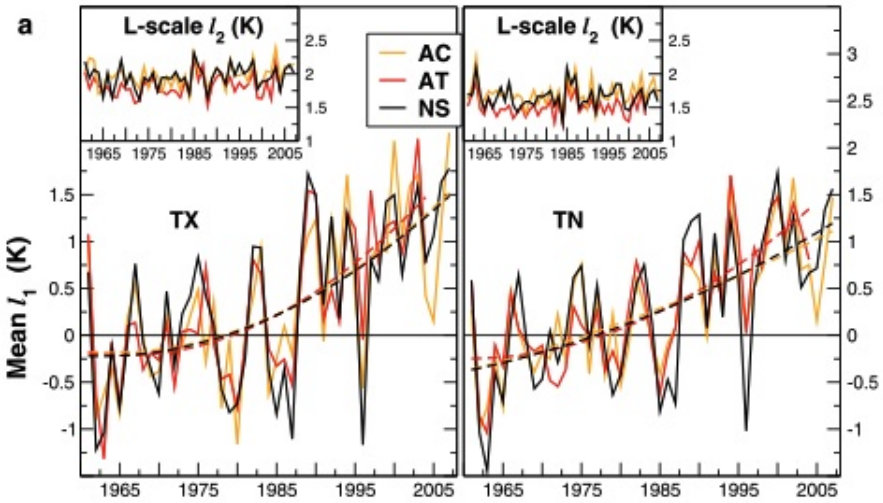

Figure 1.12. *Anomalies of annual mean with respect to 1961-1990 period for the three selected regions for maximum (left) and minimum (right) temperatures. Dashed lines represent second order polynomial fits [Simolo et al., 2011].*

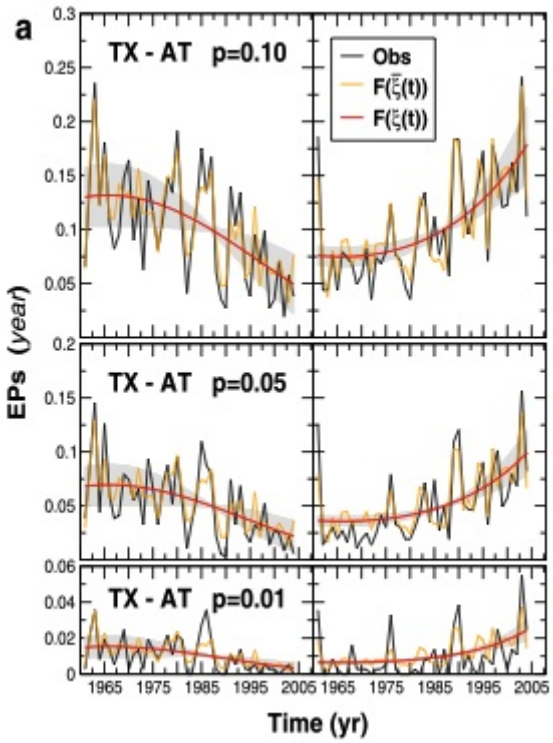

Figure 1.13. *Observed exceedance probabilities for maximum temperatures in Atlantic Region for three different thresholds and complementary ones. Black lines stand for observed data, red solid lines are the theoretical EPs and gray shaded areas represent uncertainties in the PDF's shape. [Simolo et al., 2011].*

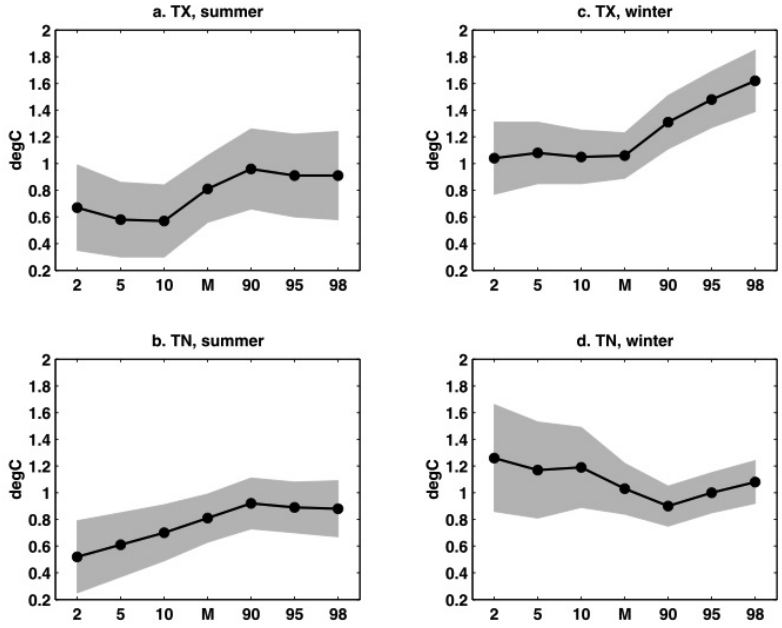

Figure 1.14. *Trends of percentiles of maximum and minimum seasonal mean temperatures in winter and summer calculated over the 20th century. Label on horizontal axis refers to 2nd, 5th, 10th percentiles, median, 90th, 95th and 98th percentiles. On vertical axis trends are shown in unity of °C/100 yr. Confidence of 95% is indicated by the shaded grey area. [Moberg et al., 2006]*

Some works have been focused on single countries. Brunet et al. [2007] (and, before, Brunet et al. [2006]) analyzed temperature trends in Spain over the period 1850-2005, finding clear warming trends especially in the 1973-2005 period. Coherently with other works for Europe they observed larger trends for maximum temperatures rather than minimum temperatures. Looking at seasonal trends they found high signals on extreme percentiles for winter and autumn but, for medium percentiles, trends have shown to be stronger for summer and spring.

Studies on Alpine Region and countries of that area revealed positive trends during second half of twentieth century (in particular after 1950) for yearly and seasonal series [Böhm et al., 2001]. Analysis for Switzerland(1864-2000 period, monthly series) showed some distinctions between northern and southern zones with respect to the main alpine ridge and differences between higher and lower stations. Northern stations showed a larger trend in mean temperatures (about 1°C/100yr vs 0.6 °C/100yr). On the other hand Begert et al. [2005] found that higher stations presented a larger increase for autumn data, while lower stations increased their temperature especially in winter.

1.5 Warming trends over Italy

Italy has been object of several works in recent years.

Trends in extreme temperature have been searched in absolute values (i.e. values not converted into anomalies or arranged into distributions). This was done, for instance, by Toreti and Desiato [2008] on the Italian context using the already introduced indices:

- frost days;
- summer days;
- tropical nights.

These indices were calculated with arithmetic averages extracted from 49 italian stations (with an homogenous spatial coverage). They showed significant trends during second half of twentieth century as displayed in figure 1.15. Frost days resulted to reduce with a rate of about -0.25 day/y; summer days showed a decrease from 1961 to 1978 (-0.98 days/y) and then an increase since 2004 of 0.73 days/y; tropical nights revealed a downward trend from 1961 to 1981 (-0.42 days/y) and from 1982 to 2004 an upward trend (0.62 days/y). These results are coherent with the weak decrease in temperature observed until the end of 1970's and a stronger increase beginning from 1979.

Looking at monthly series over Italy for 19th and 20th century Brunetti et al. [2006] observed a gradual positive trend with a secondary maximum in 1950. As already found in other works, from 1951 to approximately 1979, there was a slight decreasing trend and since then a strong positive trend with maximum values in the last decades. Gathering monthly data into seasonal series, trends were found to be mostly due to summer and spring trends, while winter showed less steep slopes. Such behaviours may be observed in figure 1.16. Brunetti et al. [2006] found a more marked trend for minimum temperatures over the whole period (since 1800) and, coherently with other studies, calculated trends from 1950 appeared to be more intense for maximum temperatures.

Another study over Italy was done by Simolo et al. [2010], that analyzed daily temperature series on the whole italian territory for the 1951-2008 period. Obtained anomalies have been fitted by skew normal distribution as described in equation 1.1 and it resulted that no significant changes in higher moments occurred. Only the distribution mean value revealed a clear shift towards warmer temperatures, as showed in figure 1.17. In the same figure is possible to notice differences between mean trends for minimum and maximum temperature. Here, contrasting what seen for global context, but coherently with works effectuated on european sample, maximum temperatures show stronger trends than minimum ones. Furthermore observed trends appeared to

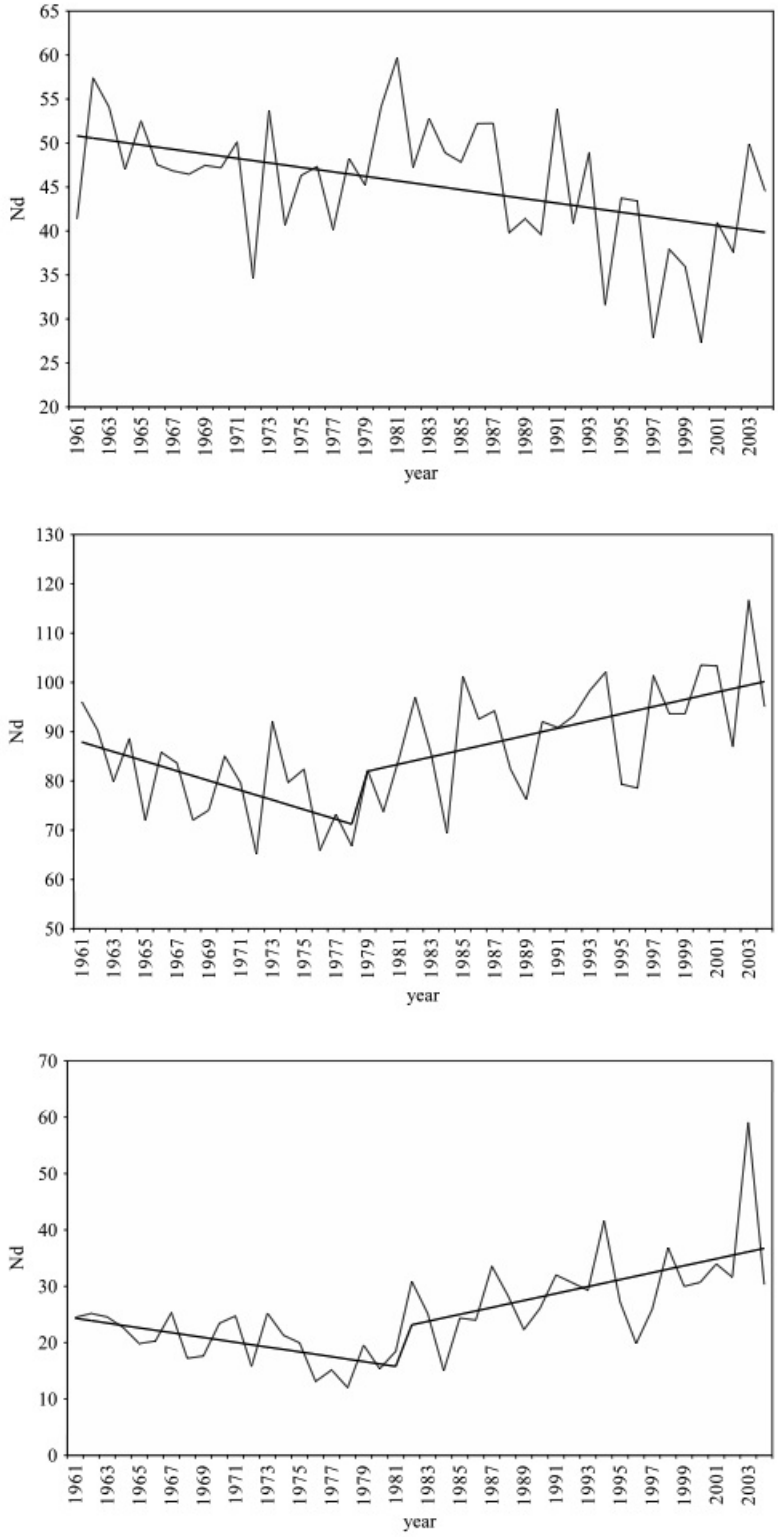

Figure 1.15. *Trends observed in frost days (top), summer days (centre), tropical nights (bottom). [Toreti and Desiato, 2008]*

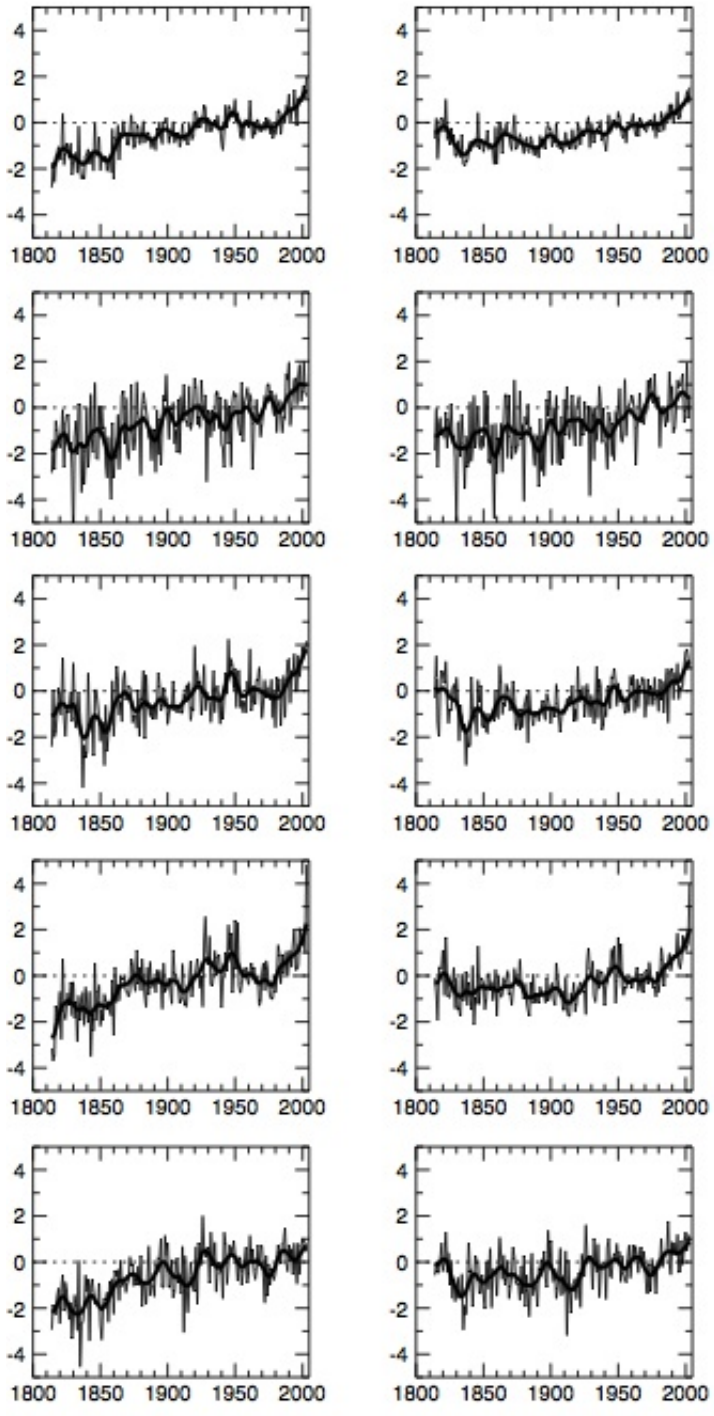

Figure 1.16. *Plots for mean maximum (left column) and minimum temperatures (right column) from 1800 to 2000. From top to bottom the five rows indicate: yearly series, winter, spring, summer, autumn. [Brunet et al., 2006]*

be almost homogeneous over the two regions of Northern and Southern Italy (individuated with a Principal Component Analysis). In particular, beginning from 1980, as found for global and european trends, warming appeared stronger. So that a simple linear trend did not represent nicely the temperature behaviour, because until 1979 data showed a weak decrease in their values (see 1.18) [Simolo et al., 2010].

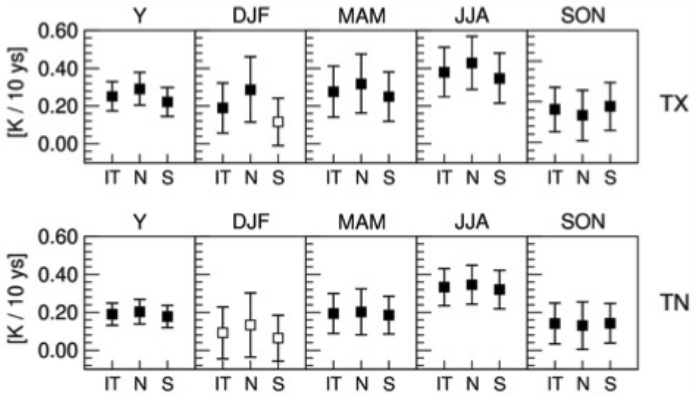

Figure 1.17. *Observed trends in mean of temperature for maxima (TX) and minima (TN) distribution. On vertical label trends in °C/10years are displayed. On horizontal labels plots are split in five frames, one for the entire year and one for each season. [Simolo et al., 2010]*

Rigid shift of the distribution was also demonstrated through the calculation of a set of 19 percentiles for each year and searching for relative trends of these indices with respect to the median. As shown in figure 1.19 each percentile, for each sub-region did not appear to have relative trends, both for maximum and minimum temperatures [Simolo et al., 2010].

Simolo et al. [2010] looked also at the exceedance probabilities (EPs) over fixed threshold and found relevant fluxes of events. These EPs, as can be seen in figure 1.20, showed to be coherent with a rigid shift of the PDF characterized by a weak decrease of temperature before 1979 and with the stronger warming found in the 1980-2008 period.

From figure 1.20 it is clear that exceedance probabilities decreased in the colder tails with a weaker rate than the one observed on warmer tails. This phenomenon has been introduced above when discussing fluxes of events with a skew normal distribution and can be easily understood looking at figure 1.21. Here it is clear how the rigid shift of a gaussian (there's no skewness in this example) distribution implies greater flows through upper thresholds than lower ones.

In this context this thesis work has the aim to analyze, keeping in mind what found by other studies and focusing on the still ongoing debate, a temperature data-set over the italian region of Trentino Alto Adige. The particular position in the center of the Alps allows to inspect warming climate at different elevations and to analyze trends in the mean and in the frequency of extreme events. All this with the goal to understand whether the latter ones belong only to shifts in the mean or to variability changes.

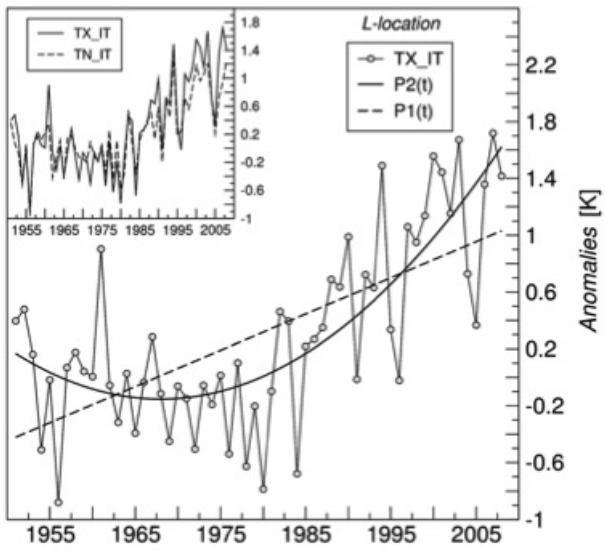

Figure 1.18. *Annual mean of maximum temperature for whole italian sample. Dashed line represents a first order linear regression, solid line a second order polynomial regression. In the little top-left window one can see the comparison between minimum and maximum temperatures. [Simolo et al., 2010]*

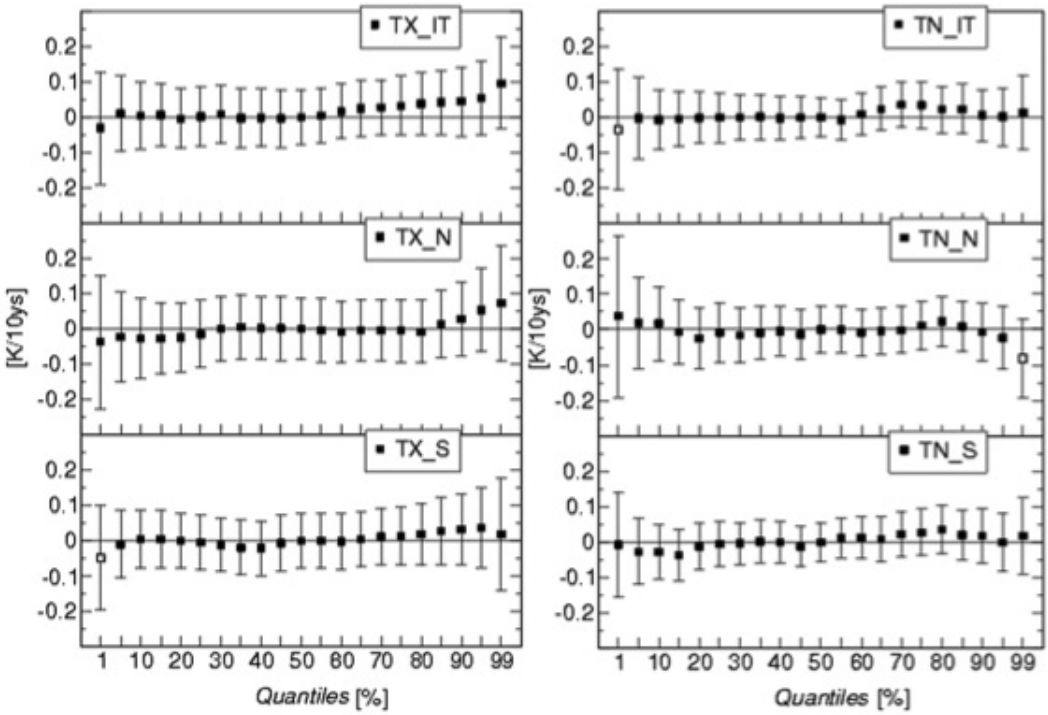

Figure 1.19. *Relative trends for each percentile with respect to the trend of the median. On vertical label degrees per decade are visible, with confidence bars of 95%. [Simolo et al., 2010] .*

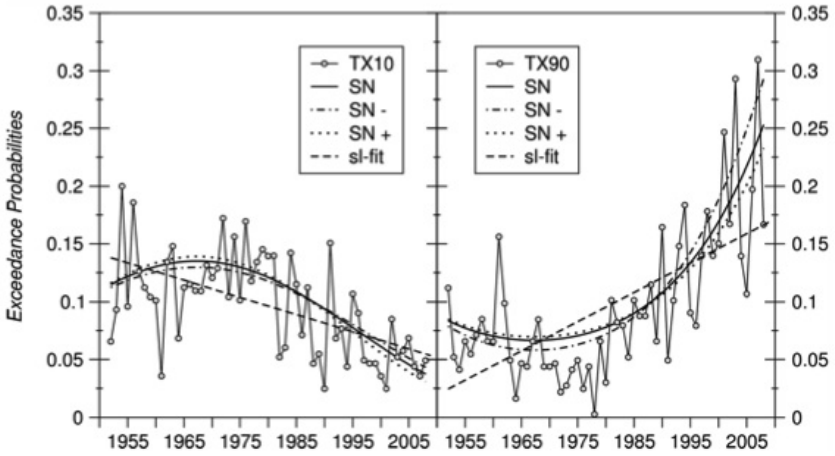

Figure 1.20. *Observed counts of maximum temperatures (for the whole italian data set) below the 10th threshold (left) and above the 90th percentile (right). Dashed lines represent the linear fit. Dotted, dash-dotted and solid lines represent different fits effectuated with three different skew normal distributions (changing shape parameter).[Simolo et al., 2010]*

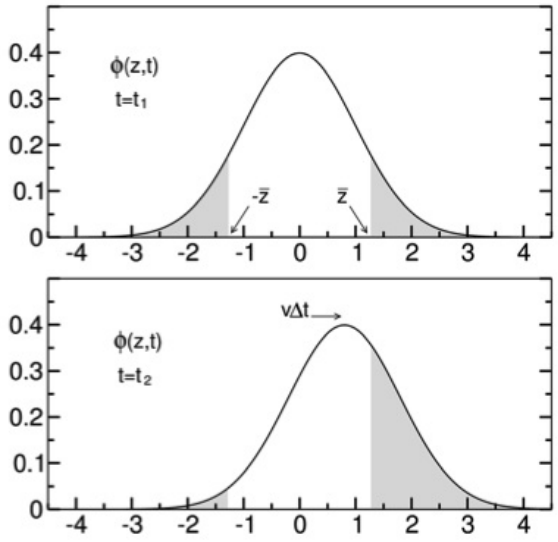

Figure 1.21. *Probability of exceeding fixed thresholds for a shifting distribution. Probabilities are identified with shaded grey areas. Here it's simple to notice consequences of rigid shift of a gaussian-like distribution and different flows through the thresholds [Simolo et al., 2010]*

Chapter 2

Data collection and quality check

2.1 Trentino Alto Adige and its geographical features

Aim of this study was then to analyze variability and changes of climate on the italian region of Trentino Alto Adige. This region is entirely located in the central-eastern Alps and its topography is characterized by high mountains (up to 3905 m, Ortles mountain) and a high number of valleys originated by the flow of creeks and rivers towards the main river: the Adige. These geographical features allowed to have a data set of station with relevant height differences. As seen in figure 2.1 and figure 2.2 stations are homogeneously distributed on the region's territory. In particular electronic series had good coverage of high mountain areas, as shown in figure 2.3.

Having data related to a high range of altitudes permitted to study how changes in climate relate to mountain regions topography, looking at valleys and steep ridges. In fact all steps of this work were done considering this features, especially when some stations were used as references for calculating anomalies and for testing inhomogeneities.

2.2 Data collection

Trentino Alto Adige is divided into two autonomous provinces (Provincia Autonoma di Trento or Trentino and Provincia Autonoma di Bolzano or Alto Adige/Sudtirol), so that they have two separated agro-meteorological services. This implied data collection to be effectuated in two steps, one for each administrative division.

Temperature series for Trentino were downloaded from Meteotrentino web site (http://www.meteotrentino.it/dati-meteo/stazioni/elenco-staz-hydstra.aspx?ID=168).

In this website, for each station present in the list, it was possible to choose the variable to download. It was also allowed to indicate time range and frequency of sample (monthly, daily).

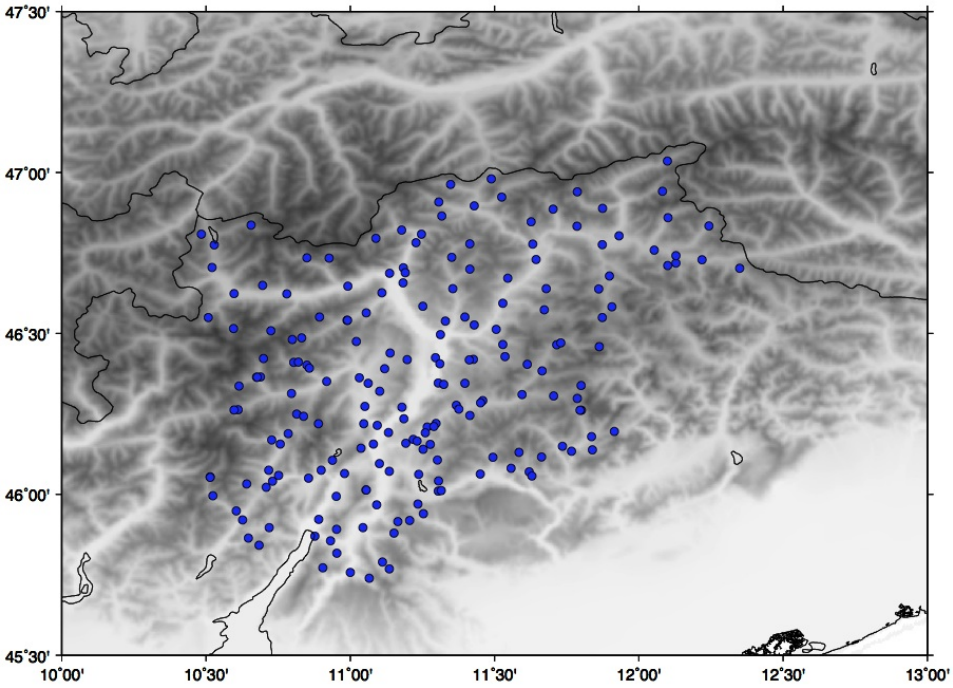

Figure 2.1. *Yearbook stations in the initial data set. Tones of gray indicate altitudes of points on the map.*

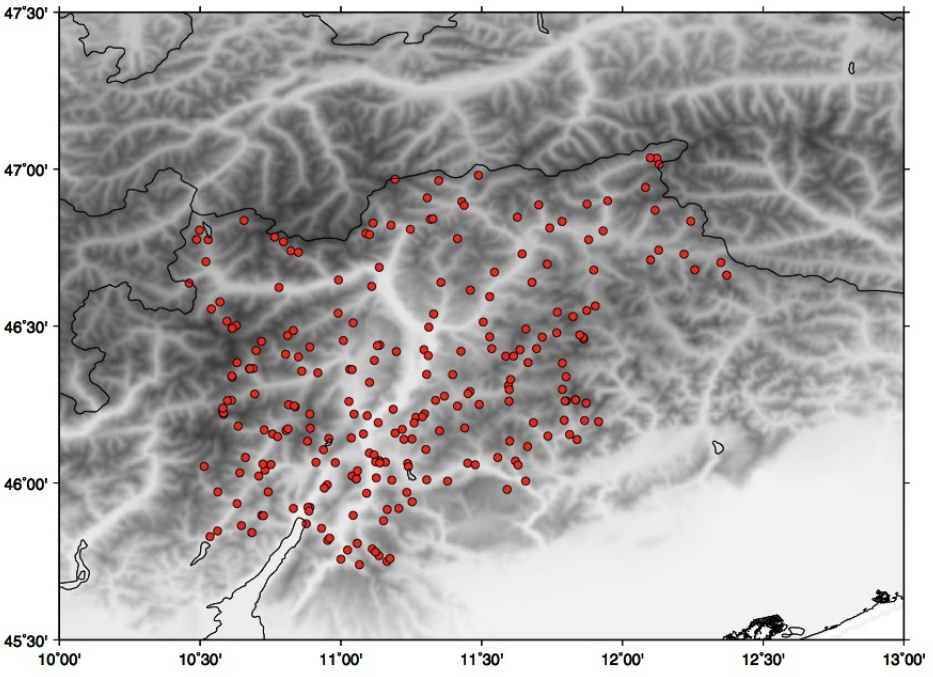

Figure 2.2. *Electronic station in the initial data set*

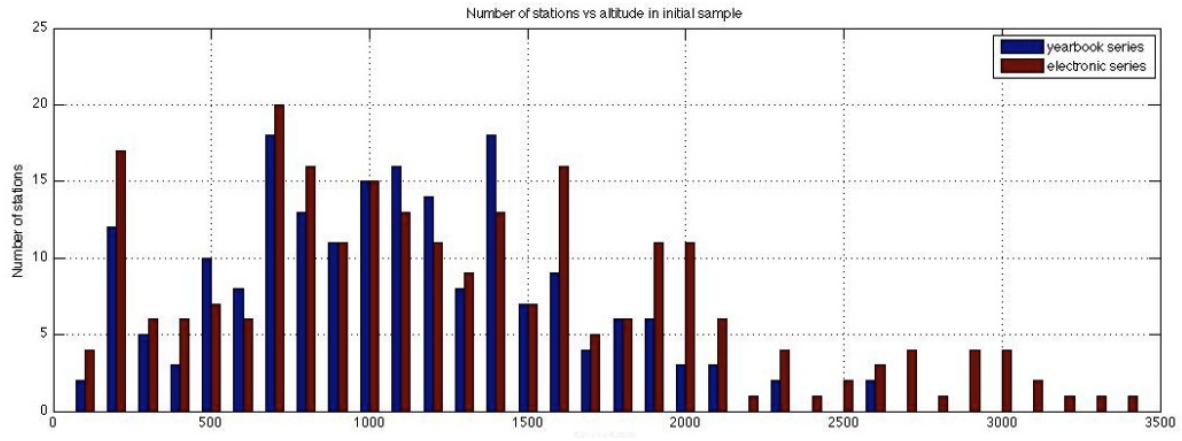

Figure 2.3. *Number of stations vs altitude bands. Bin width is 100 m. Blue columns represent number of yearbook series, red columns represent number of electronic series.*

The downloaded files were in .csv format and were converted into a defined standard format required for data elaboration thanks to a MATLAB program. Data from Alto Adige were provided by Ufficio Idrografico Provincia di Bolzano in .zrx (ASCII) format and were converted in the standard format looking at esa-decimal codes that indicated the kind and the quality of measurements.

Standard format consisted of a sequence of rows, one per each month. The structure of rows was as follows:

- the year (integer value in columns 1-5);
- the month (integer value in columns 6-8);
- the sequence of recorded temperature for each day expressed as N F7.1 floating-point variable, where N id the number of days in the month.

Downloaded series were not characterized by the same observation rules. In fact until second half of 1980's the measurements taken by each station were uniquely done with the so called yearbook method. This procedure consists in recording data each morning at 9 a.m, so that minimum and maximum temperature assigned to day i are referred to the 24 hours interval running from 9 a.m. of day i-1 to 9 a.m of day i. Such a system (from now on called "0909") causes that in general recorded maximum temperature refers to the previous day. An exception are those days in which maximum temperatures happen in the early morning (before 9 a.m.) For this reason during the "merging procedure" (see section 2.4) every maximum temperature recorded whit yearbook technique has been shifted by one day.

Starting from approximately 1985, electronic stations began to spread and replace old stations. These automatic devices record temperatures each night at midnight, avoiding doubts on the day whom the temperature refers. From now on this temporal aggregation will be called "0024".

For most of analyzed stations, at the beginning of 0024 series, yearbook series finished their record, maybe after a superimposition that could last for some months or some years. But it's also frequent to find at the same time for many years (in some case until our days) 0909 series and 0024 series together. In these cases 0909 series have been probably composed by data recorded with electronic devices, but, in order to maintain homogeneity with historical data, temperatures are stored with old temporal aggregation criteria.

After being converted to the standard format, files were renamed keeping in mind following criteria. Each name was composed by some fields separated by underscores. The fields were:

- TMND or TMXD, indicating daily minimum temperatures (TMND) or daily maximum temperatures (TMXD);
- 0909 or 0024, indicating whether records were taken with yearbook technique (0909) or electronical devices (0024);
- ITA_TAA_: indicating nation and region;
- TN o BZ: indicating the province;
- station code: (original MeteoTrentino or IdroBolzano code);
- name of the station with words separated by dashes;

Alto Adige series had been given already divided in two cathegories: first one including mechanical series (yearbook technique), the other one electronic series.

However electronic series given by IdroBolzano had been already merged with corresponding mechanical series. Since Quality Check procedure would have required to compare data from all stations related to a certain day, keeping particular attention to simultaneity of events, it was necessary to create separated data-set belonging to different record methods. Therefore, in order to check series with homogeneous ones, it became indispensable to split these electronic series into two series.

This problem was solved thanks to recording time, indicated for each data. Effectively IdroBolzano gave also, for each day of each station, exact hour of measurement. These times were recorded as 09:00 in case of mechanical station, in other cases displayed hour was the effective time of occurring of the recorded temperature (i.e. if maximum temperature were recorded at 3:45 p.m., the displayed hour was 15:45) or a generic 00:01, indicating 0024 temporal aggregation measurement. It is important to point out that in case electronic measurement began in second half of the year, IdroBolzano completed that year with yearbook-like aggregation (i.e. 0909): so electronic measurements referred to 0024 series appear from 1st January of following year. Otherwise if electronic data began before 30th June, previous mechanical data of that year had been adapted to electronic series shifting maximum temperatures to previous day.

These recording-hour informations were helpful in splitting the series but they fell into ambiguity when some minimum or maximum temperatures of a day happened at exactly 9 o'clock in the morning. At the end the solution to this issue was found individuating, thanks to hour information, the break-year between mechanical and electronic records. Furthermore this process was complicated by the fact that some series, due to technical problems in electronic measurements, went back to mechanical techniques for some periods until the retake of electronic series.

Obtained files were then ready to undergo quality check. They were renamed keeping the same station name and same code but giving different name in second field (0909/0024).

2.3 Quality check

Quality check was performed in two phases. Most important step was the second one, in which each station were compared to surrounding ones. In this process, in order to preserve simultaneity of events, comparison was made keeping separated in every step mechanical/yearbook and electronic series.

2.3.1 Removal of gross errors

The goal of the first one was to eliminate the gross errors, i.e. data clearly wrong. These outliers were discovered with a MATLAB program searching for:

- minimum and maximum temperatures above 50°C or below -50°C;
- minimum and maximum temperatures below -30°C from 1st of may to 31st of october;
- minimum and maximum temperatures above 35°C from 1st of october to 31st of march.

These wrong data were eliminated and replaced with a -90, code for a no-data.

Looking into series of Trentino, sequences of days with temperature -30°C were found. To identify all these sequences the previous program for gross errors was updated inserting criteria able to find sequences of at least 3 consecutive daily temperatures of -30°C. Results of this first step of quality check were then renamed changing first field of file names in TMNG and TMXG.

2.3.2 Splitting of yearbook series

Before proceeding with second step, a preliminary homogeneity check was made to test longest series for large inhomogeneities. These stations often had undergone modifications in their location and instruments, so corresponding temperature series

presented significant inhomogeneities that affected the mean and consequently could create problems in the following steps, when anomaly temperatures are compared to synthetic series. Effectively anomaly temperatures are calculated taking the 1976-2005 period as reference for calculating climatological averages. This implies that strong inhomogeneities appearing in 0909 series before 1975 would present large anomalies that could be labeled as suspect during quality check and then large portion of temporal series invalidated (these kinds of error may be corrected in the next homogenization step, see chapter 3). In electronic stations, beginning after 1985, inhomogeneities occur in most cases in the reference period and consequently present less large non-climatic anomalies.

For these reasons each yearbook series was analyzed with the Craddock Test (for detailed description of Craddock Test see section 3.1) to identify large inhomogeneities and to split it into "almost homogenous" sub-series, that were then checked independently. An example of Craddock Test and individuated break-points in this preliminary step is reported in figure 2.4.

The individuated breaks allowed to separate the series into almost-homogeneous sub-series. These almost homogeneous series are recognizable in Craddock Test with similar slopes. In figure 2.4 it's important to notice different slopes of the individuated sections. It may also be seen in figure 2.5 how these sub-section correspond to sub-series with nearly coherent annual mean. Indeed in this representative case sub-series 01 collected very overestimated temperatures, while sub-series 02 collected very underestimated temperatures. Even though slopes of sections included in sub-series 03 were positive, it was necessary not to gather this section to sub-series 01, since the slopes were very different.

2.3.3 Calculation of observed anomalies

Second step of quality check consisted in the comparison between values recorded in a station and values recorded in the surrounding ones. This comparison was done calculating, for each station, the temperature anomalies. These are the result of the subtraction of the annual mean cycle from daily data set. Mean annual cycle was calculated following some steps and basing on monthly means. Use of monthly data was chosen since daily temperatures presented a large number of missing data and it is more simple to reconstruct the first ones than latter ones.

Since some months presented missing daily data, a threshold of maximum 20% of no-data in a month was chosen, in order to avoid to calculate averages with few available days. Obtained series showed, as expected, many monthly missing data and only series with at least five years of data were accepted for the next steps. Series whose monthly series were created (175 "0024" series and 188 "0909" series, counting splitted series as one) are shown in figures 2.6 and 2.7, where it is shown that coverage of territory and of mountain areas was maintained (see also figure 2.8). Monthly series were named writing the prefix *mes* before the series name.

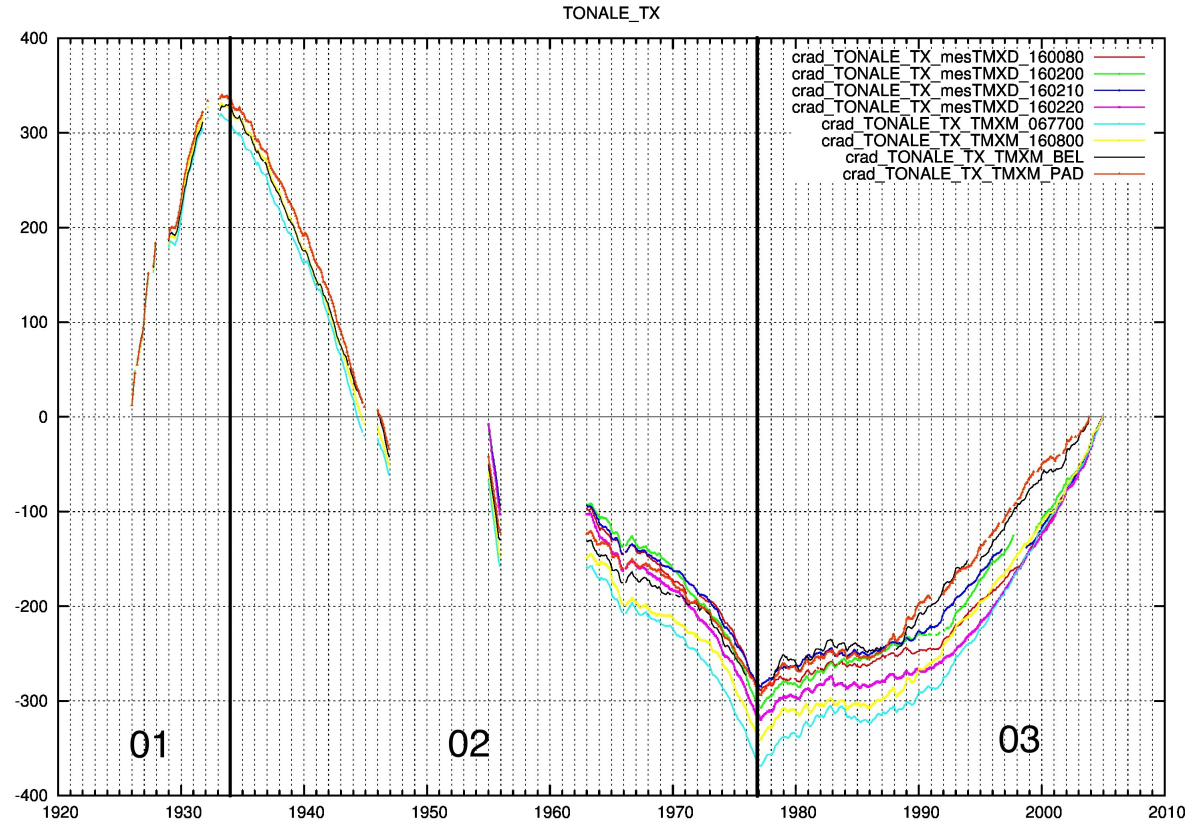

Figure 2.4. *Craddock test effectuated on maximum temperatures series of Passo Tonale . Vertical lines indicate chosen breaks and numbers stand for the separated series that section is associated.*

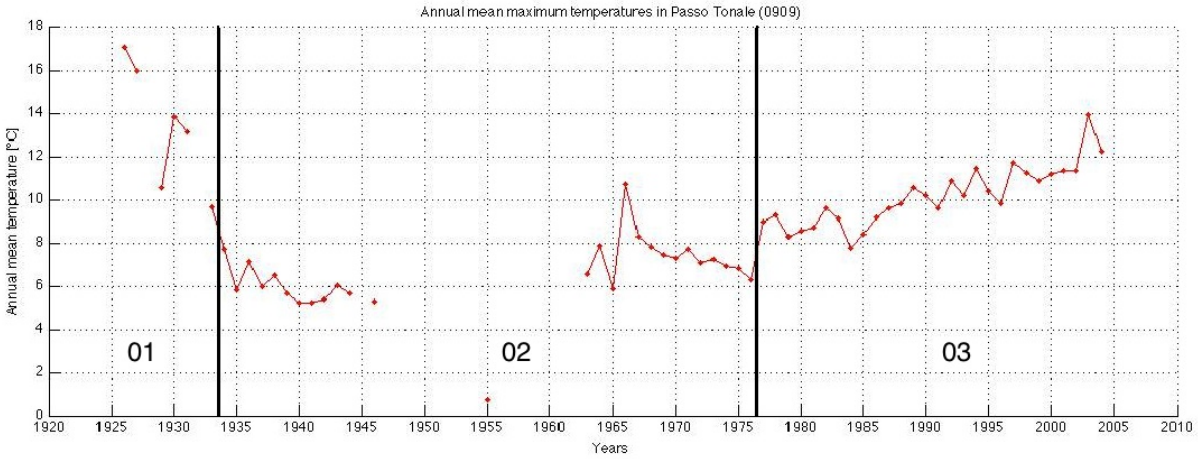

Figure 2.5. *Annual mean maximum temperature of Passo Tonale (0909). Vertical lines indicate chosen breaks and numbers stand for the separated series that section is associated.*

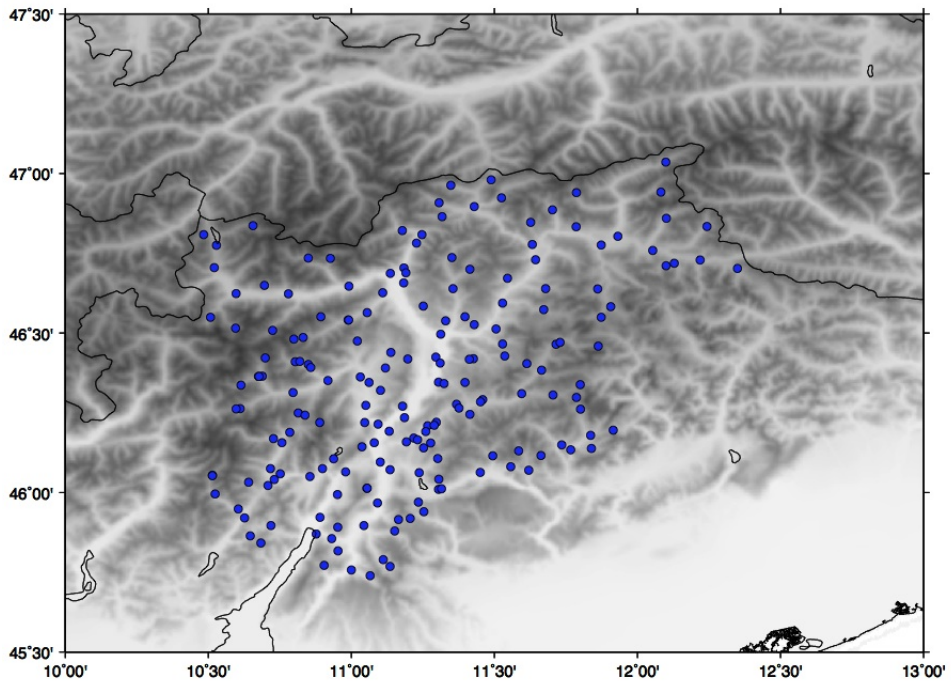

Figure 2.6. *Yearbook stations whose montlhy series was calculated. Tones of gray indicate altitudes of points on the map.*

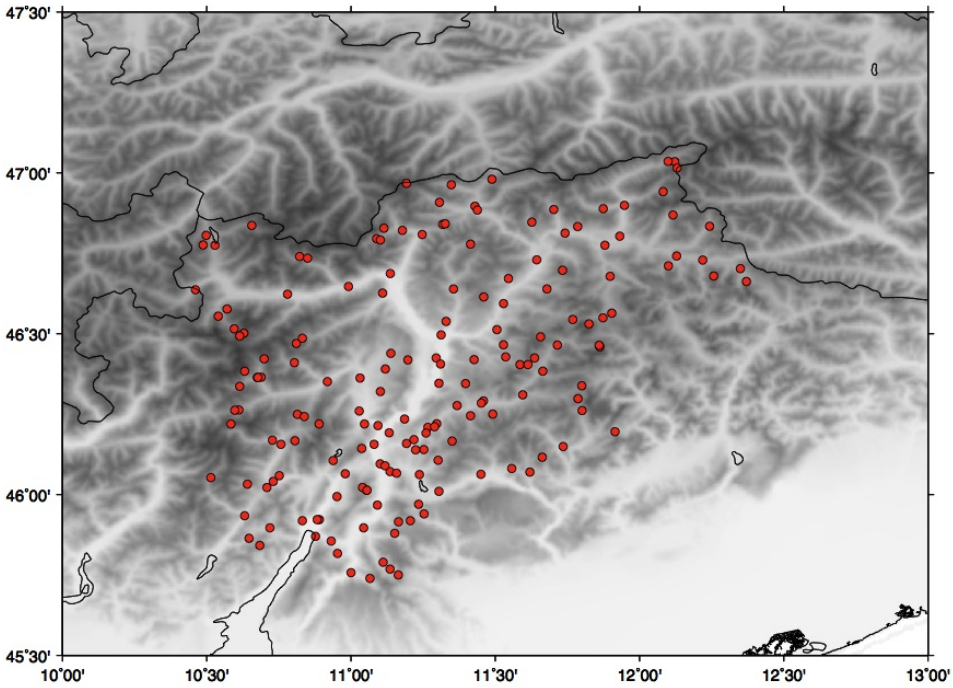

Figure 2.7. *Electronic stations whose montlhy series was calculated.*

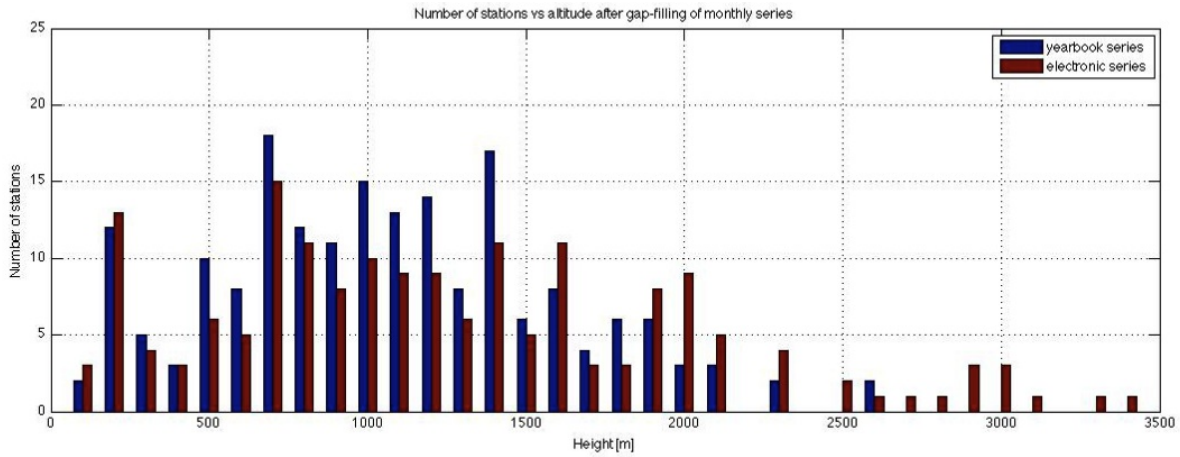

Figure 2.8. *Number of stations for altitude bands after selection made in monthly series completion. Bin width is 100 m. Blue columns represent number of yearbook series, red columns represent number of electronic series.*

Second, all monthly series were completed in their missing values over the 1976-2005 period, chosen as reference period for the estimation of anomalies, being the most complete 30-year sub-period. In fact electronic series began mostly around 1985. This would have required 1985-2014 to be the chosen range, but great part of yearbook series ended in 2005/2010. For these reasons and knowing that yearbook series were the longest ones and that long series are fundamental in this study, the choice was done in favor of the latest 30-year time range that would have included a significant part of yearbook series: i.e. 1976-2005. Reasons of this choice can be seen in figure 2.9

Gap-filling (in the 1976-2005 period) of a series was made reconstructing a synthetic monthly series of anomaly temperatures (i.e. difference from the monthly climatological mean) representative of the station location. This series was reconstructed as weighted average (see section 2.3.4) of surrounding stations not belonging to this work's data set but already homogenized.

Once synthetic series was calculated, gap-filling was made as follows (in these equations T stands for anomaly temperature):

$$T_{m,y}^{missing} = T_{m,y}^{synt} + C \tag{2.1}$$

Where m and y are the month and year whose temperature mean is missing, and C is calculated as:

$$C = \overline{T}_m^{obs} - \overline{T}_m^{synt} \tag{2.2}$$

Where $\overline{T}_m^{obs}$ and $\overline{T}_m^{synt}$ are obtained performing arithmetic averages of all data related to the selected month, available for observed and syntetic series. Therefore, reconstruction of missing data is made under the hypothesys of constant difference between observed and synthetic series.

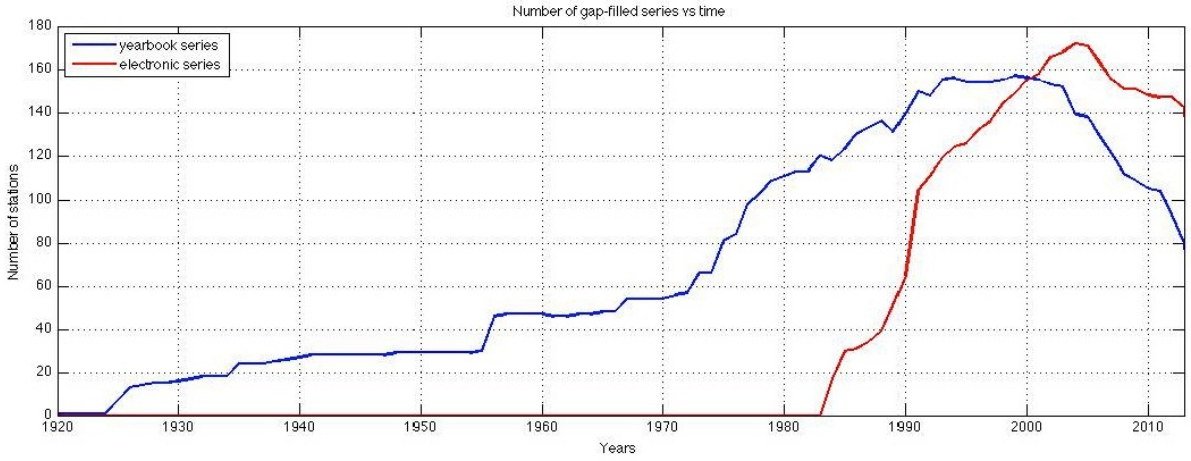

Figure 2.9. *Number of stations (whose climatology was calculated) for each year. Blue line represents annal series, here it's clear the reduction of the number of annal series after 2005. Steep increase of stations in half 1950's occurs because all series provided by Alto Adige begin in 1956. Red line represents electronic series that have been installed from 1984 to our days.*

The gap-filled monthly series were utilized to calculate the monthly climatologies overt the 1976-2005 reference period.

Daily climatologies (i.e. daily mean annual cycles) could then be calculated from monthly climatologies by means of a trigonometric smoothing. Given the 12 monthly mean, each of them was associated to the 15th day of the relative month in a 366-bin array (for example: january mean was associated to point 15, february mean to day 46, march mean to day 75 etc.). Then these points underwent a second order trigonometric regression, searching the function:

$$\mathrm{tr}(d) = \mathrm{a}_0 + \mathrm{a}_1 \cos\left(\frac{2\pi d}{Y}\right) + \mathrm{b}_1 \sin\left(\frac{2\pi d}{Y}\right) + \mathrm{a}_2 \cos\left(\frac{4\pi d}{Y}\right) + \mathrm{b}_2 \sin\left(\frac{4\pi d}{Y}\right) \qquad (2.3)$$

whose coefficients (a_0, a_1, a_2, b_1, b_2) best fitted the monthly climatology. a_0 is clearly the mean of the 12 points. Oscillation due to a_1 and b_1 can spread from the minimum (min) to the maximum(max) points so the two first-order coefficient were imposed to lay in the range $(\min - \mathrm{a}_0 - 0.5, \max - \mathrm{a}_0 + 0.5)$. At the same time a_2 and b_2 were allowed to be between -2° and 2°, since the oscillation due to second order should be less relevant than the one of first order.

Regression was done keeping fixed values for three coefficients and varying the remaining one in its range with a 0.01 °C resolution. First regression was performed on a_1, giving 0 value to the other coefficients, calculating least square for the results of each possible value of a_1 and choosing the minimum among them.

$$\mathrm{ls}(a_1) = \sum_{m=1}^{12} \left[\mathrm{a}_0 + a_1 \cos\left(2\pi \frac{\mathrm{cm}(m)}{Y}\right) - \mathrm{C}(m)\right]^2; \qquad (2.4)$$

Where:

- $a_1 \in (\min - a_0 - 0.5, \max - a_0 + 0.5)$ with 0.01 intervals;
- cm(m) is a 12-elements array indicating, for each month, the "center of the month" as number of days from the beginning of the year;
- $Y = 366$, length of the year (not chosen equal to 365 in order to have different values for 28th, 29th February when dealing with leap years);
- C(m) is the climatology of the month m.

When found the value $\overline{a_1}$ for which ls(a_1) is minimized, the same process was done for b_1, imposing $a_1 = \overline{a_1}$:

$$\mathrm{ls}(b_1) = \sum_{m=1}^{12} \left[a_0 + \overline{a_1} \cos\left(2\pi \frac{\mathrm{cm}(m)}{Y}\right) + b_1 \sin\left(2\pi \frac{\mathrm{cm}(m)}{Y}\right) - \mathrm{C}(m) \right]^2; \tag{2.5}$$

where $b1 \in (\min - a_0 - 0.5, \max - a_0 + 0.5)$ with 0.01 intervals.
After individuating $\overline{b_1}$, the same was done for a_2 and b_2:

$$\mathrm{ls}(a_2) = \sum_{m=1}^{12} \left[a_0 + \overline{a_1} \cos\left(2\pi \frac{\mathrm{cm}(m)}{Y}\right) + \overline{b_1} \sin\left(2\pi \frac{\mathrm{cm}(m)}{Y}\right) + a_2 \cos\left(2\pi \frac{\mathrm{cm}(m)}{Y}\right) - \mathrm{C}(m) \right]^2; \tag{2.6}$$

And:

$$\begin{aligned} \mathrm{ls}(b_2) = \sum_{m=1}^{12} \Bigg[& a_0 + \overline{a_1} \cos\left(2\pi \frac{\mathrm{cm}(m)}{Y}\right) + \overline{b_1} \sin\left(2\pi \frac{\mathrm{cm}(m)}{Y}\right) + \\ & + \overline{a_2} \cos\left(2\pi \frac{\mathrm{cm}(m)}{Y}\right) + b_2 \cos\left(2\pi \frac{\mathrm{cm}(m)}{Y}\right) - \mathrm{C}(m) \Bigg]^2; \end{aligned} \tag{2.7}$$

This 4-step regression was re-iterated until difference between new and old coefficients was found to be less than 0.01 for all of them (for first iteration old values utilized are 0 for every coefficient). Generally the program required two iterations to reach convergence. Obtained coefficients were then substituted in equation 2.3 and plotted with monthly climatologies, as seen in figure 2.10.

Calculated daily climatologies were then utilized to create observed daily anomalies.

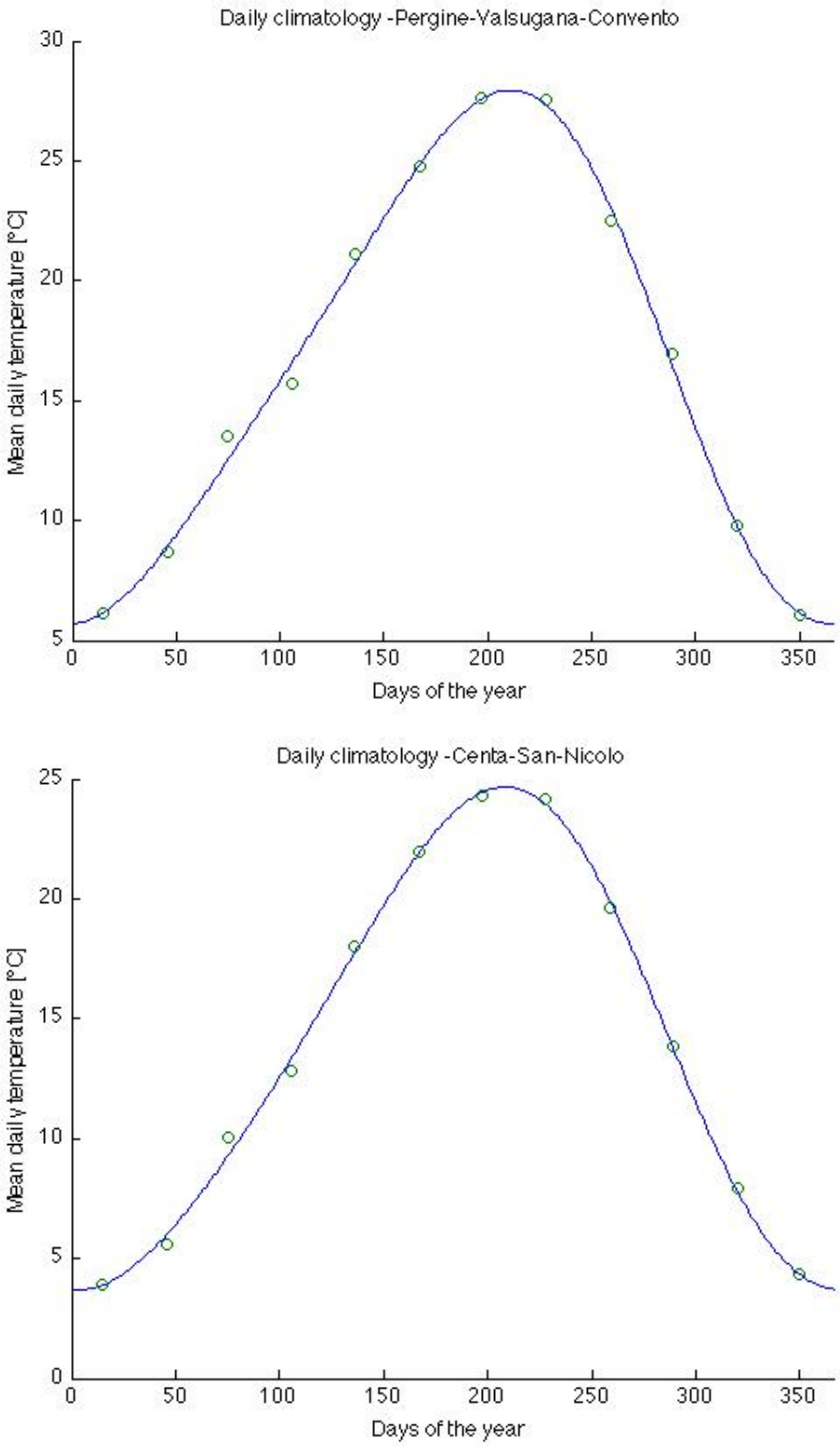

Figure 2.10. *Trigonometric regression for maximum temperatures of Pergine Valsugana (top) and Centa San Nicolò (bottom). On x-label days of the year appear, while on y-label temperature in Celsius degrees. Green circles represent monthly climatologies, blue line is the result of trigonometric regression*

2.3.4 Calculation of synthetic anomalies

Quality check was mainly based on the comparison between observed anomalies and synthetic anomalies.

The selection of reference series to construct the synthetic series was done among the anomaly series resulted from the gross-error removal, choosing those that showed less inhomogeneities and less number of missing data. In some cases it was necessary to delete from reference series some years of data, recognized as deeply different from the rest of the series (for example years that showed a significant higher or lower mean temperatures). At the end, together with these reference series, an additional series already homogenized, having data since 1920, was considered (Cortina d'Ampezzo, provided by ARPA Veneto)

Synthetic series were reconstructed as weighted averages of surrounding reference series having the same temporal aggregation of the site, where weights depended by horizontal and vertical distance of reference series from the site the synthetic series was referred to.

If (ϕ_1, θ_1, h_1) are the coordinates of the synthetic series site and (ϕ_2, θ_2, h_2) coordinates of the reference series:

$$d = R\,\Delta\alpha \tag{2.8}$$

where R is the radius of the Earth (6371 km) . $\Delta\alpha$ is the angular distance of the two points in the latitude-longitude grid, and is calculated doing:

$$\cos(\Delta\alpha) = \sin(\theta_1)\sin(\theta_2) + \cos(\theta_1)\cos(\theta_2)\cos(\phi_1 - \phi_2) \tag{2.9}$$

At this point, known d and known Δh ($\Delta h = h_1 - h_2$), weight might be calculated using following expression:

$$w^r_{1,2} = e^{-\frac{d^2}{c_r}} \tag{2.10}$$

$$w^h_{1,2} = e^{-\frac{\Delta h^2}{c_h}} \tag{2.11}$$

$$w_{1,2} = w^r_{1,2} w^h_{1,2} \tag{2.12}$$

$$c_r = -\frac{d_0^2}{\ln 2} \tag{2.13}$$

$$c_h = -\frac{h_0^2}{\ln 2} \tag{2.14}$$

d_0 and h_0 are the horizontal and vertical distances at which the corresponding weight decreased to 0.5.

These parameters have been searched running several time the program and looking for the combination of the two parameters that minimized the root mean square error (RMSE) (synthetic minus observed anomalies). The chosen values were $d_0 = 30$ km and $h_0 = 700$ m, found with an iterative process. It consisted in keeping one parameter as constant (and equal to its optimized value of the previous step) and varying the other one, searching for the minimum RMSE of the synthetic series. This process was stopped when the two parameters converged. Report of this research can be seen in table 2.1.

To avoid using stations at very different height, only stations whose difference in altitude from the site was lower than the maximum between 500 m and half of the site elevation were considered among reference series. For example: if a station was 655 m high, reference series had altitudes ranging from 155 m to 1155 m; while if a station was 1200 high, the range went from 600 m to 1800 m.

Synthetic series might then be built thanks to a MATLAB program. Starting from the first day of the observed series, the program searched among the reference series the ones with data available for that day. Collected data were then ranked from highest to lowest observed anomalies, the highest and the lowest were removed in order to avoid synthetic anomaly to be affected by outliers. Remaining values underwent a weighted mean, in which each anomaly temperature had the weight relative to the reference series it belonged to. If the removal of highest and lowest valued had deleted the only available data for that day, synthetic series would have had, for the considered day, a -90°C value. This procedure was repeated for each day of the checked series until its end.

height scale: 300 m

(d_0[km])	*(RMSE)*
10	2.0604
20	1.9360
30	1.9059
40	1.8984
50	1.8969*****
60	1.8975
70	1.8990
80	1.9005
90	1.9019
100	1.9031

distance scale: 50 km

(h_0[m])	*(RMSE)*
50	2.1857
100	2.0744
150	2.0135
200	1.9672
250	1.9276
300	1.8969
350	1.8736
400	1.8565
450	1.8445
500	1.8368
600	1.8306*****
800	1.8374

height scale: 600 m

(d_0[km])	*(RMSE)*
20	1.8506
30	1.8241*****
40	1.8252
45	1.8277
50	1.8306

distance scale: 30 km

(h_0[m])	*(RMSE)*
300	1.9059
400	1.8604
500	1.8357
600	1.8241
700	1.8209*****
800	1.8223

height scale: 700 m

(d_0[km])	*(RMSE)*
25	1.8252
30	1.8209*****
35	1.8220
40	1.8250
45	1.8286
50	1.8332

Table 2.1. *Iterations of height scale and distance scale optimization. For each iteration, optimum value is indicated by five stars. Note that the value emphasized by the stars is that used in the following iteration, as explicated in text.*

2.3.5 Selection of thresholds and removal of suspect data

Most important part of quality check was the comparison of observed anomalies and synthetic anomalies. The basic concept in this phase of quality check was that observed anomaly should not differ too much from synthetic anomaly. This "too-much" was quantified through the calculation of variance of each series. For this reason, before proceeding with analysis of single daily data, using a MATLAB program, it was necessary to determine standard deviations of both synthetic and observed anomalies series.

Figure 2.11 shows behaviours of observed anomaly variance with respect to the elevation of the stations. Here it may be observed how high mountain stations present higher standard deviation (the ”main sequence” is slightly sloped to the right) both for maximum and minimum temperatures. Group of electronic stations have a more narrow range of standard deviation than the one observed for yearbook series. Even if distribution of st. dev. of yearbook is wider, it is possible to assess that the median value of st. dev. of these series is lower than that obtained for electronic series. This is probably due to the splitting process that avoided yearbook series to have extremely high variances.

Standard deviations of synthetic series (see figure 2.12), as expected, had lower values than observed anomaly standard deviations. While st. dev. of electronic series did not show great differences between maximum and minimum temperatures, differences observed for yearbook series are relevant. In particular splitted yearbook series present significantly lower st. dev. for minimum temperatures. This is probably an effect of the splitting of yearbook series that didn't affect in the same way st. dev. of yearbook maximum temperatures .

For each examined day, observed and synthetic daily anomalies were then normalized with respect to standard deviation and the following index was estimated:

$$\text{ind} = \frac{\text{an}_{\text{obs}}}{\sigma_{\text{an}_{\text{obs}}}} - \frac{\text{an}_{\text{syn}}}{\sigma_{\text{an}_{\text{syn}}}} \tag{2.15}$$

Where an_{obs} is the observed anomaly, an_{syn} is the synthetic anomaly, $\sigma_{\text{an}_{\text{obs}}}$ is the standard deviation of observed anomalies series and $\sigma_{\text{an}_{\text{syn}}}$ is the standard deviation of synthetic anomalies series. If absolute value of the indicator was larger than a chosen threshold (in this work selected threshold was 1.5), the value was labeled as suspect.

Each suspect classified daily anomaly of test series was compared to all neighboring series of that day, keeping in mind to consider only reference series of the same temporal aggregation (i.e. 0909 series compared with 0909 series and 0024 series compare with 0024 series). Series utilized in these steps will be called ”reference series” from now on, but it is important not to confuse them with those used for creation of synthetic series, which are a sub-set of them with a higher quality in terms of homogeneity and data availability.

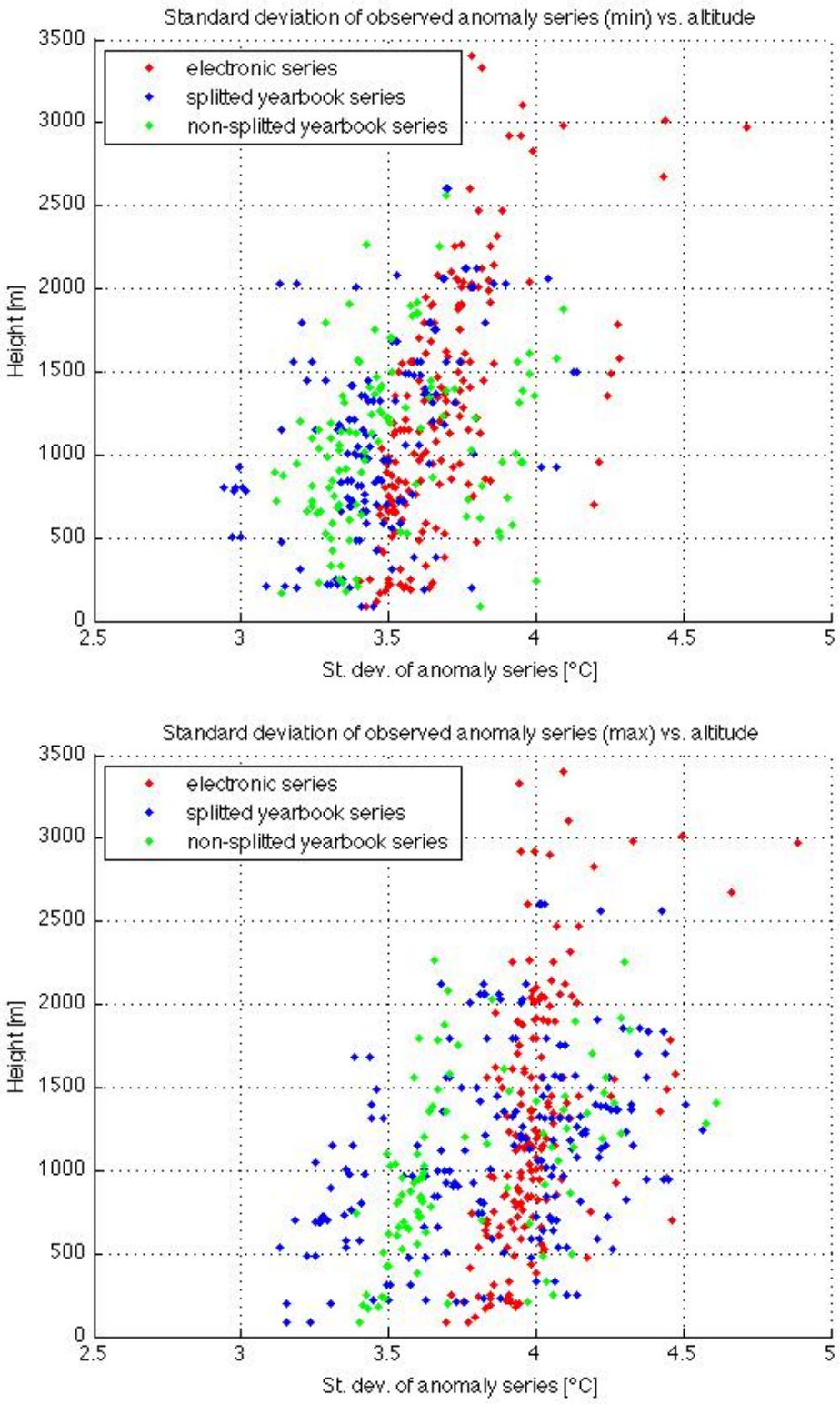

Figure 2.11. *Standard deviation of anomaly series for minimum (top) and maximum temperatures (bottom). As before, blue dots are for annal series and red dots are for electronic series*

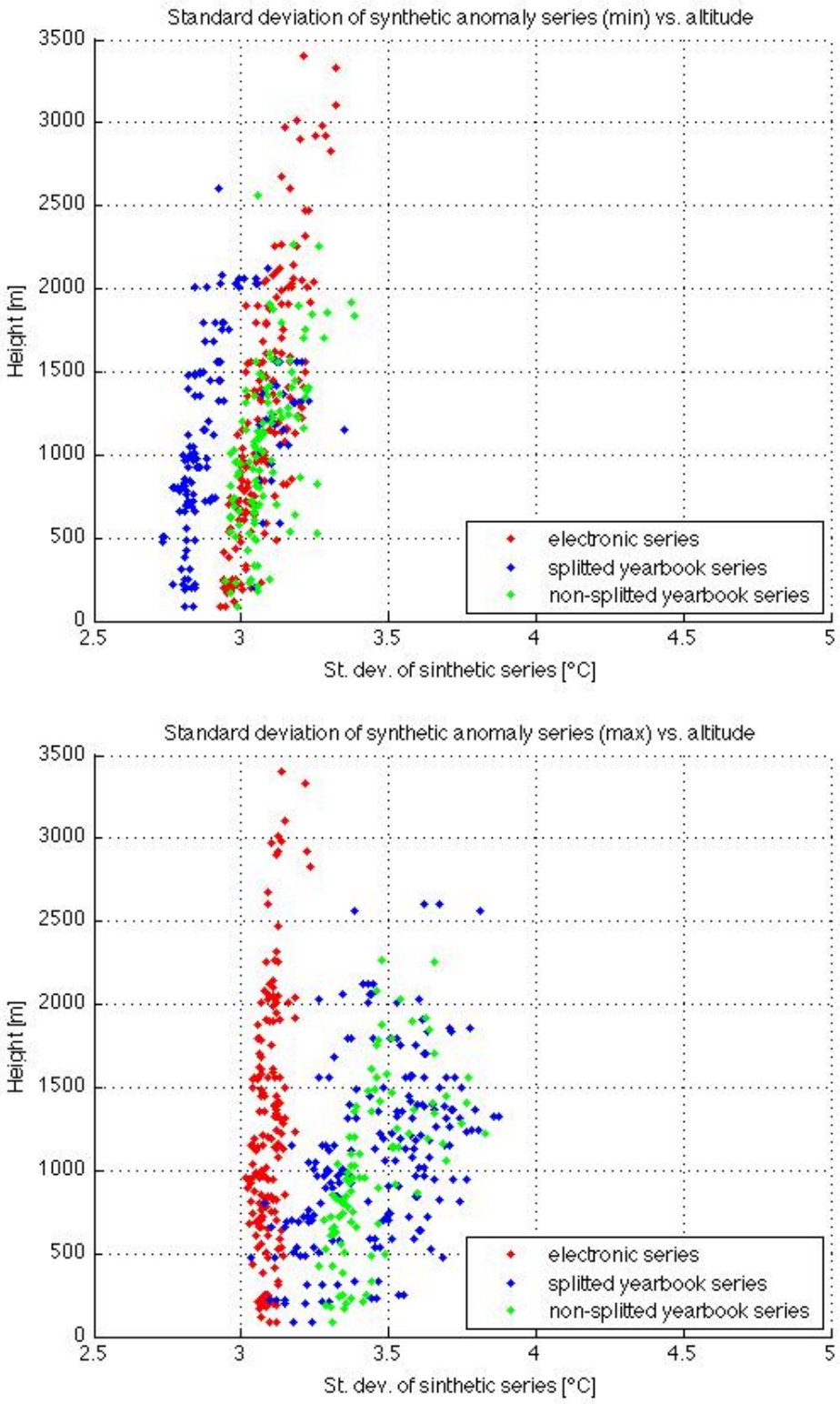

Figure 2.12. *Sigma of synthetic anomaly series for minimum (top) and maximum temperatures (bottom). Colors are same as in 2.11*

Therefore reference data were collected, considering only those stations whose difference in elevation from the checked was lower than the maximum between 500 m and half of the site elevation. Then these reference anomalies were ranked, excluding the highest and the lowest values, in order to avoid outliers to affect the range. Remaining data were then analyzed, taking note of maximum, minimum and variance of their distribution.

In order to be considered acceptable, observed anomaly of the test series should not overcome by a chosen quantity the maximum and the minimum values of the reference range. This quantity varied day by day depending on the variance of reference data and on the elevation of the checked station. If altitude was lower than 1500 m, anomaly should lay in the range $(\min - \sigma, \max + \sigma)$; while, for higher altitudes the range was $(\min - 1.5\sigma, \max + 1.5\sigma)$, where σ is the standard deviation of the reference series anomalies for the day under consideration.

Different ranges for different altitudes showed to be necessary since different temperature profiles would have affected in different ways the quality check process. Three representative cases are displayed in figures 2.13, 2.14 and 2.15.

In the first case (figure 2.13) it is possible to observe a profile that probably is due to thermal inversion. Here normalized difference between observed and synthetic anomaly is above the chosen threshold, as displayed by the large distance between red and green dots. If all stations would be taken as references, this temperature would not be labeled as suspect. Though it is clear that the red dot is outside of the main sequence. So it appears necessary to focus reference series in a limited elevation range, in order to better represent the anomaly profile close to the test station elevation.

Second case (figure 2.14) is a clear example of a climatological profile. All anomalies have nearly same values and, consequently, absolute temperature follows approximately the climatological profile, with some shifts. Here the normalized difference would be sufficient to determine the suspect values.

In the third case profile is probably interested by a more-adiabatic-than-climatology behavior and the checked point, even if distant from its corresponding synthetic value, is clearly inside the main sequence and, thanks to the reference range check, is not deleted from data-set.

Particular treatments were necessary for days with observed suspect anomalies but without available synthetic anomalies. In these cases the indicator introduced in equation 2.15 could not be utilized and the only available parameter was the observed anomaly itself. It was chosen that a datum without synthetic anomaly was to be considered suspect if absolute value of observed anomaly was larger than 3 times relative standard deviation and simultaneously occurred conditions of laying outside range of surrounding data. If there were no data available among reference series or these had been deleted in the removal of highest and lower values, data were not to be considered suspect and were not eliminated. This circumstance occurs when reference series are less than 3.

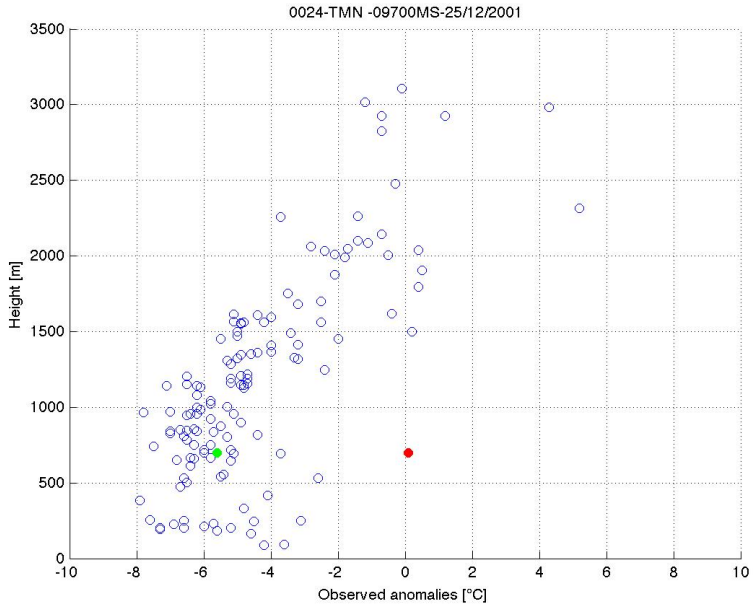

Figure 2.13. *Scatter plot of observed anomalies vs height. Empty dots represent reference series, red dot is the observed anomaly of the checked series, green dot represent the synthetic anomaly calculated as described above. Here lowest stations present "more negative" anomalies than highest ones.*

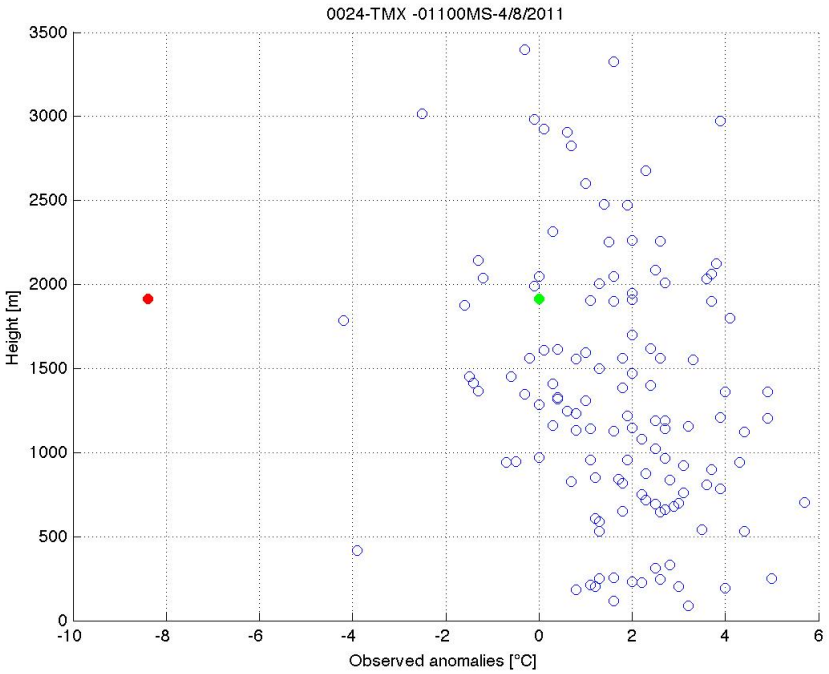

Figure 2.14. *Same as figure 2.13. Here every station presents approximately same anomaly values.*

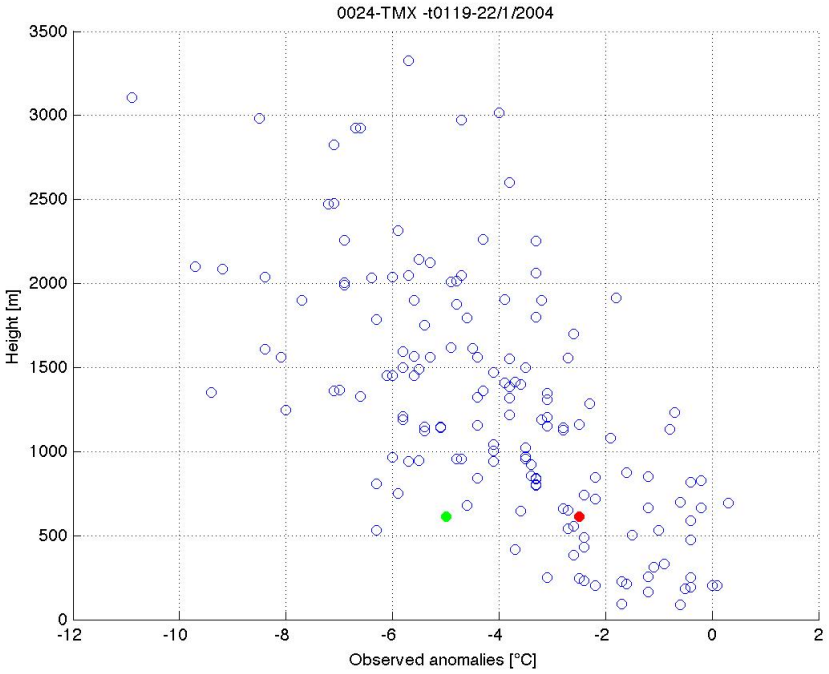

Figure 2.15. *Same as figure 2.13. Here high stations presents "more negative" anomaly than low ones.*

Summarizing, data were removed:

- if synthetic anomaly existed and reference series had data:

  $\text{ind} \notin (-1.5, +1.5)$

  AND

  $\text{an}_{\text{obs}} \notin (\min - c \cdot \sigma_{\text{range}}, \max + c \cdot \sigma_{\text{range}})$

  Where

  $$c = \begin{cases} 1.5 & \text{height} > 1500\text{m} \\ 1 & \text{height} \leqslant 1500\text{m} \end{cases}$$

- if synthetic anomaly did not exist but reference series had data:

  $\text{an}_{\text{obs}} \notin (-3\sigma_{\text{series}}, 3\sigma_{\text{series}})$

  AND

  $\text{an}_{\text{obs}} \notin (\min - 1.5\sigma, \max + 1.5\sigma)$

This process was performed thanks to a MATLAB program.

In figures 2.16, 2.17, 2.18 it is possible to see other three examples of possible situations occurred during quality check. These examples represent cases of clearly wrong data, false positive and clearly right data.

First plot is related to a clearly wrong datum whose indicator is equal to 3.4 (note the distance between green and red dots) and whose anomaly (red dot) is without doubt not included in the main sequence .

Second plot describes a case in which indicator (ind=2.2) is greater than the threshold but some reference series have greater anomalies, furthermore the main sequence is not well defined as in the other cases; for these reasons the suspect data cannot be deleted.

Last plot is related to a clearly right data: red and green dots are very close one to the other, indicator has a very low value and the main sequence is defined, showing values above and below the checked one.

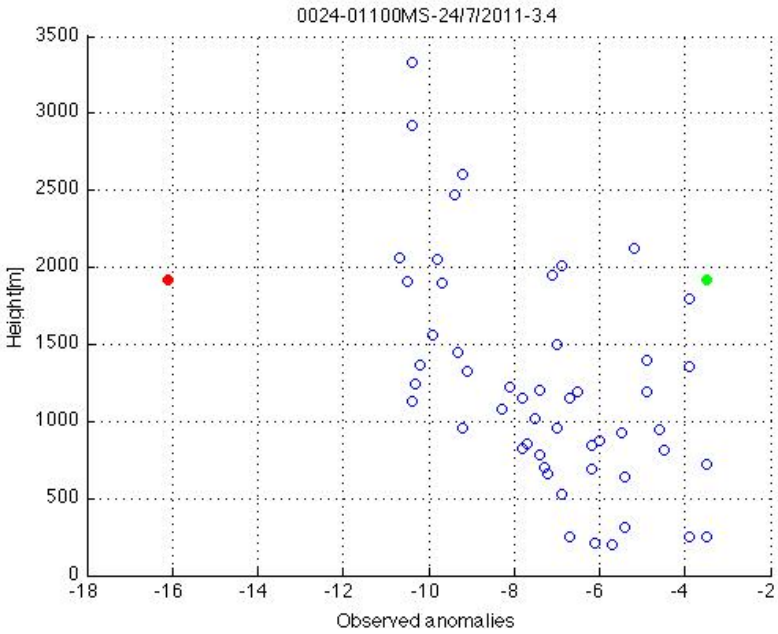

Figure 2.16. *Same as 2.13.*

Data individuated as suspect with these criteria were removed and replaced, in the original temperature series, by a -90°C. Since there exists the possibility that in the same day more than one station presented some problems, quality check was effectuated twice. In second iteration the new series, results of first iteration, were utilized as reference series. This second quality check allowed to find anomalous data that in the first check were masked by other wrong data with higher anomalies.

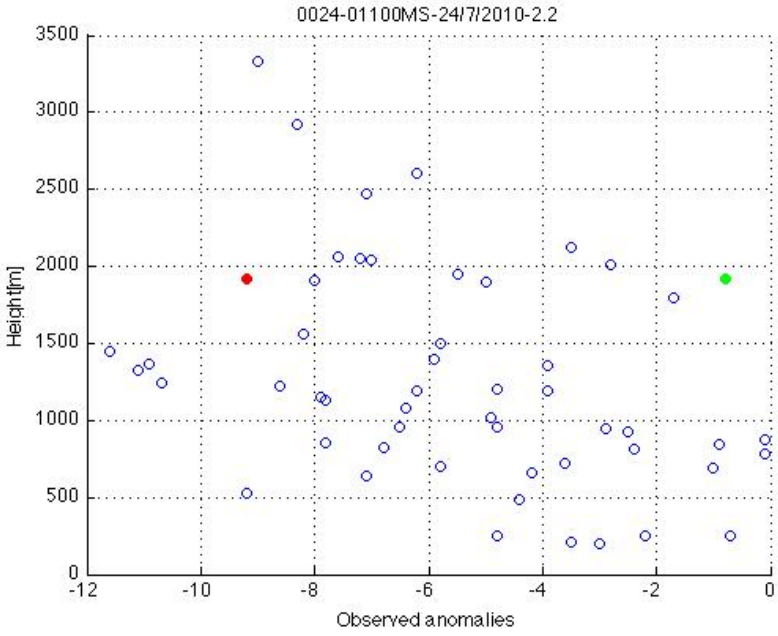

Figure 2.17. *Same as 2.13.*

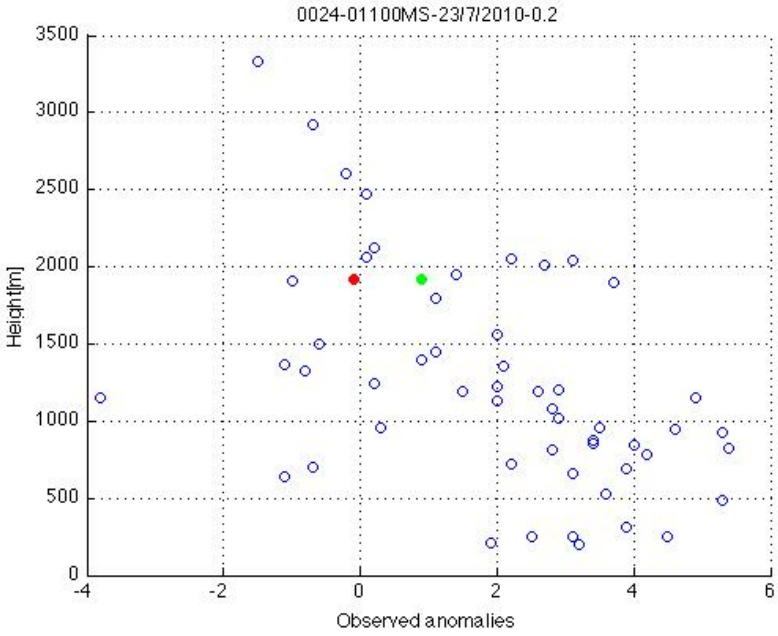

Figure 2.18. *Same as 2.13.*

At this point new series were compared with old ones in order to individuate months whose data underwent a significant removal. When it was found that a certain month had lost more than five daily data after the two quality check iterations , it was chosen to invalidate the whole month. Therefore every datum from first to last day of that month was removed and substituted by a -90°C. Percentage of data removed after simple quality check and after monthly invalidation can be examined in figures 2.19 and 2.20.

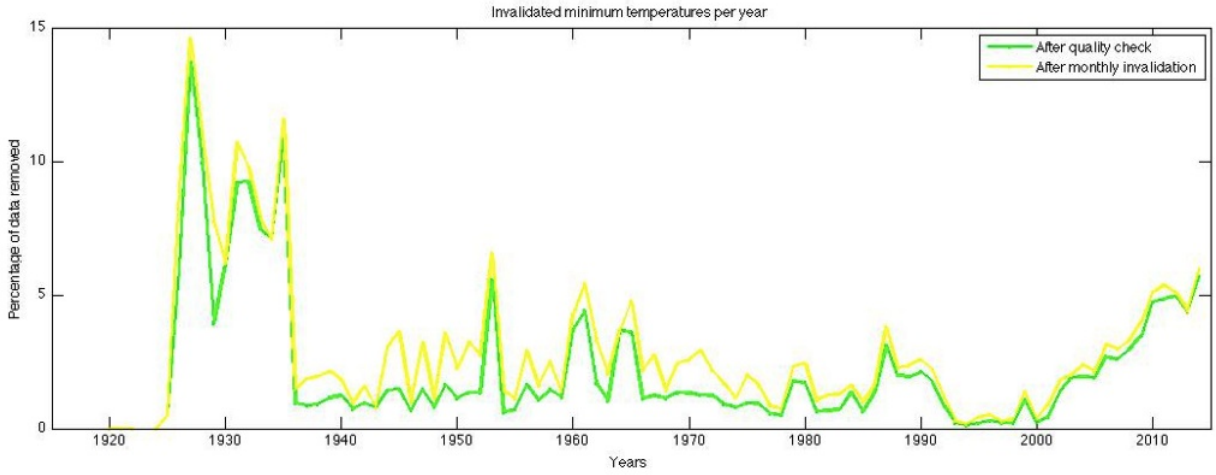

Figure 2.19. *Percentage of minimum temperatures removed by quality check (green lines) and by monthly removal (yellow lines).*

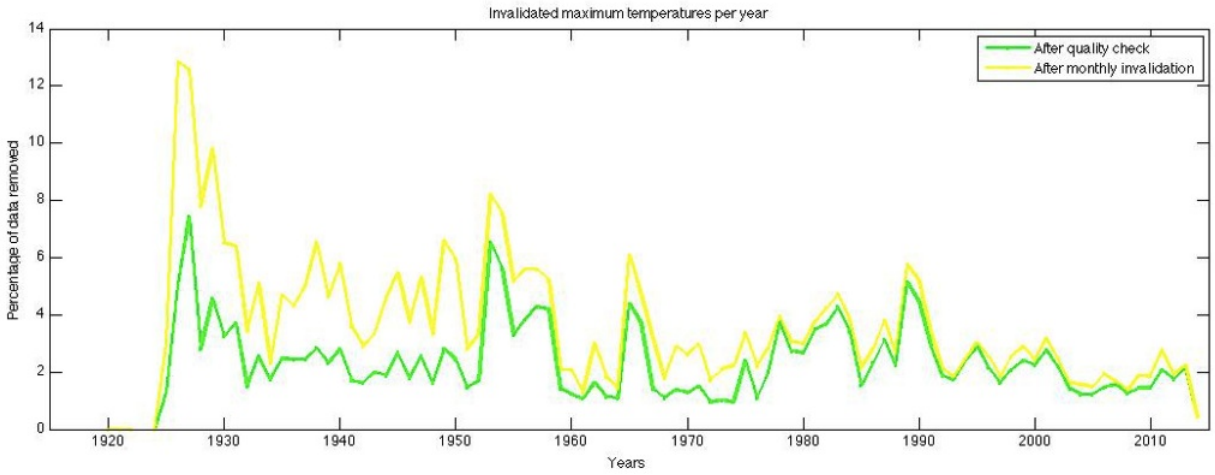

Figure 2.20. *Percentage of maximum temperatures removed by quality check (green lines) and by monthly removal (yellow lines).*

At the end of quality check yearbook series that had been separated before the beginning of the control were gathered with results of quality check coming from each sub-series.

2.4 Merging

Since for climatological goals is useful to deal with series as long as possible, series belonging to same station or to stations very close one to the other were merged. First step of the "merging" process was gathering of yearbook and electronic series of the same station. As said in section 2.2, each station could have yearbook or electronic series, or even both. In general yearbook series are not updated but they were dismissed and substituted by electronic series.

Merging process allowed to create series in which yearbook series appeared until its last datum and then data from electronic series began. This operation was effectuated thanks to a MATLAB program that searched for the last available datum in a yearbook series. The month in which this temperature appeared was chosen as the last one whose data would have come from mechanical series; beginning from following month data belonged to electronic series.

Some particular cases required to change criteria for the individuation of connection points. In fact some yearbook series presented one or more data after years of no-data, while corresponding electronic series had continuous series of temperatures. For this reason it was decided to anticipate connection between the two series to the date in which a ”no-data” in yearbook series was followed by at least two years of no-data and corresponding electronic series had an uninterrupted sequence of data (minimum 24 days per month required). So-obtained series were named writing ”MERG” in second field of file names.

Once series related to same stations were gathered, second step of merging process consisted in individuating closest neighboring station with a distance lower than 2 km and with a height difference less than 100 meter. Merging of closer station were accepted if the resulting series was longer than the original one, otherwise old series would have been retained. In this case the resulting files have been named with both codes of the two stations, separated by a dash.

Spatial and Final group of station can bee seen in figure 2.21 and 2.22.

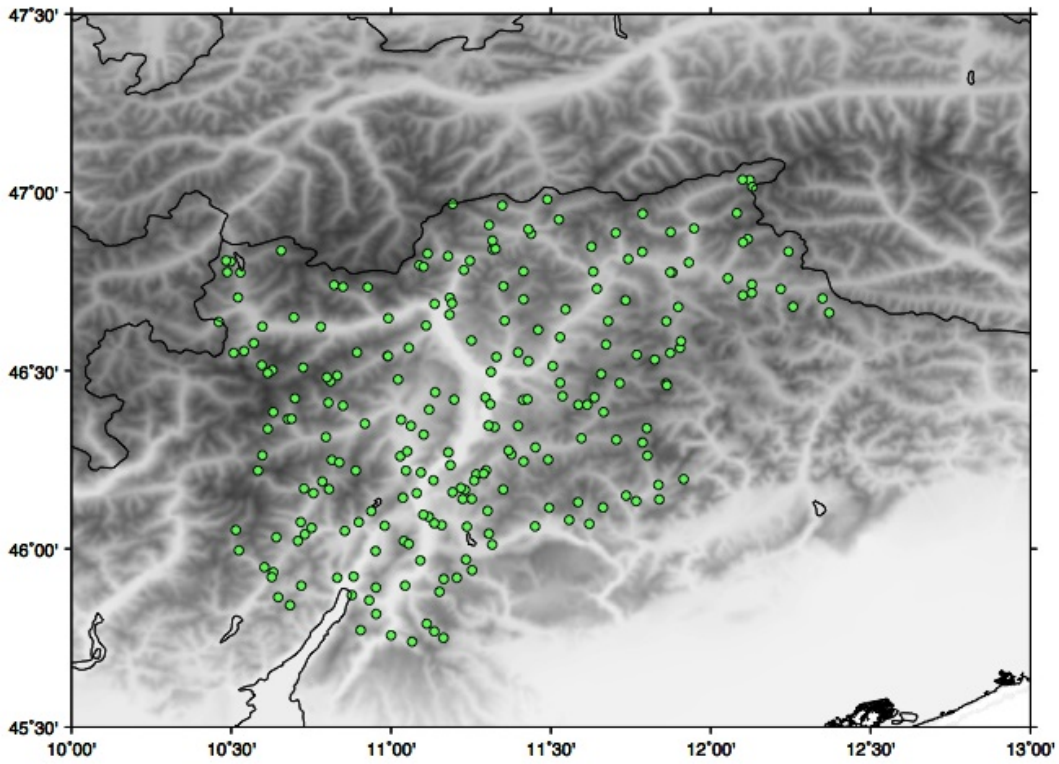

Figure 2.21. *Stations whose montlhy series have been calculated.*

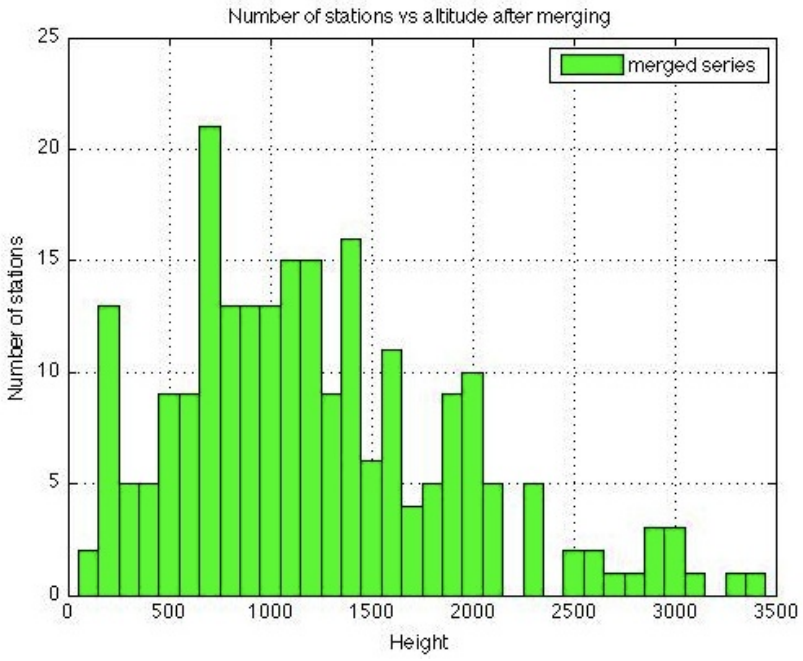

Figure 2.22. *Number of stations for altitude bands after merging process. Bin width is 100 m*

Chapter 3

Homogenization

Climatological analysis require to work on series whose recording methods and station position were not subjected to variations in time. Changes in position can indeed affect up to some degrees minimum and maximum temperatures, especially when stations are moved in height. Effectively topography of the examined region causes that even a little change in horizontal position of a station causes changing in its altitude. Non-climatic signal in temperature series may also be caused by changes in instrumental equipment.

Therefore these and other changes in stations features implied important variations in recorded temperatures causing several points of non-homogeneity, called "breaks". For these reasons lacking of homogeneity would made difficult to distinguish climatic signal in the analyzed series and corrections were necessary to make series suitable to statistical analysis.

3.1 Craddock Test

Homogenization was done applying to each station a Craddock Test. The test is based on the hypothesis of the constancy of temperature differences between a reference and a test series. Given two stations, where the first one (x) is the one to be homogenized and the second one (y) is a reference series, x and y can be written in the following way:

$$x_i = \overline{x} + x'_i \tag{3.1}$$

$$y_i = \overline{y} + y'_i \tag{3.2}$$

Here i indicates temporal instant, bar indicates arithmetic average and prime stands for the deviation from the mean. Series are then brought to same average with a correcting factor ($c = \overline{y} - \overline{x}$). At this point series of differences (d) is calculated:

$$d_i = x_i - y_i + c = \bar{x} + c - \overline{y} + x'_i - y'_i = x'_i - y'_i \tag{3.3}$$

Craddock Test is based on the plot of the s_i series calculated in the following way:

$$s_i = \sum_{j=1}^{i} d_j \tag{3.4}$$

This is a cumulative series that shows increasing trend when series x_i is overestimated and decreasing trend when the series is underestimated.

Series checked with Craddock Test in this work was monthly series. Breaks were recognizable in Craddock Test through changes in the mean slope of the plot (filtering natural noise) i.e. discontinuities in the first derivative of the Craddock curve. In order to make a more confident evaluation, Craddock Test was always performed comparing checked series to 10 reference series. The break signals of the check series against all the reference series are then collected in a decision matrix and the breaks are assigned to the check series according to probability. This caution avoided non-homogeneities in a single reference series to affect the homogenization process and permitted to individuate more carefully slope changes common to a higher number of reference series.

After homogenization the Craddock curves should contain only a noise signal. Two examples of series before and after homogenization are displayed in figure 3.1 (Bezzecca, 698 m) and figure 3.2 (St Veit in Prags, 1285 m). Please note the different scale in y axis before and after homogenization.

In some cases simple Craddock Test was not sufficient in detecting breaks. Some problems indeed can affect only limited parts of the year and for these reason Craddock Test program allows to look in a separated way to summer (from april to september) and winter (from october to march) data. This was definitely not a secondary check, since in some cases overestimation of winter (summer) data and underestimation of summer (winter) data might balance each other and produce no signal in the general Craddock Test if all months are considered together.

Moreover, this detailed observation of series permitted to detect outlier months that were not individuated during the quality check. These data were recognized through very steep increase or decrease in craddock curve lasting only one or few months. After verifying whether these data were really consequences of wrong measurements, they were removed and replaced by -90°C code.

3.2 Correction of the series

Homogenization was performed changing data with correcting factors calculated accounting for a reference period. Since most of the considered series are still taking measurements, reference period was chosen to be the last one, going from most recent break to end of the series. This would allow updates to the series to be homogeneous to the rest of sample.

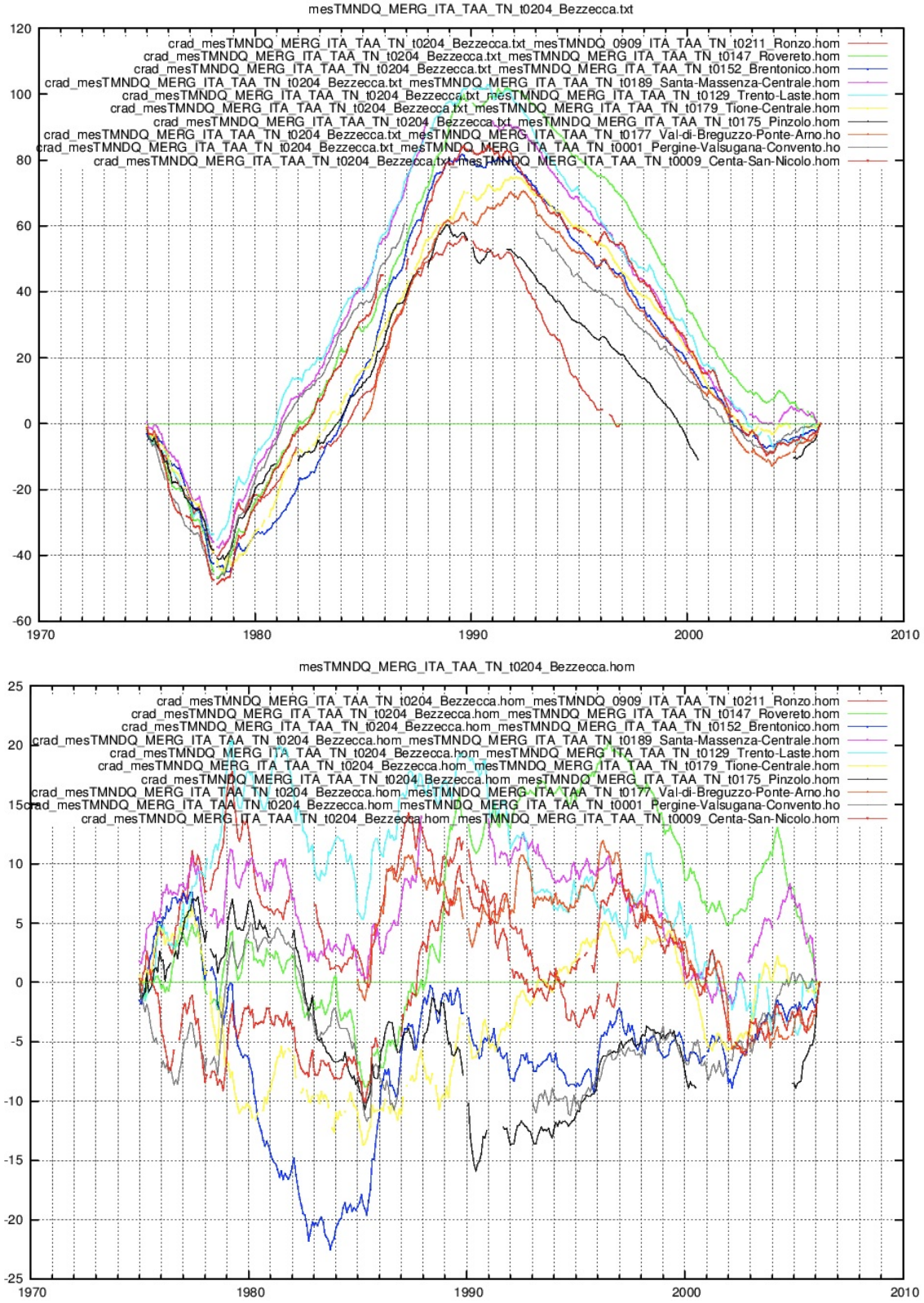

Figure 3.1. *Craddock test effectuated on minimum temperature series of Bezzecca before homogenization (top) and after (bottom). In the top plot breaks are clearly individuable in september 2003 (2003-09), 1988-10, 1978-11 and 1977-12. Bottom plot is an example of craddock test operated on an homogeneous series: it appears as bruise around zero and reference series do not "agree" indicating overestimated and underestimated periods.*

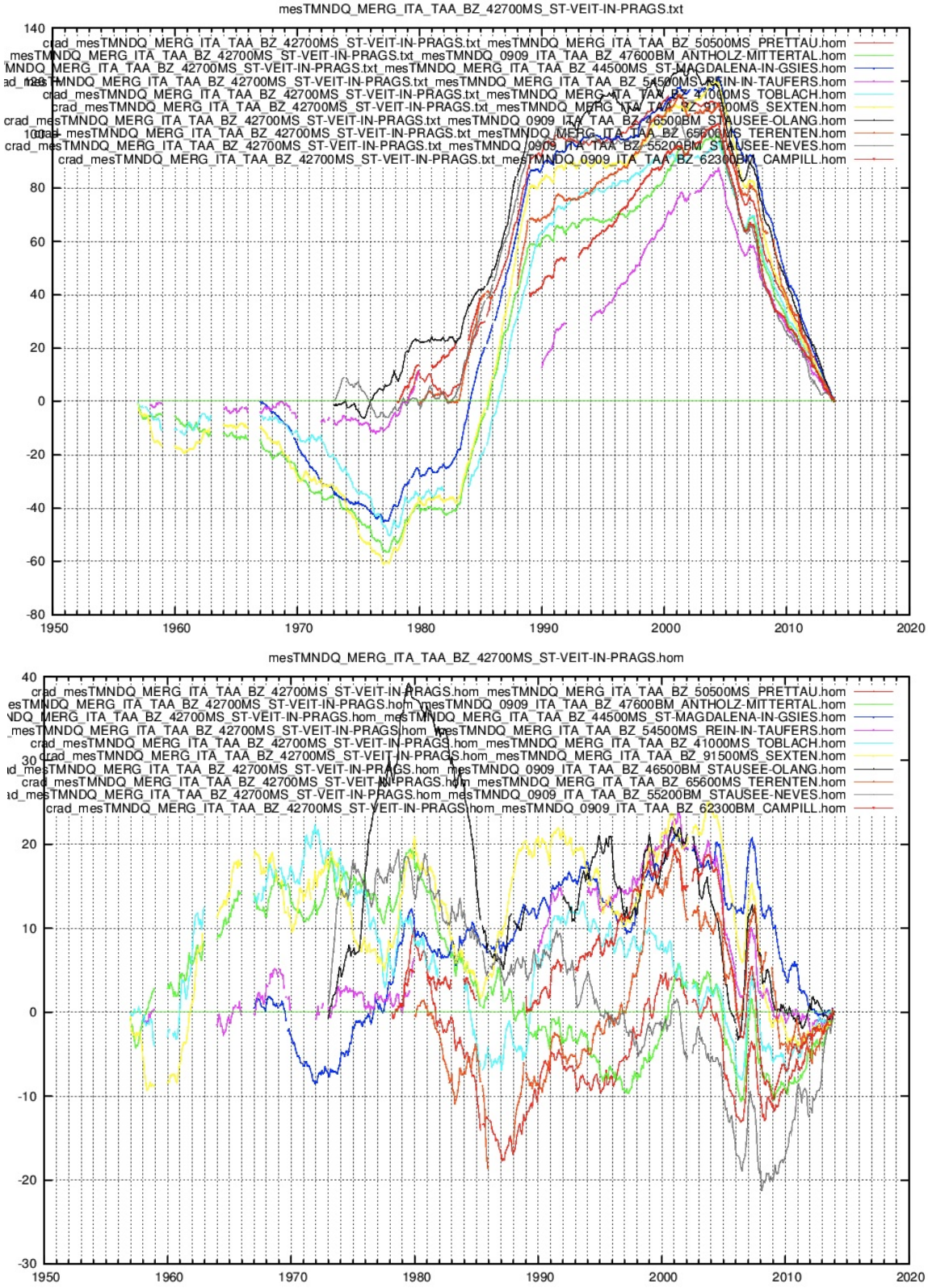

Figure 3.2. *Same as figure 3.1 but for St Veit in Prags. Breaks found are 2004-06, 1989-01, 1983-01 and 1977-01. Correcting factors used for the interval going from 1983 to 1989 will be discussed hereinafter.*

Correcting factors utilized in homogenization were calculated independently for each month in the following way:

$$C_m^y = (\overline{x}_m^U - \overline{y}_m^U) - (\overline{x}_m^H - \overline{y}_m^H) \tag{3.5}$$

Where C_m^y is the correcting factor, $\bar{x}_m^U$ is the average of the check series calculated in the period laying on the left of the break (non-homogenized yet), $\bar{x}_m^H$ is the average of the check series calculated in the period laying on the right of the break (already homogenized), $\bar{y}_m^U$ and $\bar{y}_m^H$ are the averages of the reference series calculated in the period laying on the left and on the right of the break (both homogenized). Index m indicates months from 1 to 12.

Using in this process a single reference series might cause wrong correction, since reference series could have inhomogeneities or periods of missing data. For this reason final correcting factors were obtained as arithmetic mean of correcting factors calculated for a higher number of series, from 2 to 8. Choice of reference series was done looking at series with high correlation and that showed agreement among them in the individuated annual cycle of correcting factors. Number of utilized reference series was due to data availability for the examined period. When particular conditions caused a low number of reference series (for example very old data or high mountain stations) it was decided to use reference periods as long as possible in order to avoid possible extreme (but not wrong) monthly data to affect final result.

An example of correcting factor can be seen in figure 3.3, where it is evident the agreement among reference series in individuating an annual cycle. It is a sort of ensemble of correcting factors.

Since daily series are studied, corrections had to be effectuated on daily data. This was done thanks to a trigonometric regression of the second order, searching coefficients of the function:

$$C_d = a_0 + a_1 \cos\left(\frac{2\pi d}{Y}\right) + b_1 \sin\left(\frac{2\pi d}{Y}\right) + a_2 \cos\left(\frac{4\pi d}{Y}\right) + b_2 \sin\left(\frac{4\pi d}{Y}\right) \tag{3.6}$$

that best fitted the sequence of 12 monthly values. Results of trigonometric regression may be observed in figure 3.4.

Homogenization brought all periods of the series to be coherent with the last one and was effectuated correcting from one break to the previous one step by step going back in time. After homogenizing second last period of the series, Craddock Test was used to individuate the previous break. Time interval going from new break to the following one was then homogenized taking as reference period the recent part of the series that already had been homogenized.

In some cases reference period after most recent break was shorter than three years. Three data for each month is a too little sample to be reliable for calculating correcting factors. For this reasons some series have been shortened by removing data after last break.

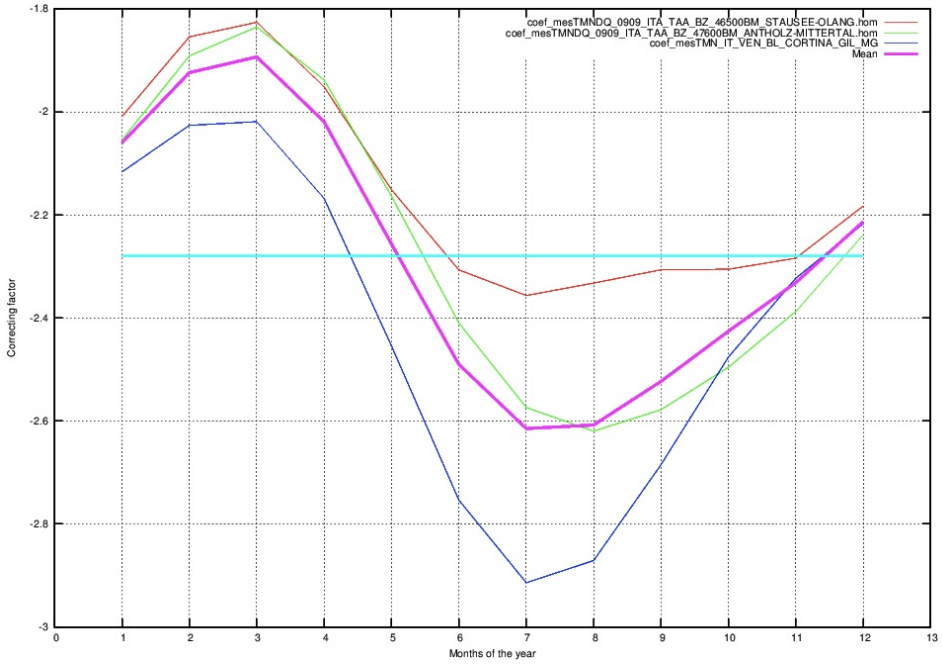

Figure 3.3. *Monthly correcting factor calculated with the procedure described above. Thick line represents arithmetic mean of correcting factors relative to the 3 reference series. This figure is taken from the homogenization process of minimum temperature series of St Veit in Prags and is relative to the homogenization of the third last period to the last one.*

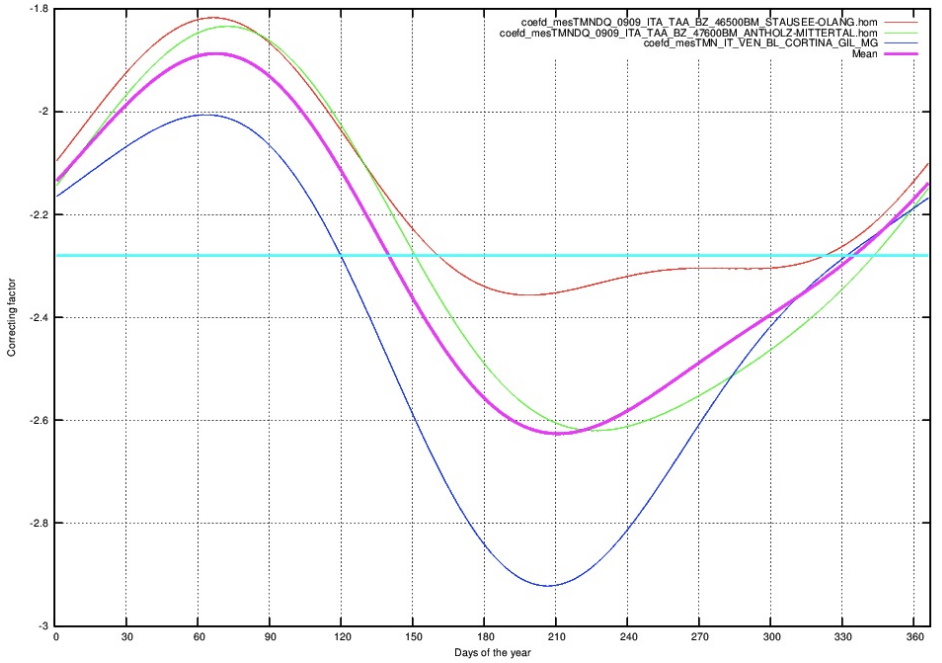

Figure 3.4. *Daily correcting factor calculated with a trigonometric regression. Thick line represents arithmetic mean of correcting factors relative to the 3 reference series.*

Homogenization was effectuated only on series having at least 30 years of effective data. Furthermore some series became too short after having been shortened for the reason explicated above. This selection reduced significantly the sample to 98 series. Since it was needed for this work to have a good coverage of the entire region, two series with less than 30 years of data were ″saved″ and underwent homogenization anyway (Rabbi and Passo Valles).

Final geographical and altitudinal distribution of series may be observed in figures 3.5 and 3.6.

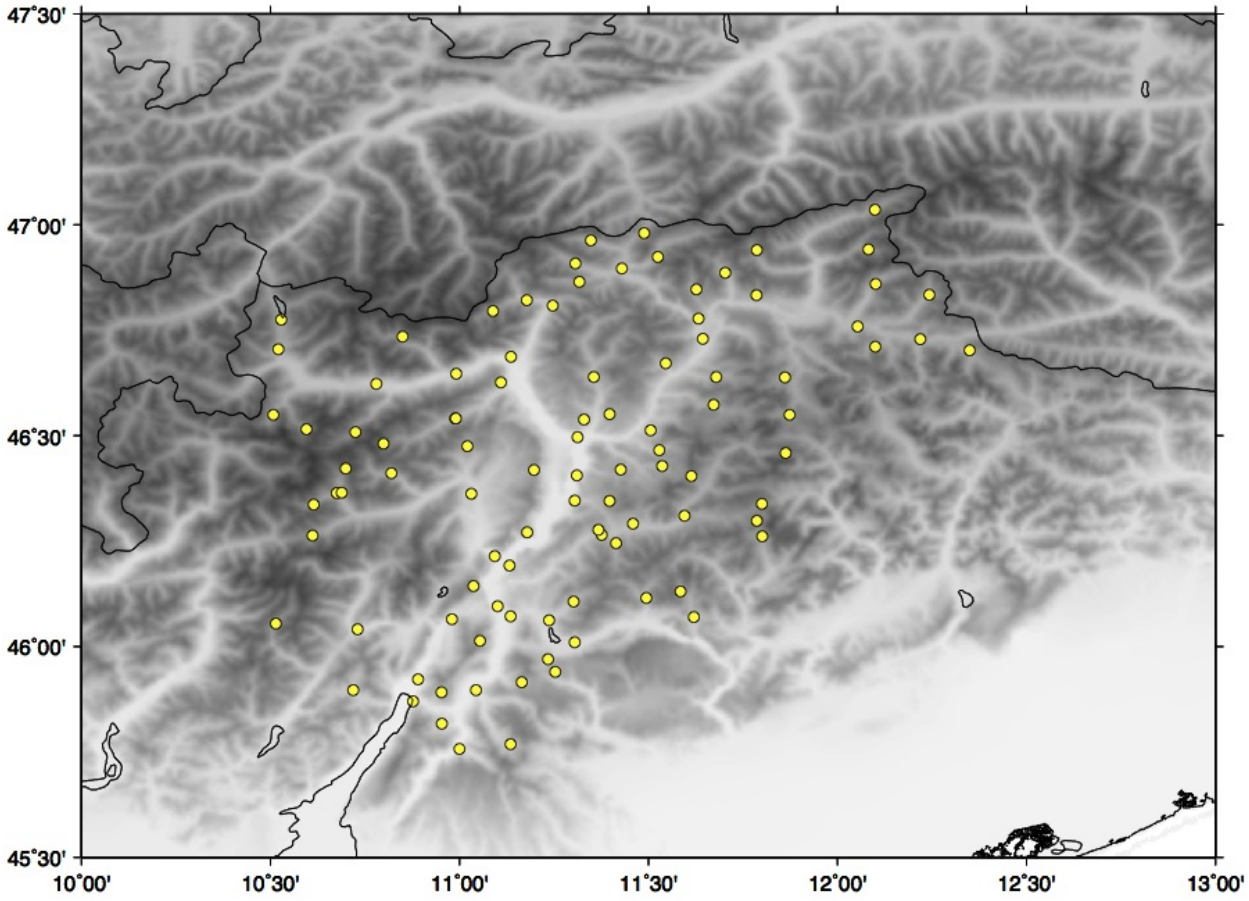

Figure 3.5. *Homogenized series.*

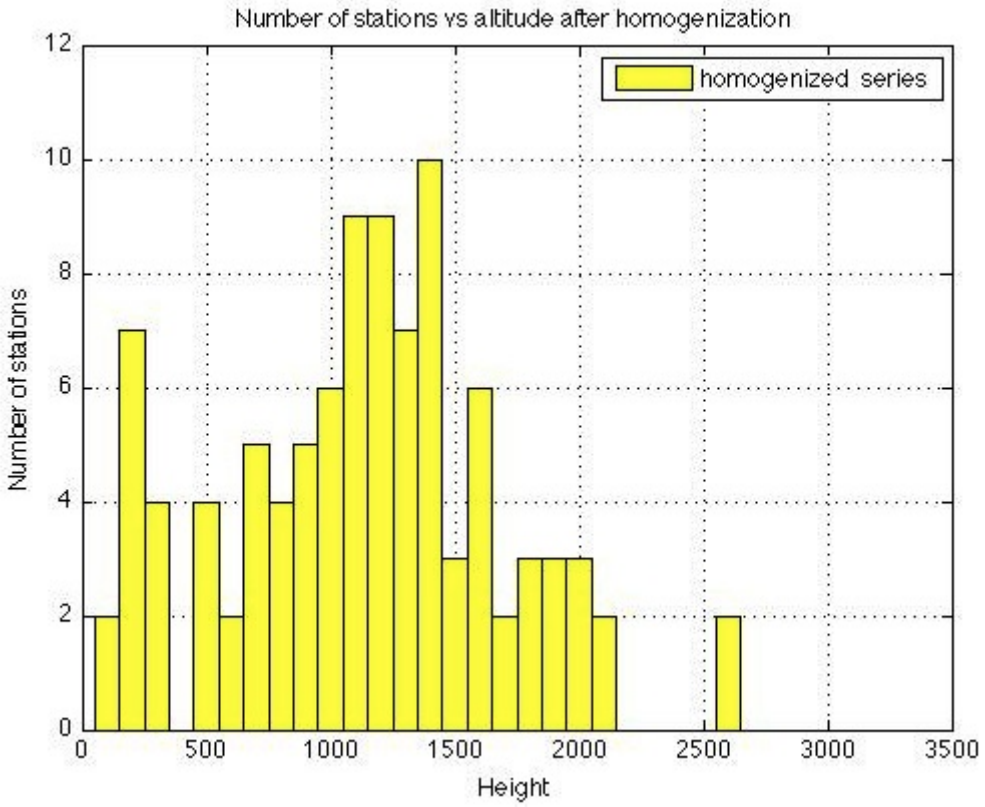

Figure 3.6. *Number of series for altitude bands after homogenization. Bin width is 100 m*

3.3 Series of the correction

In order to inspect the effects of the homogenization corrections on the sample, series of the mean corrections were created. In particular for each series i it was calculated the monthly correction series:

$$\mathrm{d}_{i,m} = \mathrm{T}^{hom}_{i,m} - \mathrm{T}^{ori}_{i,m} \tag{3.7}$$

where m runs along the months of the series, $\mathrm{T}^{hom}_{i,j}$ is the monthly mean temperature of the homogenized series and $\mathrm{T}^{ori}_{i,j}$ is the monthly mean temperature of the original series. After performing annual averages ($\mathrm{d}_{i,y}$), general mean series was created, calculating:

$$\mathrm{D}^{av}_{y} = \frac{1}{98}\sum_{i=1}^{98} \mathrm{d}_{i,y} \tag{3.8}$$

At the same times two series for maximum and minimum corrections were created:

$$\mathrm{D}^{max}_{y} = \mathrm{max}_i\{\mathrm{d}_{i,y}\} \tag{3.9}$$

$$\mathrm{D}^{min}_{y} = \mathrm{min}_i\{\mathrm{d}_{i,y}\} \tag{3.10}$$

Behaviour in time of these series may be observed in figures 3.7, where it is clear that correction made on minimum temperatures did not introduce a relevant trend (calculated with a linear regression). Instead for maximum temperatures a strong and significant negative trend is found (-0.24 ± 0.02 °C/dec), this means that original temperature have been increased in the early period by homogenization and that eventual warming trends obtained forward in the text would have been larger if the sample were not homogenized.

Considering the trend in the mean corrections and the range between maximum and minimum corrections, it is clear how homogenization is a necessary step before studying climatic changes or calculating trends.

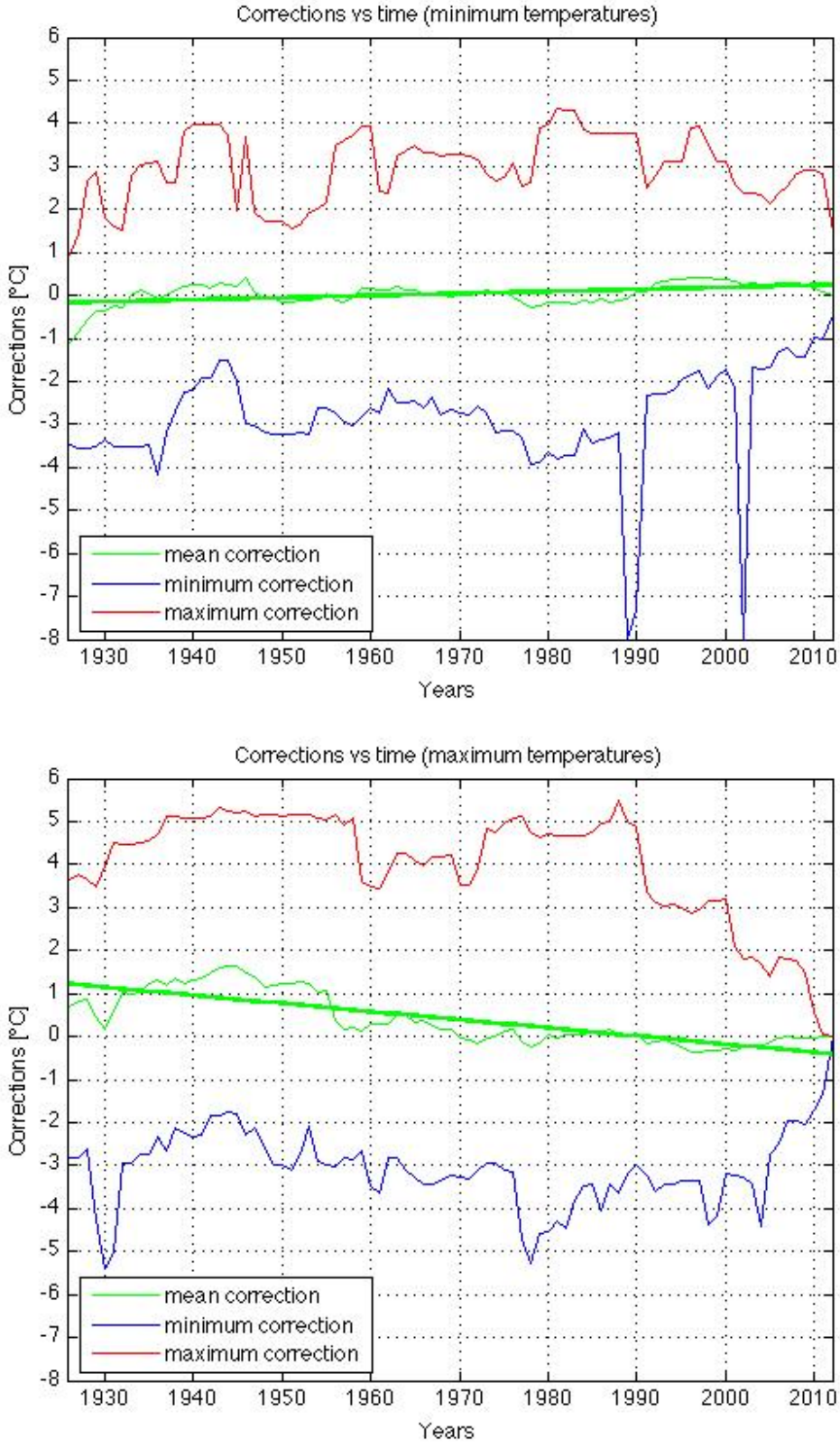

Figure 3.7. *Correction series for minimum (top) and maximum (bottom) temperatures. Red line stands for the maximum annual correction, blue line for the minimum annual correction. Green line represent the mean annual correction and green straight line is the calculated trend with a linear regression, whose confidence level (calculated with a Mann-Kendall test) has a p-value lower than 0.01.*

Chapter 4

Data analysis

Once homogenization was complete, obtained series underwent a gap filling of the monthly average series with the same process described in section 2.3.3, but considering as references the series themselves. After completing the series, a Principal Component Analysis (PCA) was performed on the mean temperature series (i.e. the average of maximum and minimum temperatures monthly series) to identify climatically homogeneous regions.

4.1 Principal Component Analysis

4.1.1 PC calculation and truncation

This is a technique aimed at simplify data reducing dimensionality without losing information on variability. This process consists in a linear transformation in which data-set is projected in a new cartesian system where the new variables (Principal Components, PC) are non-correlated one to the other and sorted by decreasing variability. This implies that the PC with the highest variance is linked to the first axis, the second higher to the second axis and so on.

It is worth recalling the definitions of covariance, variance and correlation of two series X_i and X_j:

$$\mathrm{cov}[X_i, X_j] = E[(X_i - E[X_i])(X_j - E[X_j])] \tag{4.1}$$

$$\mathrm{var}[X_i] = E[(X_i - E[X_i])]^2 \tag{4.2}$$

$$\mathrm{corr}[X_i, X_j] = \frac{\mathrm{cov}[X_i, X_j]}{\sqrt{\mathrm{var}[X_i]}\sqrt{\mathrm{var}[X_j]}} \tag{4.3}$$

Before operating on the sample it is useful to standardize the original data subtracting the mean and dividing by its standard deviation:

$$z_{i,j} = \left(\frac{x_{i,j} - \overline{x_j}}{\sigma_j} \right) \tag{4.4}$$

where $x_{i,j}$ is the i^{th} element of the series X_j.

This last calculation allows to have a system whose total variance is N, where N is the number of original series. Correlation matrix may be calculated as:

$$\mathrm{R} = \mathrm{Z}^T \cdot \mathrm{Z} \tag{4.5}$$

where Z is the matrix of the normalized series. This implies that the R matrix is written such that $\mathrm{R}_{i,j} = \mathrm{corr}[X_i, X_j]$. At this point first step of PCA may be done operating a linear diagonalization of the correlation matrix.

Diagonalization matrix (E) is composed by the normalized eigenvectors e_k (with k between 1 and N) of the correlation matrix and the diagonalized matrix (having the eigenvalues on the diagonal) is calculated as:

$$\Lambda = \mathrm{E}^T \cdot \mathrm{R} \cdot \mathrm{E} \tag{4.6}$$

The coefficients of the first PC, with respect to the original series, are given by the components of the eigenvector with highest eigenvalue; similarly the coefficients of second PC can be found in the components of eigenvector having second highest eigenvalue and so on for the other ones. The eigenvectors are also called Empirical Orthogonal Functions (EOF) and the PC corresponding to the k^{th} EOF is obtained writing:

$$\mathrm{PC}_k = \mathrm{Z} \cdot \mathrm{e}_k \tag{4.7}$$

Reduction of dimensionality in a Principal Components Problem is done choosing a limited number of PCs, the ones with highest eigenvalues, in order not to lose significant part of the variability.

In this work this process was effectuated on the 98 series obtained at the end of the homogenization process.

Truncation of the PCs at a certain number is not determined by objective criteria [Wilks, 2011] and this choice was made selecting the first two components, since the first one represented over 97 units (out of 98) of the entire system variance, while the second PC represented more than a half of the variance of a single station.

In figure 4.1 one may see (in a semilogarithmic scale) the eigenvalues sorted by decreasing order. Here it is clear that almost all the variance in represented by the first PC, this is probably due to the reduced geographical dimensions of the sample and the high spatial coherence of the variable. Nevertheless, as already said, the second PC represents more than half of the variance of a single station; so it was chosen to keep the first two PCs in order to perform the regionalization of the sample.

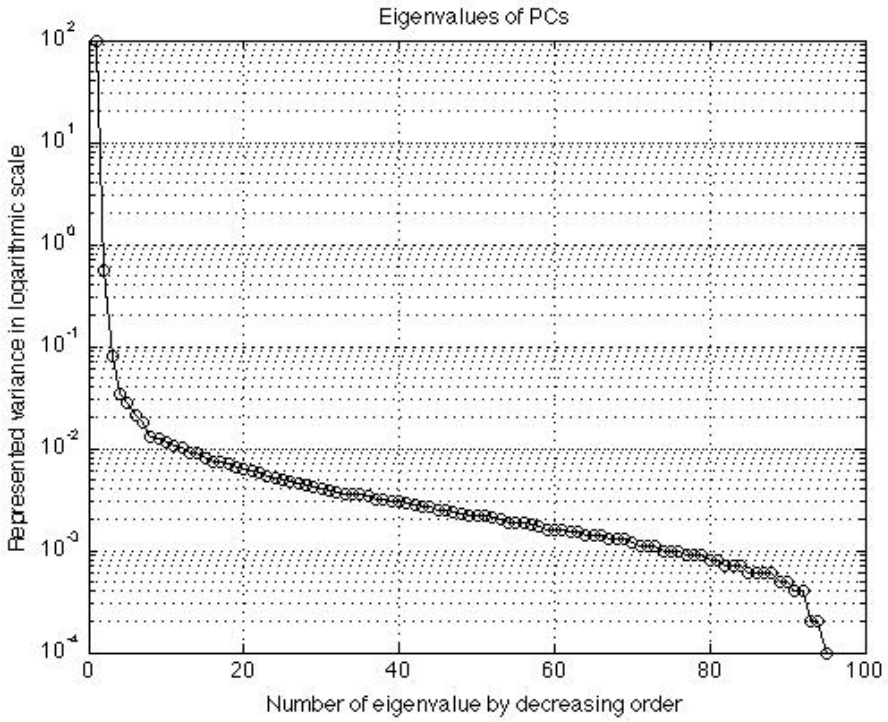

Figure 4.1. *Plot displaying eigenvalues of PC sorted by decreasing order (logarithmic scale).*

4.1.2 Rotation of the PCs and Regionalization

The so-selected eigenvectors (each one linked to a PC) then underwent a rotation:

$$E^{Rot} = E \cdot T \tag{4.8}$$

where E is indeed the eigenvectors matrix and T is an orthonormal rotation matrix whose elements represent the directional cosines. The elements of each column of E and E^{Rot} are called "loadings". The loadings describe the coefficients used to multiply the original series matrix when calculating the PC (as displayed in equation 4.7).

Rotation of axis is aimed at finding a coordinate system where, for each EOF, few loadings have high values and the other ones are approximately zero. This implies that after a rotation the sum of the loading variances must be the highest, for this reason this process is called VARIMAX. After this process each old variable is represented by only one of the new EOFs. Such a method allows to identify sub-areas of the sample stations having similar behaviour, each one describing different features of the system variability.

In this work rotation was made on the first two PCs. It permitted to identify two regions or, better, two altitudinal bands: first one for low elevations and second one for high elevations with separation at about 1200 m o.s.l.. In fact in figure 4.2 it is clear how regionalization didn't determine separate regions on the horizontal plain.

It was though noticed that loadings had a recognizable behaviour when analyzed with respect to the vertical coordinate. In figure 4.3 one can see how each loading relates with elevation. Here it was possible, thanks to a linear fit, to determine the changing point between the two regions. This critical altitude was found to be 1205 m above mean sea level.

Thanks to rotation of the axis and regionalization the sample was then divided into two sub-set:

- LOW: group of the 53 stations with elevation lower than 1205 m and high loading for the EOF 1 (figure 4.3). These stations are mainly located in the valleys and in great part of the urban settlements.
- HIGH: group of the 45 stations with altitude higher than 1205 m and high loadings in the EOF 2 (figure 4.3). These stations are distributed in particular on the mountains that surround the valleys.

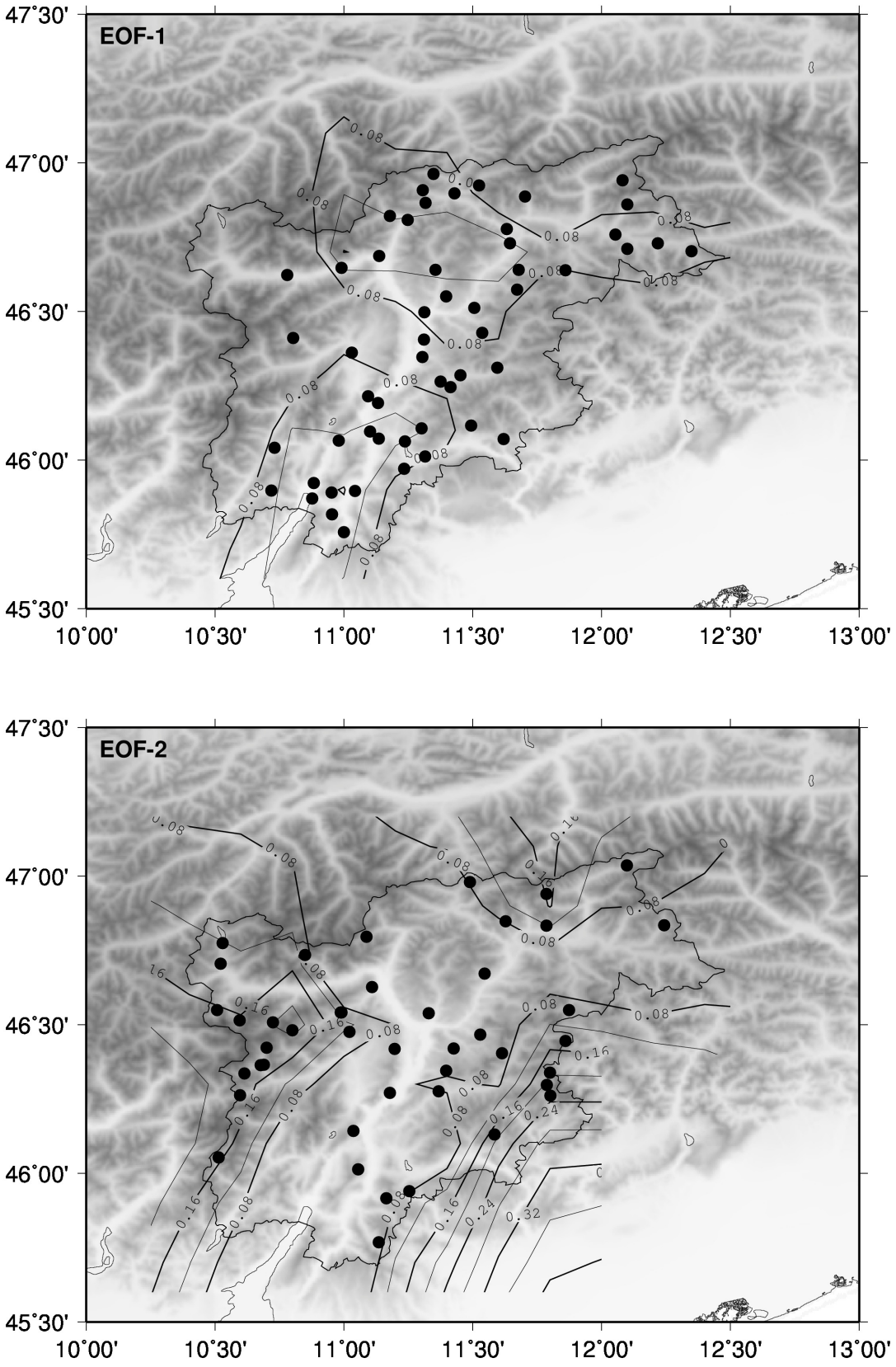

Figure 4.2. *Results of regionalization on the horizontal view. EOF1 stations (top) and EOF2 station (bottom) with isolines of corresponding loadings.*

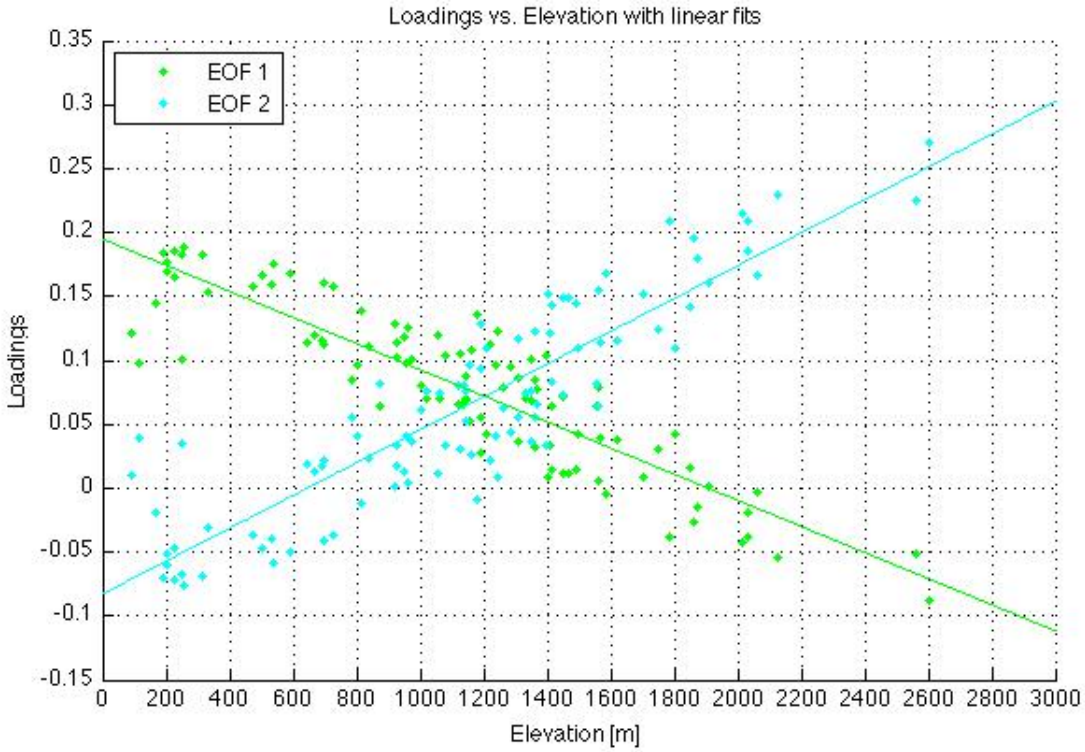

Figure 4.3. *Scatter plot displaying relationships between the rotated EOFs and elevation of the stations. The two solid lines represent linear fits operated with the least square method. Green line is linked to the EOF with high values for lower stations, cyan line is linked to the EOF with high values for higher stations.*

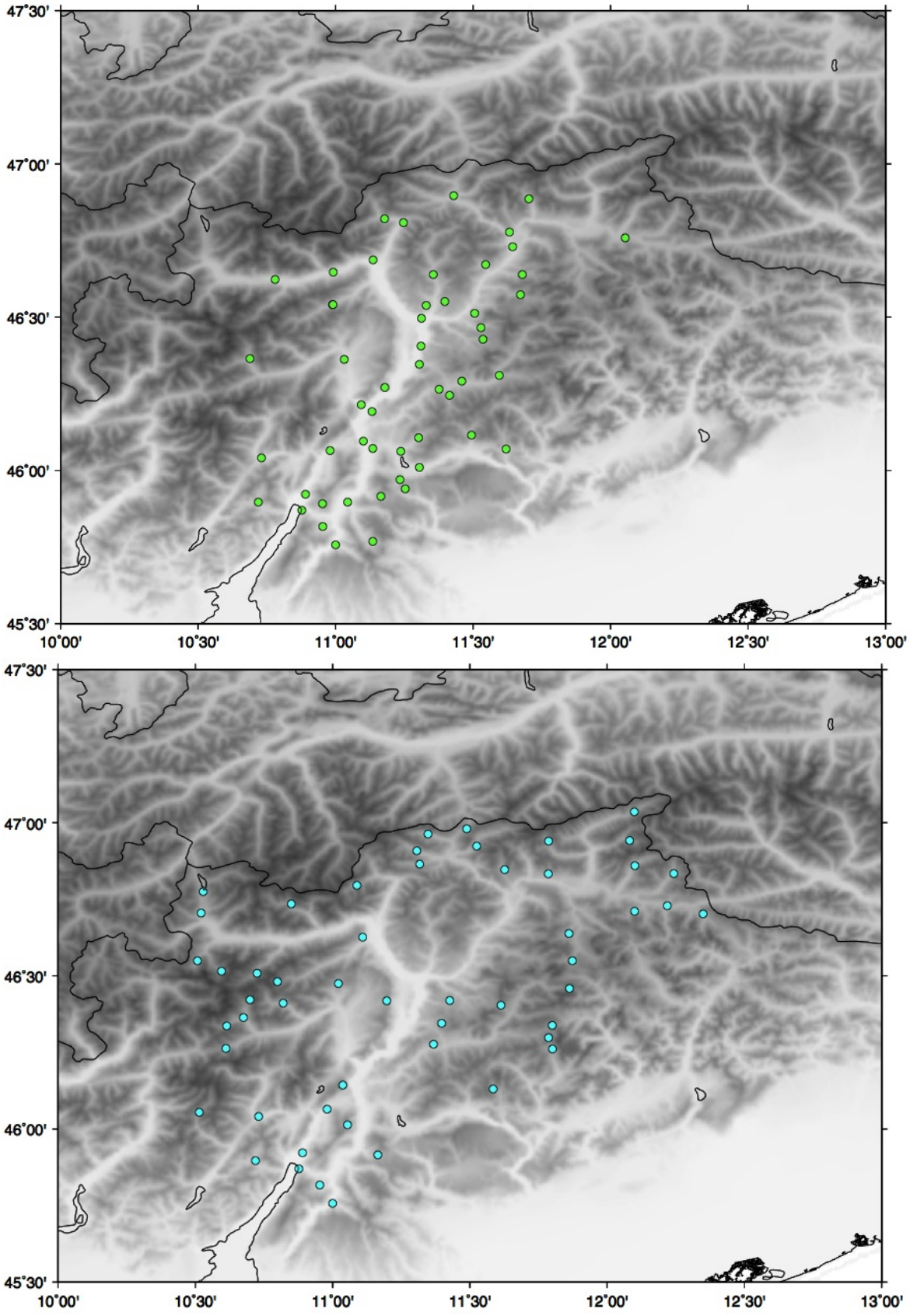

Figure 4.4. *Maps of stations for LOW sub-set (top) and HIGH sub-set (bottom), determined by the linear fit displayed in figure 4.3*

4.2 Series interpolation on a grid

Series that were selected after the homogenization process didn't show to be equally distributed on the Trentino Alto Adige territory. For this reason it was possible that the regional mean series, calculated with simple arithmetic averages of the available data, were affected by the concentration in limited areas of higher quantity of stations than in other parts of the region.

This problem was tackled calculating mean monthly series on a set of grid points having 0.25 degree resolution. Interpolation was realized calculating weighted averages, where weights are based on a radial and an angular term.

The radial weight was calculated as follows:

$$\mathrm{w}_i^{rad}(x,y) = \mathrm{e}^{-\frac{\mathrm{d}_i^2(x,y)}{\mathrm{c}_r}} \tag{4.9}$$

Where

$$\mathrm{c}_r = -\frac{\left(\frac{\overline{\mathrm{d}}}{2}\right)^2}{\ln 0.5} \tag{4.10}$$

Where index "i" identifies each station, $\mathrm{d}_i(x,y)$ is the distance of the i^{th} station from the grid point (x,y) and $\overline{\mathrm{d}}$ is defined as the mean distance between two grid points whose difference in both longitude and latitude is of one grid step. In this case the $\overline{\mathrm{d}}$ value is about 32 km.

The angular terms, considered in order to avoid areas with high station density to influence too much values in a grid point, were calculated performing:

$$\mathrm{w}_i^{ang}(x,y) = 1 + \frac{\sum_{l=1}^{n} \mathrm{w}_l^{rad}(x,y)[1-\cos\theta_{(x,y)}(i,l)]}{\sum_{l=1}^{n} \mathrm{w}_l^{rad}(x,y)} \tag{4.11}$$

where $\theta_{(x,y)}(i,l)$ is the angular separation of the i and l station with the angle vertex centered on the grid point (x,y).

Values on a grid point in a certain month were calculated if at least one of the following conditions was satisfied:

- at least one series was found with radial distance less than $\overline{\mathrm{d}}$;
- at least two series were found with radial distance less than $2\overline{\mathrm{d}}$.

Keeping in mind these criteria it was possible to calculate monthly series for high and low altitudinal bands, both for maximum and minimum temperatures (4 series per grid-box indicated in figure 4.5). Some of the obtained series, unfortunately did not have data for the whole 1920-2014 sample period, but the longest common period was restricted to 1956-2013.

These series underwent then an averaging process creating seasonal mean series and were written in a format having on each row:

- year;
- the 4 seasonal averages: winter, spring, summer, autumn;
- meteorological year average.

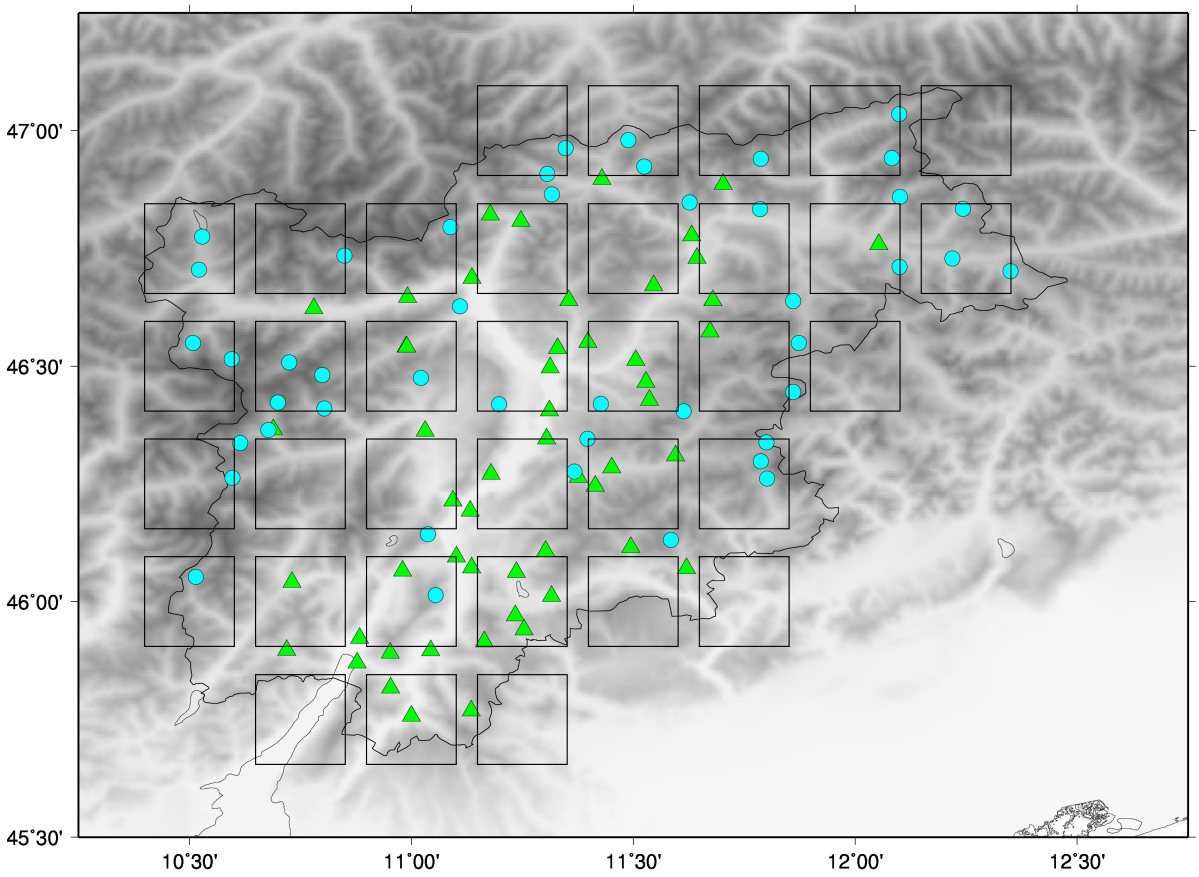

Figure 4.5. *Map of the generated grid boxes. Green triangles represent LOW stations, cyan circles represent HIGH stations.*

4.3 Trends on the grid-points

Seasonal series then underwent a trend analysis, performing a linear regression. In this process it was also calculated the root mean square error and the significance of the regression with a Mann Kendal test, expressed through the p-value . When possible trends were calculated over the entire length of the sample (1926-2013, first and last complete year) and over some sub-periods. In the case of grid-point series trends were calculated for 1956-2013.

The maps of figure 4.6 and 4.7 show the calculated trends for each grid-point, for HIGH and LOW bands and for minimum and maximum temperatures. Each trend is represented by a square whose color belongs to the trend values and whose size depends on the significance of the calculated trend:

- large square: $p<0.01$;
- medium square: $p<0.10$;
- small square: $p>0.10$.

These maps allowed to find a homogeneous significant positive trend in all grid points for the annual series ranging between 0.15 and 0.25 °C/dec for minimum temperatures and between 0.25 and 0.35 °C/dec for maximum temperatures.

Trends of winter series have low significance for minimum temperatures (especially for HIGH series) with the exception of LOW series corresponding approximately to mid Adige Valley (Bolzano area) and Non Valley (Cles area). Maximum temperatures show stronger trends with medium significance. In both cases trends are slightly higher (but coherent with the other ones) on the northern part of the examined region. In particular LOW series show steeper increase on the north-east and HIGH series on the north-west, up to 0.35 °C/dec in the Passeier Valley.

Spring series are interested by high and significant trends in all cases. In minimum temperatures it is to be noticed the weakly higher trends on the north-west. Maximum temperature present evidently higher trend, especially for LOW series. The increase of LOW maximum series appears to involve the northern part of the region, up to 0.55 °C/dec. HIGH maximum temperatures instead show a more homogeneous distribution.

The stronger increase of temperature may be observed for summer series at both altitudinal bands and, in particular, for maximum temperatures, where the trend ranges between 0.45 and 0.55 °C/dec.

Autumn series are those with the less significance trends. Minimum temperatures show only weak positive trends in the eastern part of the region for HIGH series and in the northern for LOW series (coherent with non-significant trends of the other grid points). Maximum temperatures are even less significant but present a mid-high significance in 4 grid-points in the north-west of the region (Venosta Valley) for the LOW series, whose trends lay in the 95% confidence interval of the other grid-points' trends.

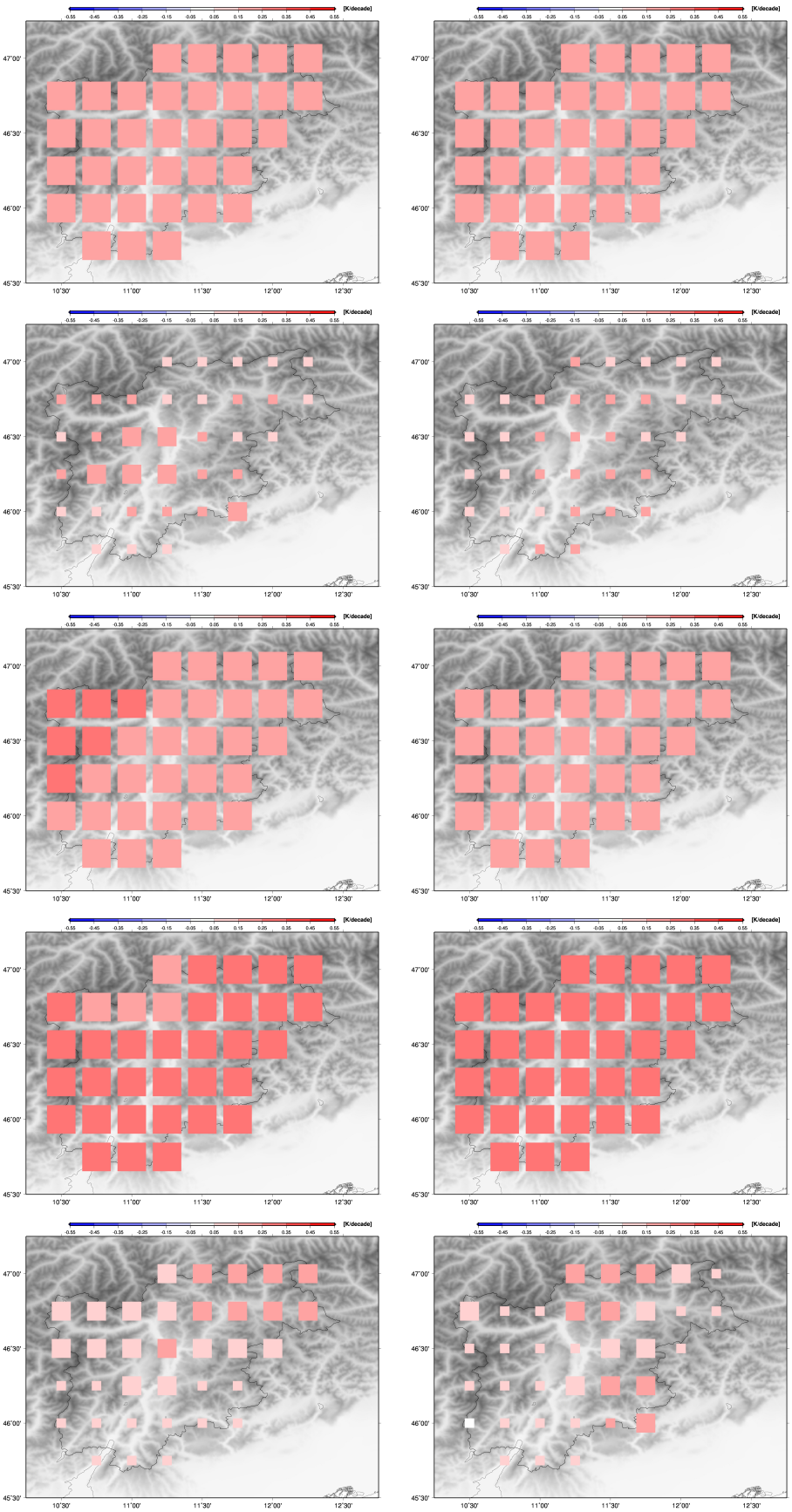

Figure 4.6. *Trends of minimum temperatures. or each grid point. Left column stands for LOW series and right one for HIGH series. Rows stand for: Year, Winter, Spring, Summer, Autumn. Dimensions of the squares represent significance with the same critical values as above.*

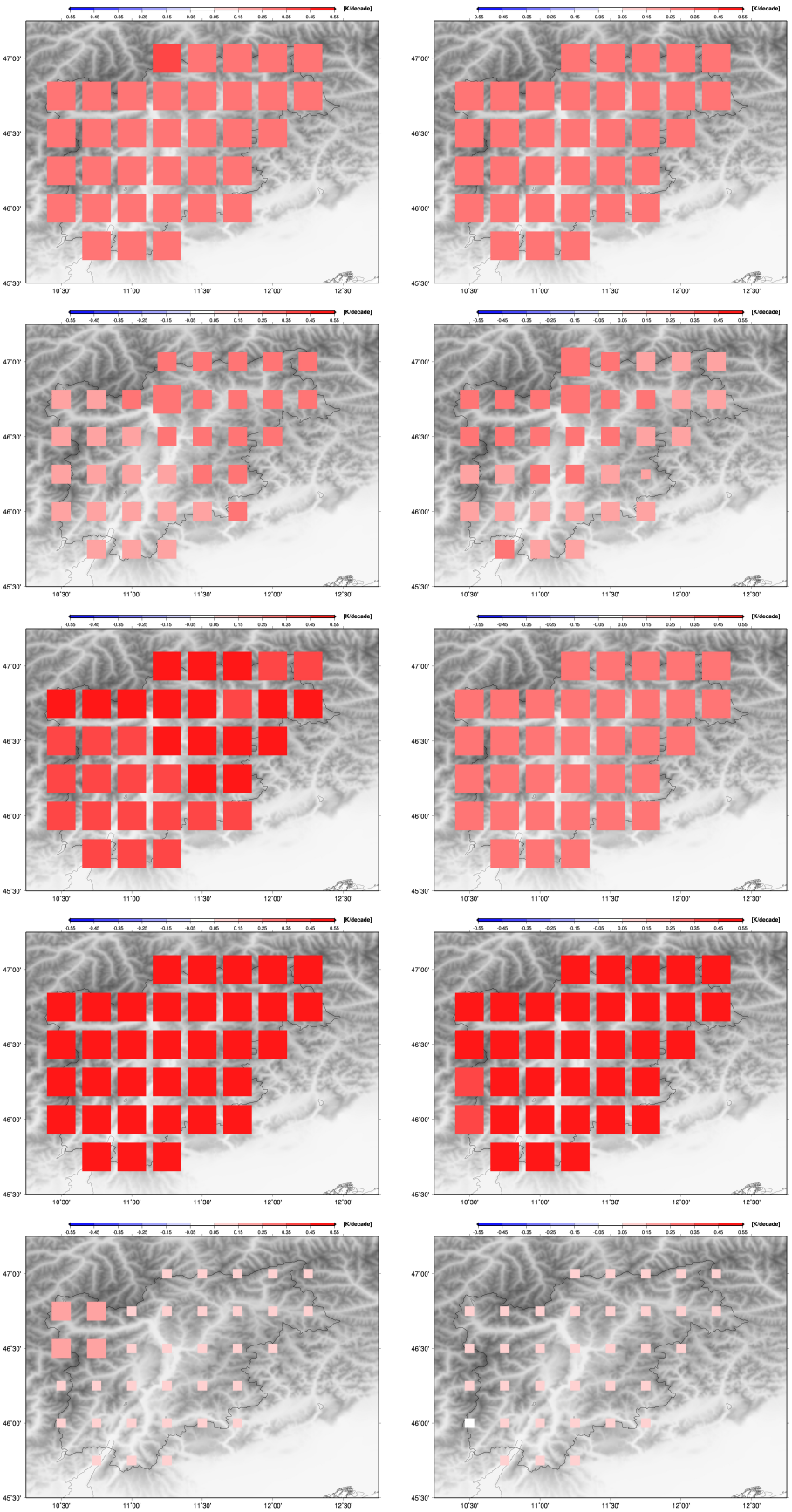

Figure 4.7. *Same of figure 4.6 but for maximum temperatures.*

4.4 Trends in regional seasonal series

As displayed above, trends of temperatures over the analyzed region are homogenous with negligible differences. For this reason it was possible to represent temperature behaviour considering one single mean regional series obtained as arithmetic averages of the gridded series (when available), obtaining 4 series: 2 series for LOW sub-set (maximum and minimum temperatures) and 2 series for HIGH sub-set (maximum and minimum temperatures).

The calculated trends on the seasonal grid-average HIGH and LOW series may be observed in table 4.1 and are displayed in the plots of figures 4.8, 4.9, 4.10 and 4.11. In these graphics annual and seasonal series are shown together with their estimated trends (straight lines). Thickness and type of the trend lines belongs to their significance calculated with the Mann Kendall test:

- Thick and solid line: p<0.01;
- Thick and dashed line: p<0.10;
- Thin and dashed line: p>0,10.

	Year		Winter		Spring		Summer		Autumn	
	Min [°C/dec]	Max [°C/dec]	Min [°C/dec]	Max [°C/dec]	Min [°C/dec]	Max [°C/dec]	Min [°C/dec]	Max [°C/dec]	Min [°C/dec]	Max [°C/dec]
LOW	**0.07±0.02**	**0.13±0.03**	+	0.15±0.05	0.07±0.04	**0.22±0.05**	**0.12±0.03**	**0.17±0.05**	-	+
HIGH	**0.07±0.02**	**0.11±0.03**	+	+	0.09±0.04	**0.20±0.05**	**0.10±0.03**	**0.15±0.04**	-	-

Table 4.1. *Calculated trends over the 1926-2013 period for LOW and HIGH seasonal series. Bold indicates p<0.01, normal font indicates confidence level with p<0.10. When significance had p>0.10 only the trend sign has been written.*

Here one can see a clear trend to warming temperatures for both regions in the annual series, especially for maximum temperature and in particular for lower elevations.

Seasonal data show significant trends mainly for warm seasons. In particular all trend for Summer have p<0.01 and values above 0.1 °C/dec. Spring presents lower tendencies for minimum temperatures and very high trends for maximum temperature (with high significance), up to 0.22 °C/dec, as found for grid-point series. It is to be noticed that larger trends for minimum temperatures are recorded in Summer, while steeper trends for maximum temperatures are obtained over Spring.

Colder seasons instead show non-significant trends for nearly all series. Autumn in particular wasn't found to have any significant trends and in 3 cases (out of 4) the trend sign is negative. Winter instead shows positive trends in all cases (significant only for maximum LOW series).

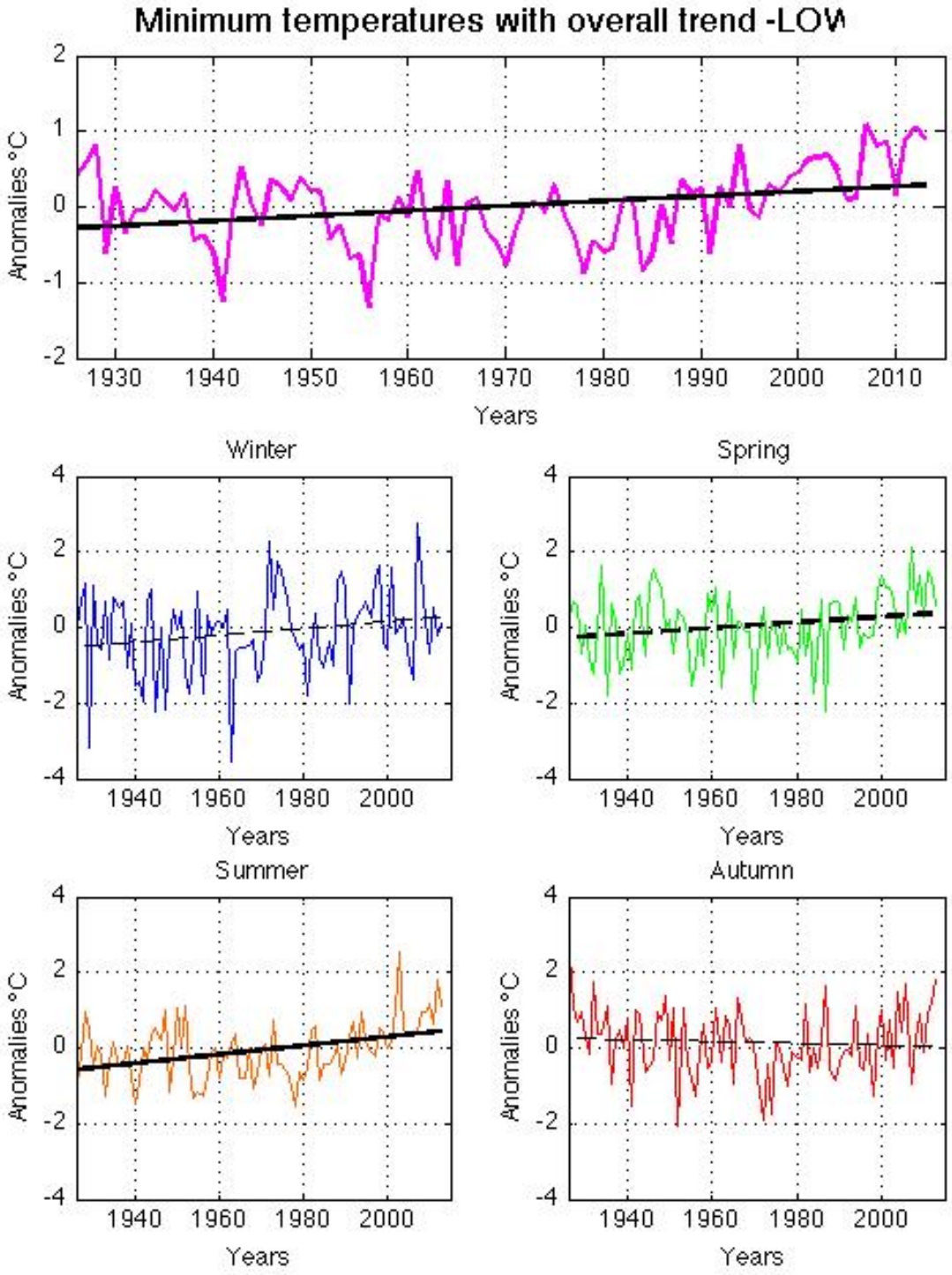

Figure 4.8. *Minimum grid-average seasonal series for LOW sub-sample with estimated trends(straight lines). Plots represent: annual series and trends (magenta, top), winter series and trends (blue, center-left), spring series and trend (green, center-right), summer series and trends (orange, bottom-left), autumn series and trends (red, bottom-right). For a better visualization trends are displayed with black lines. As explained in the text thickness and type of the trend line depends on its confidence level.*

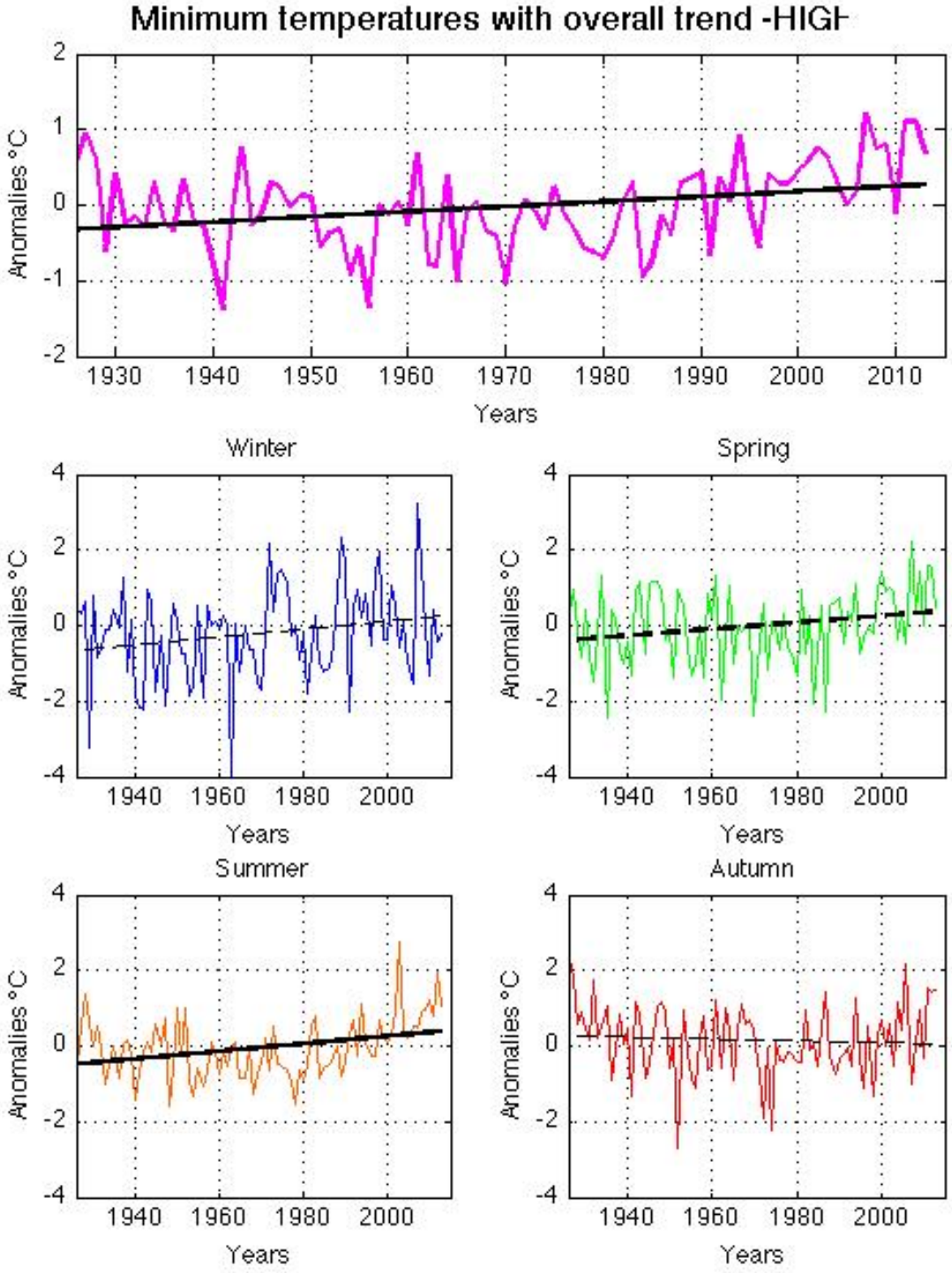

Figure 4.9. *Same as figure 4.8 but for minimum grid-average seasonal series of HIGH sub-sample.*

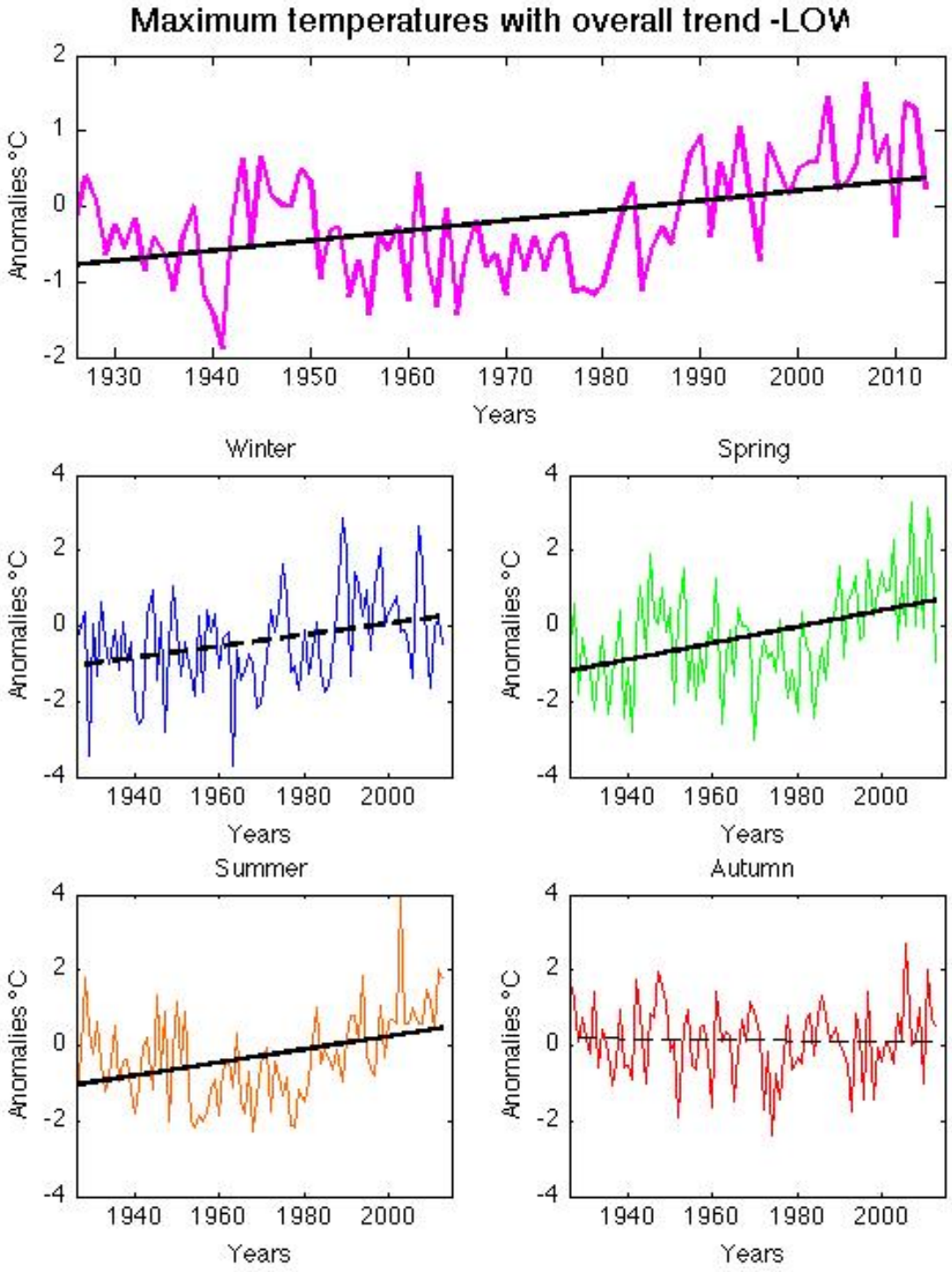

Figure 4.10. *Same as figure 4.8 but for maximum grid-average seasonal series of LOW sub-sample.*

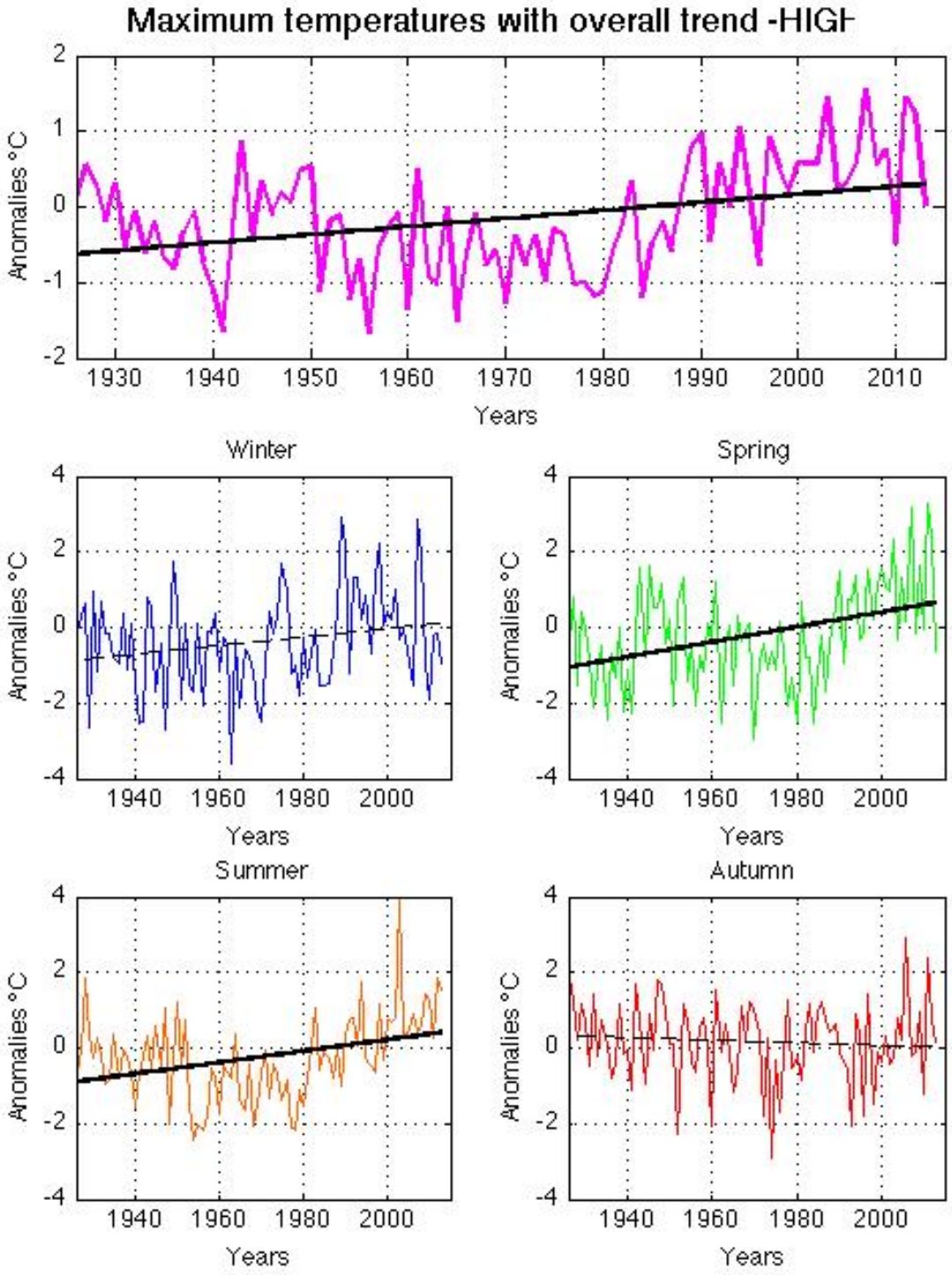

Figure 4.11. *Same as figure 4.8 but for maximum grid-average seasonal series of HIGH sub-sample.*

Looking at Summer and, in particular, Spring plots in figures 4.10 and 4.11 it can be clearly noticed that temperature series may not have constant trends during the considered time range. For instance period from 1950's to 1970's decades appears to have lower temperatures and looks like it is interested by a weak cooling trend (especially for maximum temperatures). This suggested to split the period in three parts:

- 1926-1950: expected to have a slight warming trend with possible cooling trends in minimum temperatures;
- 1951-1979: expected to present a weak cooling trend with possible warming trends in minimum temperature;
- 1980-2013: expected to be the period with the strongest warming trends.

First two periods have less than 30 years of data, for these reasons it is not expected to find significant trends, but generalized trends. Subdivision of the analyzed period was done keeping in mind also sub-periods utilized in works as Vose et al. [2005], Alexander et al. [2006], Toreti and Desiato [2008], Simolo et al. [2010] even if they considered different geographical scales.

MIN	Year			Winter			Spring			Summer			Autumn		
	1926-1950	1951-1979	1980-2013	1926-1950	1951-1979	1980-2013	1926-1950	1951-1979	1980-2013	1926-1950	1951-1979	1980-2013	1926-1950	1951-1979	1980-2013
LOW	-	+	**0.39±0.06**	-	+	+	+	-	**0.51±0.14**	+	-	**0.50±0.10**	-	-	0.30±0.14
HIGH	-	+	**0.38±0.07**	-	+	+	+	-	**0.51+0.15**	-	-	**0.51±0.11**	-	-	0.30±0.14

Table 4.2. *Calculated trends for minimum grid-average series LOW and HIGH for each sub-period. Font code is the same as table 4.1. Values are still expressed in °C/dec.*

MAX	Year			Winter			Spring			Summer			Autumn		
	1926-1950	1951-1979	1980-2013	1926-1950	1951-1979	1980-2013	1926-1950	1951-1979	1980-2013	1926-1950	1951-1979	1980-2013	1926-1950	1951-1979	1980-2013
LOW	+	-	**0.42±0.10**	+	+	+	0.07±0.03	-	**0.78±0.20**	-	-	**0.62±0.16**	+	-	+
HIGH	+	-	**0.41±0.11**	-	+	+	+	-	**0.83±0.20**	-	-	**0.59±0.15**	-	-	+

Table 4.3. *Same as table 4.2 but for maximum temperatures.*

Annual series in figures 4.12 and 4.13 allow to observe the different behaviours of the three sub-periods. It is clear and unmistakable the warming trend since 1980 (with elevated significance) in both regions and both minimum and maximum temperatures.

Trends observed for the first two periods on annual series are always non-significant. But showing a decrease of minimum and an increase of maximum in the first sub-period (increasing daily temperature range, DTR) and an increase of minimum and decrease of maximum temperatures in the second period (decreasing DTR).

These weak trends may be better examined looking at trends in the seasonal series in figures 4.14 and 4.15 and tables 4.2 and 4.3. Here it is possible to see how all trend are non-significant except the positive trend obtained on the first period for LOW maximum temperatures in spring.

First period shows strong positive trends for Spring, especially for LOW maximum temperatures. At the same time trend for the other seasons are not homogenous.

Second period shows weak positive trends for minimum and maximum temperature in winter and negative trends in all the other cases. There are no cases of different seasonal sign of the trend between HIGH and LOW in any season. Positivity of winter trends dominates only in minimum series.

Last period instead shows warming trends for all the cases, but Winter appears to have less steep slopes (always non-significant). Autumn shows high-confidence-leveled warming trends only for minimum temperatures. Trends of Spring and Summer are significant for all cases and show even steeper trends (up to 0.83 °C/dec).

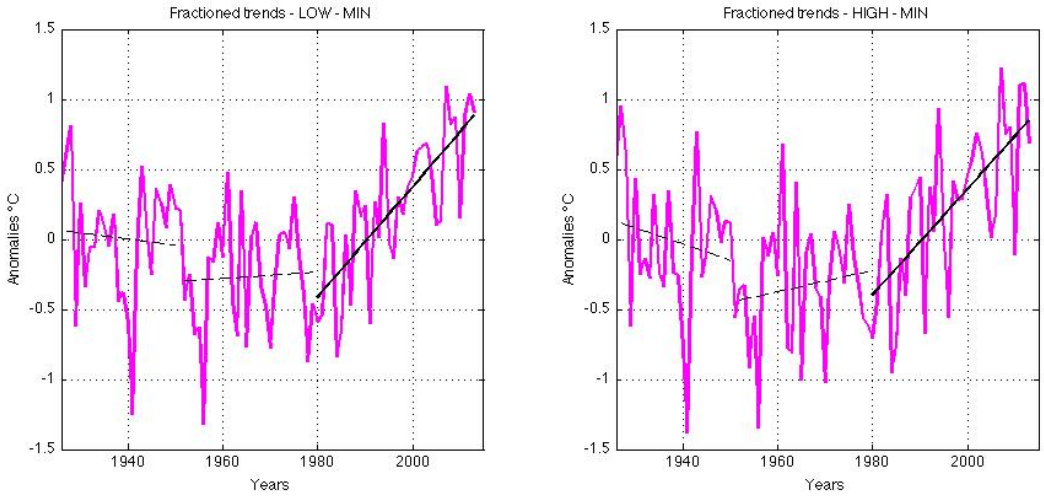

Figure 4.12. *Obtained trends over the three sub-periods for yearly minimum series. The two plots stand for LOW (left) and HIGH (right) series.*

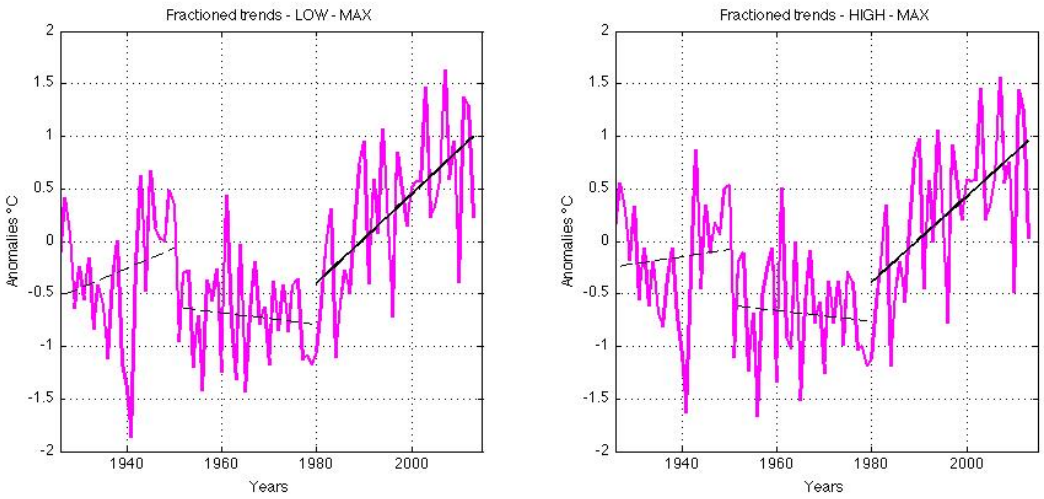

Figure 4.13. *Same as 4.12 but for maximum temperatures.*

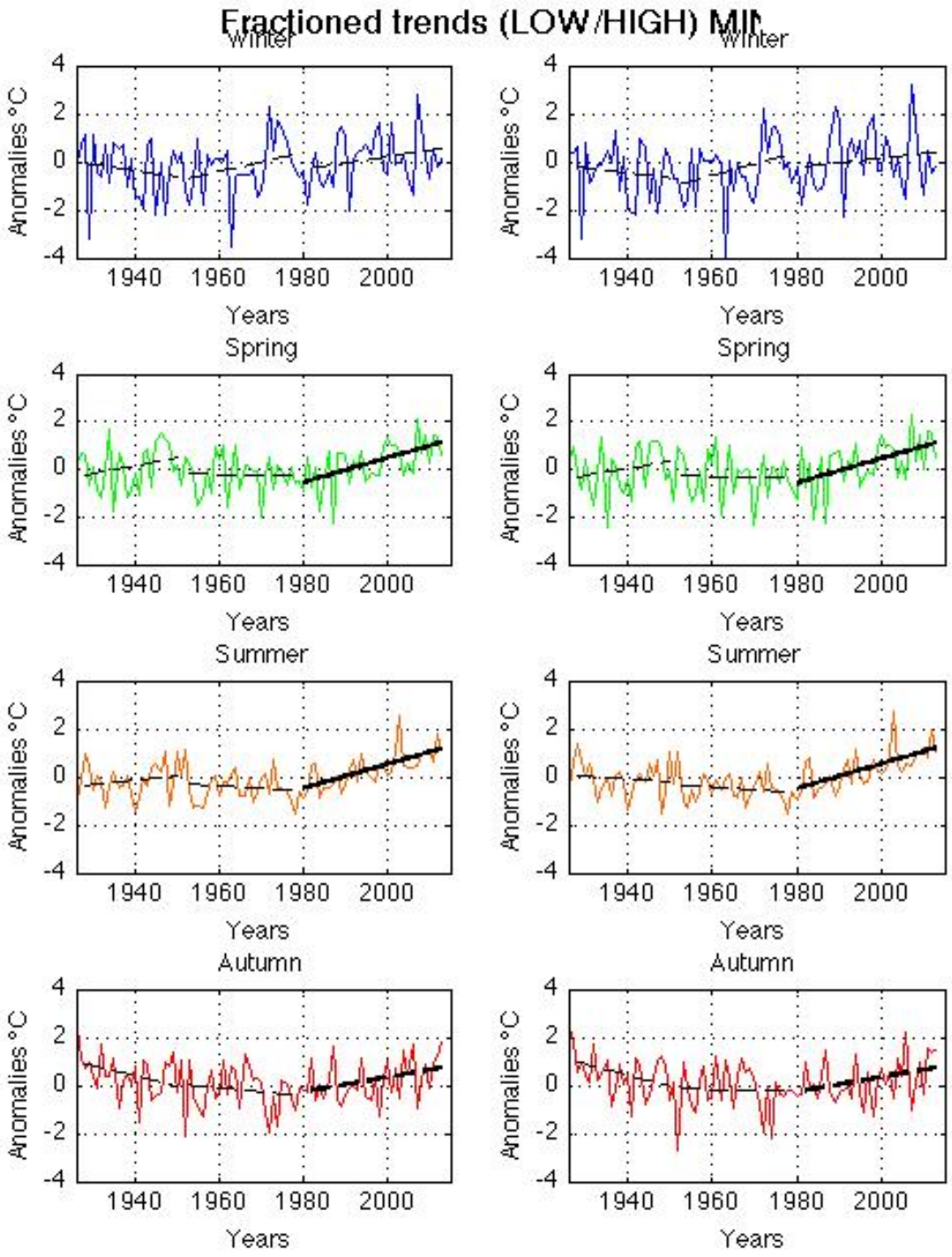

Figure 4.14. *Same as 4.12 but for seasonal series of minimum temperatures.*

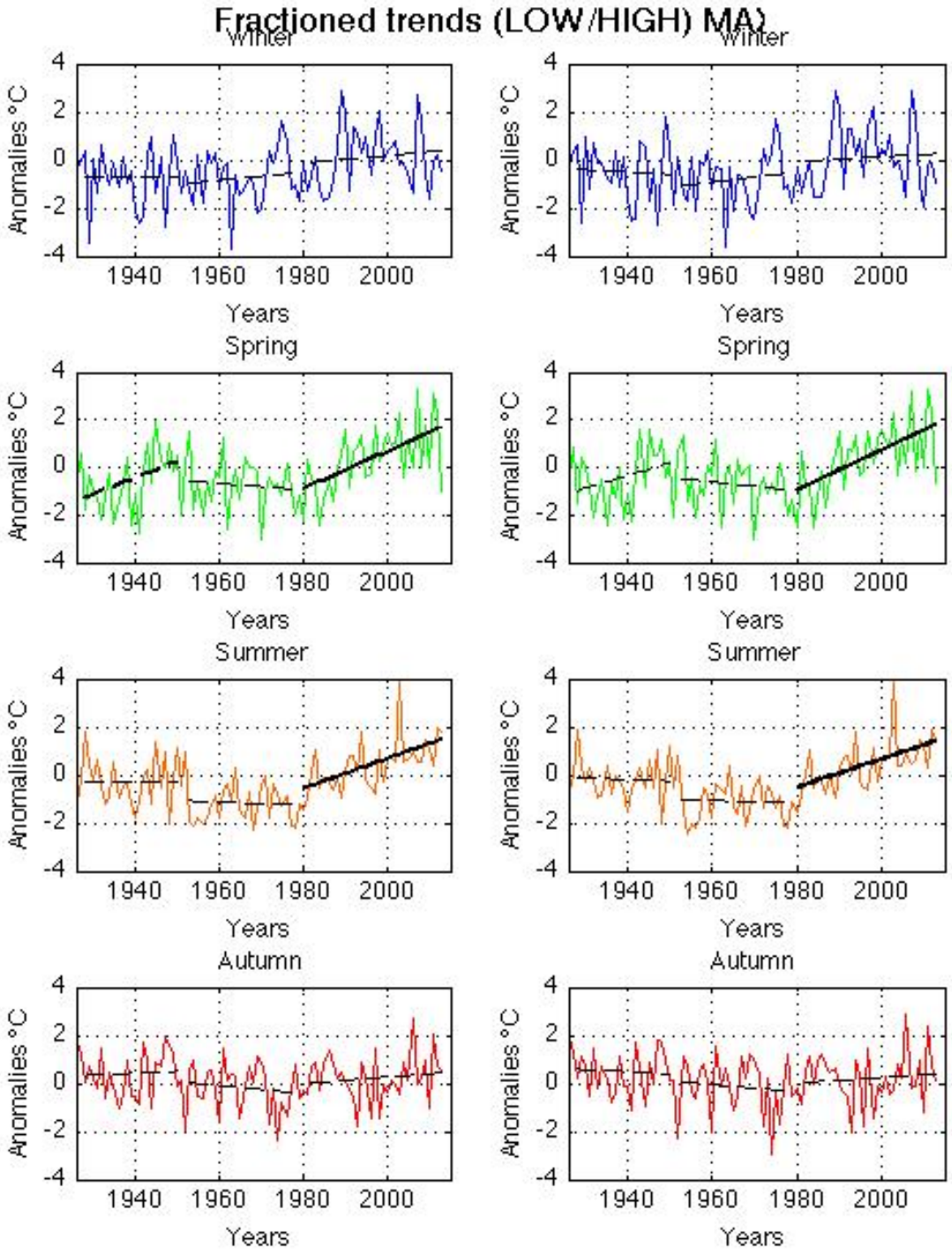

Figure 4.15. *Same as 4.14 but for maximum temperatures.*

4.5 Comparison with ISAC-CNR data set

Together with the already treated series, trend analyses were also made on seasonal series obtained performing gridding on the whole sample without separating it in two groups. These series were called "ALL" and their seasonal averages were calculated with the same criteria described above.

ALL series were compared with seasonal series coming from the ISAC-CNR database and consisting in the average of three seasonal series related to three grid points centered on the Trentino Alto Adige territory belonging to an Italian grid system (having grid step of 1° both in longitude and latitude) , presented in Brunetti et al. [2006]. Since no data for this Italian region are available before 1951, series on these grid points in the oldest period are calculated using data coming from near stations as Belluno, Padua, Mantua and Milan. For these reasons trends are calculated also on the 1951-2013 period.

Coordinates of these three points were:

- 12°E 47°N
- 12°E 46°N
- 11°E 46°N

Plots in figures 4.16 and 4.17 display relationships between the ISAC-CNR mean seasonal series and the ALL seasonal series. Corresponding trends are shown in table 4.4.

In the comparison between ISAC-CNR and ALL series it is clear that the two series are almost everywhere consistent one to the other especially for maximum temperatures. Minimum temperatures show more differences with steeper trends for ISAC-CNR series, especially in spring, that is the only case with relevant differences. This is due to the fact that minimum temperatures are more sensible to local features. By consequence, ISAC-CNR data-set before 1951 (calculated only with external station) may not nicely describe behavior of minimum temperatures over this one. For these reasons same comparison was made on the 1951-2013. Results are displayed in table 4.5 and figure 4.18. Here accordance between ALL and ISAC is more evident. In particular coherence between trends of minimum temperatures reflects what said above: availability of local series allows a better representation of minimum temperature features.

	Year		Winter		Spring		Summer		Autumn	
	Min [°C/dec]	Max [°C/dec]	Min [°C/dec]	Max [°C/dec]	Min [°C/dec]	Max [°C/dec]	Min [°C/dec]	Max [°C/dec]	Min [°C/dec]	Max [°C/dec]
ALL	**0.07±0.02**	**0.12±0.03**	+	0.12±0.05	0.08±0.04	**0.20±0.05**	**0.11±0.03**	**0.16±0.05**	-	+
ISAC-CNR	**0.13±0.02**	**0.14±0.03**	0.12±0.05	0.17±0.05	**0.20±0.04**	**0.21±0.05**	**0.17±0.03**	**0.17±0.05**	+	+

Table 4.4. *Calculated trends over the 1926-2013 period for ALL and ISAC-CNR grid-average seasonal series.*

1951-2013	Year		Winter		Spring		Summer		Autumn	
	Min [°C/dec]	Max [°C/dec]	Min [°C/dec]	Max [°C/dec]	Min [°C/dec]	Max [°C/dec]	Min [°C/dec]	Max [°C/dec]	Min [°C/dec]	Max [°C/dec]
ALL	**0.19±0.03**	**0.29±0.04**	+	0.25±0.08	**0.20±0.06**	**0.37±0.08**	**0.26±0.04**	**0.46±0.06**	0.14±0.06	+
ISAC-CNR	**0.20±0.03**	**0.27±0.04**	+	0.20±0.08	**0.25±0.06**	**0.33±0.08**	**0.35±0.04**	**0.46±0.06**	0.14±0.06	+

Table 4.5. *Calculated trends over the 1951-2013 period for ALL and ISAC-CNR grid-average seasonal series.*

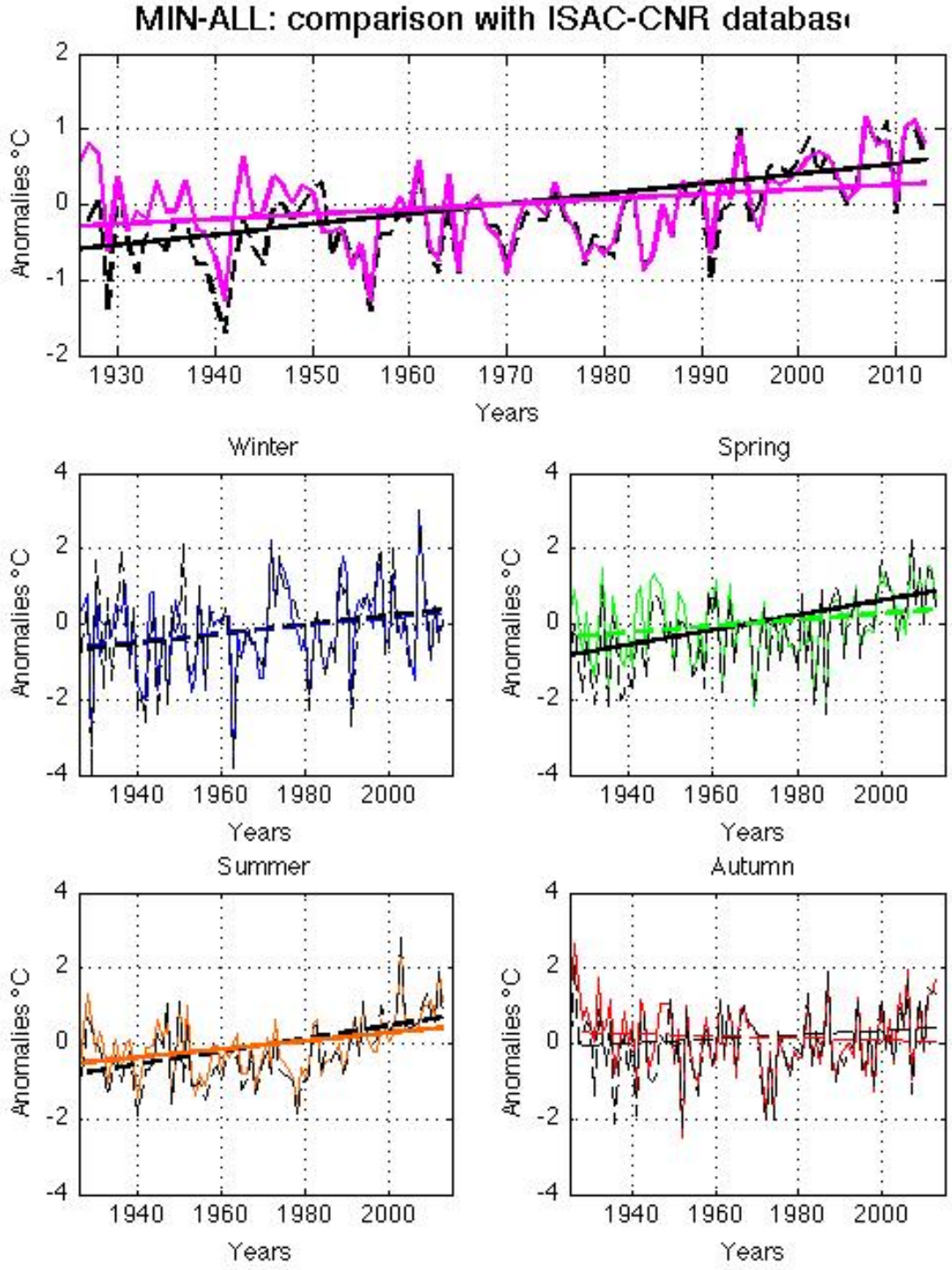

Figure 4.16. *Comparison of anomaly minimum temperatures and trends (straight lines) between seasonal series ALL and ISAC. Black lines stand for ISAC series, colored lines stand for ALL series.*

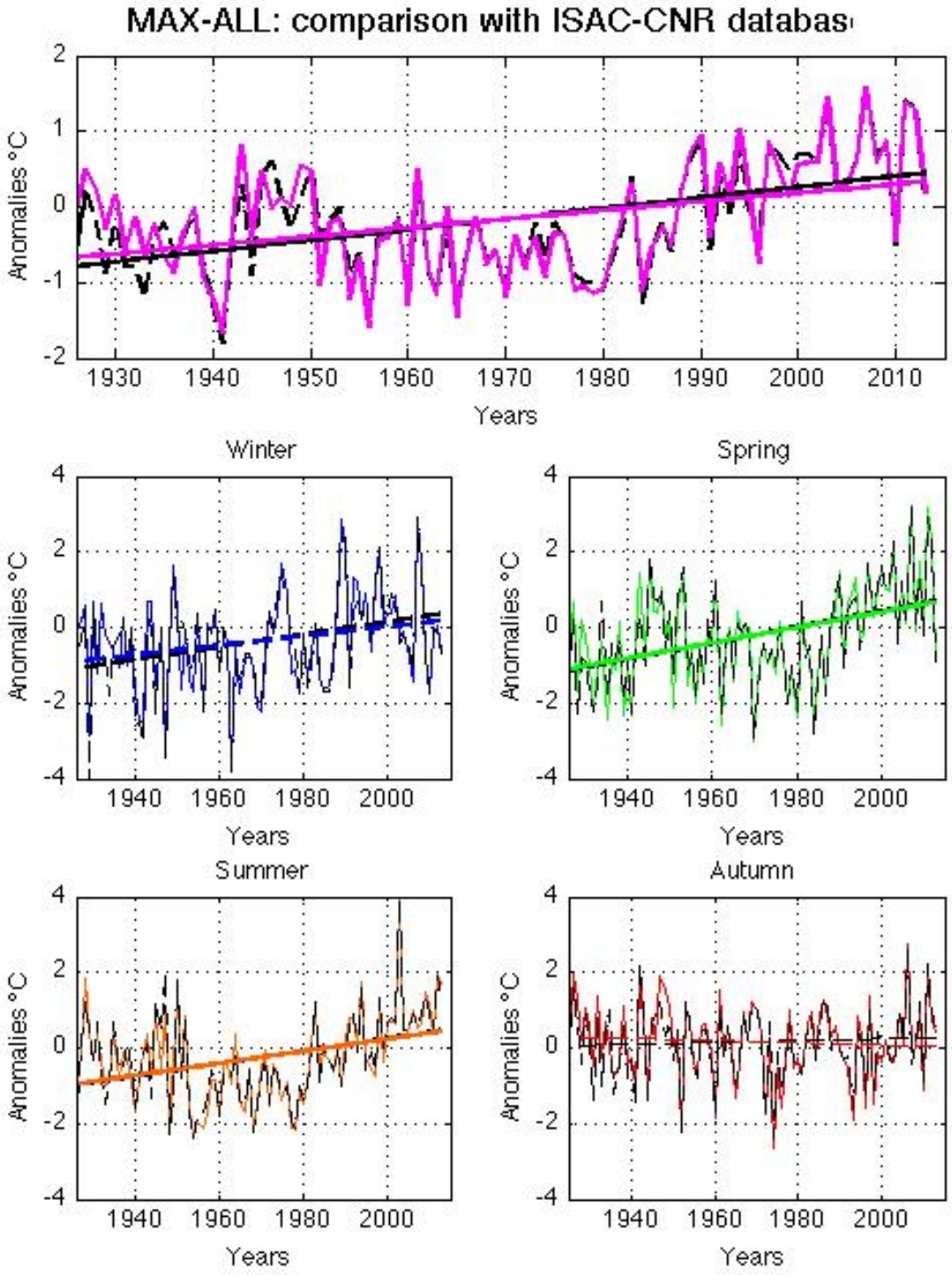

Figure 4.17. *Same as figure 4.16, but for maximum temperatures.*

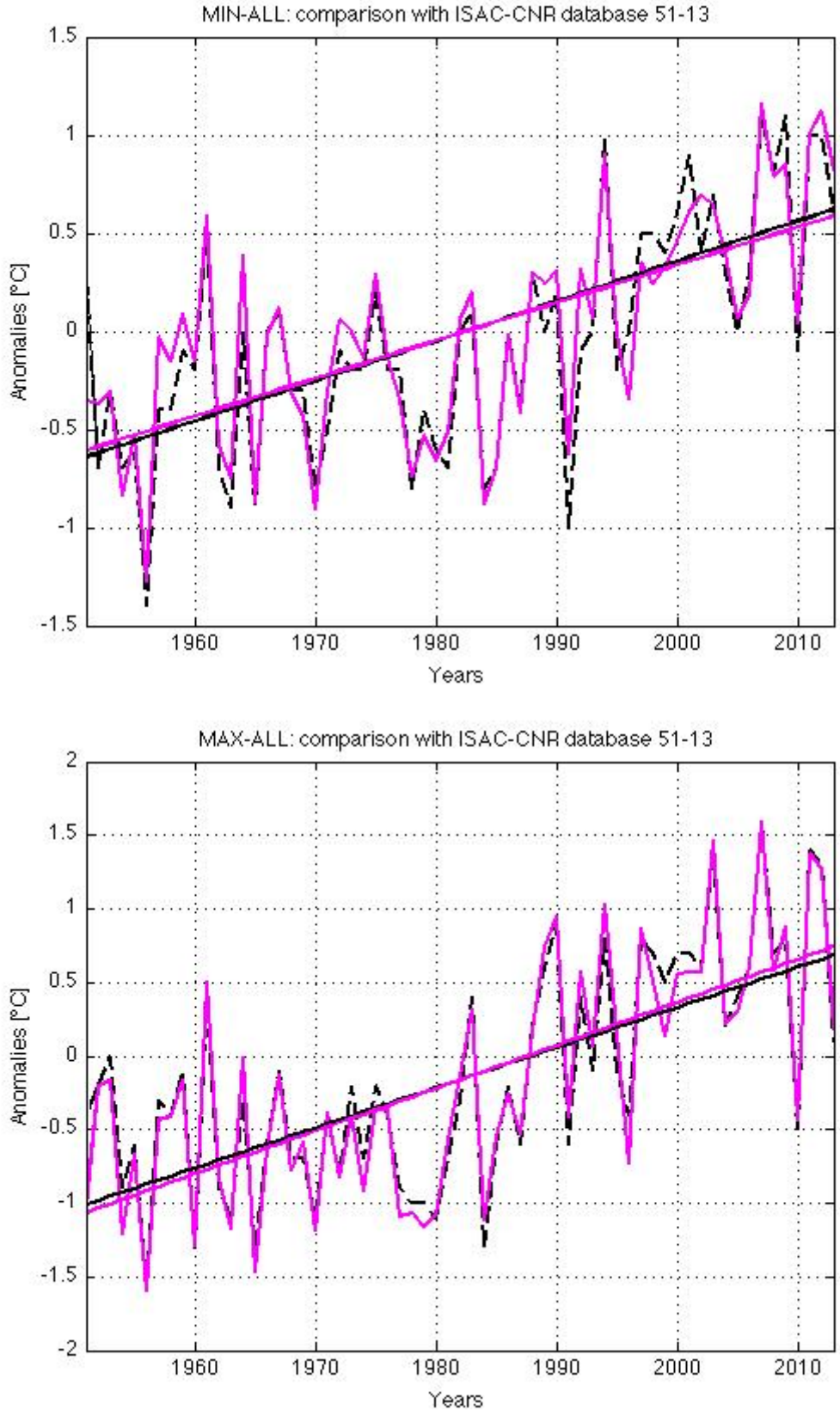

Figure 4.18. *Same as figure 4.16, but only for annual trend and for the 1951-2013 range.*

4.6 Exceedance probability trends

Aim of this work is to detect changes in the mean temperatures but also changes in the frequency of extreme temperature events and in the variability of the sample through the years. Effectively, analyzed seasonal series show a clear warming trend in their mean values. But changes in the variability or in the frequency of extreme events are better studied through the analyses of tails of the daily temperature distributions. For these reasons next step was to calculate the daily mean series for each regional subset. In fact daily series allow to preserve the features of the distribution tails, whose characteristics get lost during the averaging process performed to obtain seasonal and annual series. It was chosen to operate with regional mean series and not on single station series since temperature changes highlighted by trend analysis performed on gridded data-sets are spatially homogeneous and because of the greater robustness of the regional daily series.

The regional daily series were then calculated as arithmetic averages of all the available data for each day of the series.

Evidences of changes in extreme events were first searched in the number of days above and below some fixed thresholds, chosen to be 1st, 5th, 10th, 90th, 95th, 99th percentiles.

These thresholds were indeed different for each day of the year and were calculated considering moving windows of 31 days centered in the analyzed day. This means that for the calculation of thresholds related to a day "i", all data of every year ranging from day i-15 to day i+15 were collected and sorted by increasing order. In this list it was then possible to individuate the selected percentiles.

Next step was counting, for each season and each year, how many days stood below lowest thresholds or above their corresponding high thresholds. The so obtained seasonal and yearly series underwent a trend analysis on the entire period (1926-2013), whose results are displayed in table 4.6 and figures 4.19 and 4.20 (here only for annual series, seasonal series may be observed in appendix A).

Annual series show a clear increasing of warm extreme events. Daily minimum temperatures above high thresholds have increased with significant rates for both altitudinal bands with trends slightly larger for high elevations. At the same time maximum temperature show even steeper trends (nearly twice those observed for minimum temperatures) with similar values between LOW and HIGH. As expected, fluxes of events through low and complementary high threshold (1st vs 99th, 5th vs 95th and 10th vs 90th) are not symmetric, since temperature distributions take a nearly-gaussian shape (see figure 1.21). For these reasons trends of events below low thresholds appear to be almost all non-significant, with the exception for minimum LOW temperature trends, whose results (negative trends) confirm tendencies to warming climate.

Calculated seasonal trend show non-homogeneous attitudes.

Winter presents negative trends of exceedance probabilities in all cases for lowest threshold, with higher confidence-levels at low elevations. LOW sub-sample shows high differences between minimum (non-significant trends) and maximum temperatures, while HIGH sub-set presents coherent trends between them. It is to observe the very high values obtained for 99th percentile, whose exceedance probabilities for HIGH minimum series represents almost a half of the annual trend.

Also Spring shows exceedance probabilities decreasing for lowest thresholds (with significant values for minimum LOW temperatures). Observed trends for high thresholds present large values, consistent between HIGH and LOW, but with slightly higher trends for HIGH sub-set. As noticed for annual trends, calculated tendencies for maximum temperatures are prominently larger than ones for minimum temperatures, even more than double the amount in some cases.

Fluxes of events through warmer threshold reach their highest values in Summer, up to an increase of 1.75 days/dec for the 90th percentile of LOW maximum temperature (19 %, with respect to the value of the mean: 9 days). Minimum temperatures show a different behaviour for the two altitudinal regions, in fact increase of warm extreme events is more marked for LOW. At the same time trends observed for maximum temperatures show nearly same results for HIGH and LOW. Fluxes through low threshold have significant values only for minimum LOW sub-set with negative values. Nonetheless looking at maximum temperatures, even if non-significant, in 5 cases out of 6 it is observed an increase of events below colder thresholds.

The only season that seems to strongly disagree with annual trends is Autumn. This attitude was already observed when analyzing trends of the average temperatures (see table 4.1) and here it is confirmed since this season shows significant increase of exceedance probabilities both for colder and warmer thresholds, suggesting an increasing variability of the sample, especially for HIGH sub-sets.

		MIN	[day/dec]	MAX	[day/dec]
	percentiles	LOW	HIGH	LOW	HIGH
Year	1	-0.31±0.13	-	-	+
	5	**-1.00±0.37**	-	-	+
	10	**-1.39±0.55**	-	-	+
	90	+2.07±0.67	**+2.45±0.69**	**+4.77±0.76**	**+4.70±0.69**
	95	+1.36±0.47	**+1.58±0.45**	**+2.97±0.49**	**+2.94±0.43**
	99	+0.36±0.15	**+0.46±0.16**	**+0.91±0.18**	**+0.98±0.16**
Winter	1	-0.16±0.08	-	-0.07±0.06	-
	5	-0.55±0.23	-	**-0.48±0.21**	-
	10	-0.71±0.31	-	-0.66±0.29	-
	90	+	+0.64±0.24	**+0.90±0.32**	+0.63±0.30
	95	+	**+0.48±0.14**	+0.50±0.19	+
	99	+	**+0.21±0.06**	+0.19±0.06	**+0.18±0.07**
Spring	1	-0.10±0.05	-	-	-
	5	-0.28±0.18	-	-	-
	10	-0.41±0.26	-	-	+
	90	+0.71±0.27	**+0.81±0.28**	**+1.63±0.33**	**+1.69±0.31**
	95	**+0.50±0.17**	**+0.52±0.19**	**+0.93±0.24**	**+1.11±0.21**
	99	+0.13±0.06	+	**+0.27±0.08**	**+0.35±0.08**
Summer	1	-	+	+	+
	5	-0.36±0.17	-	+	+
	10	**-0.67±0.22**	-	-	+
	90	**+1.16±0.32**	+0.98±0.33	**+1.75±0.36**	**+1.74±0.30**
	95	**+0.74±0.23**	+0.50±0.23	**+1.14±0.24**	**+1.07±0.21**
	99	**+0.17±0.07**	**+0.06±0.08**	**+0.37±0.09**	**+0.28±0.08**
Autumn	1	+	+	+	+
	5	+0.18±0.19	+0.25±0.19	+0.27±0.18	**+0.43±0.19**
	10	+	+0.46±0.29	+0.50±0.28	**+0.75±0.27**
	90	-	+	+0.50±0.30	+0.60±0.27
	95	+	+	+0.39±0.20	+0.38±0.17
	99	+	+0.08±0.07	+	**0.13±0.07**

Table 4.6. *Calculated trends for number of days above and below the fixed thresholds. Font code is the same as table 4.1. Values are expressed in day/dec.*

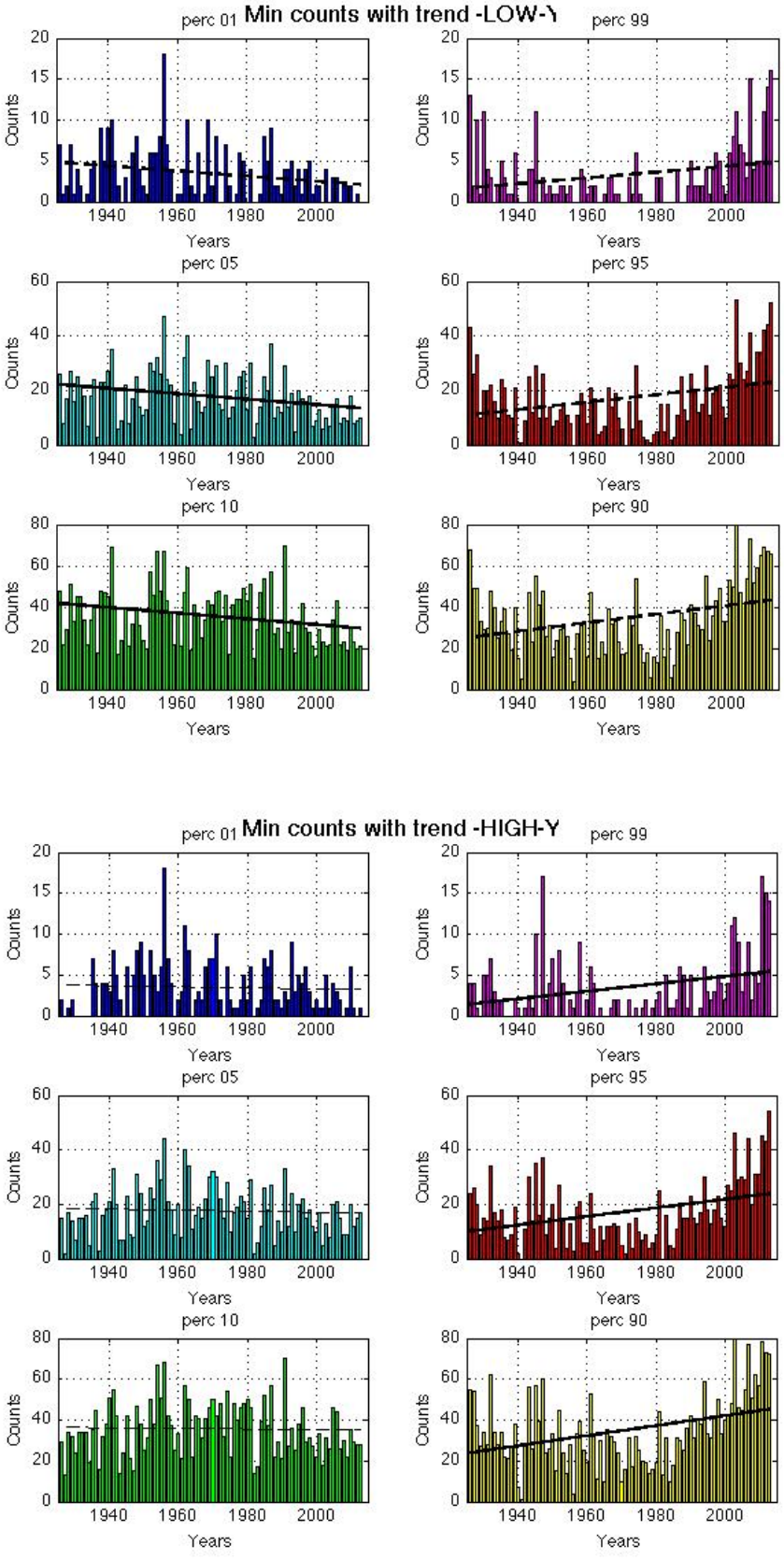

Figure 4.19. *Histograms representing number of events above or below the indicated thresholds for each year. Straight lines stand for calculated trends and follow the line-type code introduced above. These graphics deal with minimum temperatures. Group on the top (bottom) is for LOW(HIGH) data-set.*

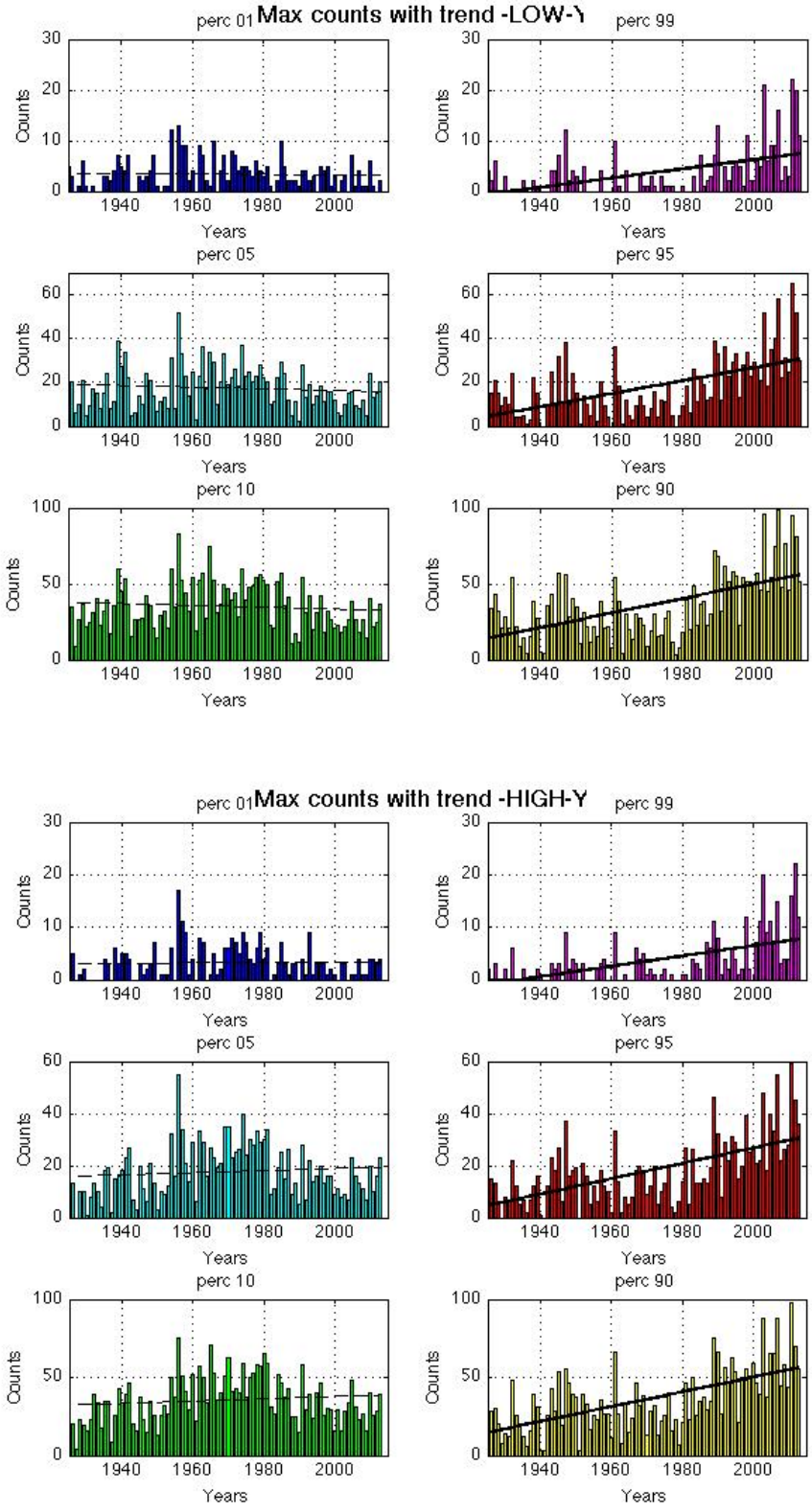

Figure 4.20. *Same as 4.19 but for maximum temperatures.*

These particular behaviour, observed in some seasons, suggested to analyze, also in this case, trends over some sub-periods, choosing, as before, the three yearly ranges of 1926-1950, 1951-1979 and 1980-2013. Obtained trends are displayed in table 4.7 and 4.8 and may be also observed in the histograms of figures 4.21 and 4.22.

The first sub-period doesn't show homogeneous trends in extreme temperatures but obtained yearly fluxes of events suggest an increase in variability. This may be inferred by the positive, but generally non-significant, trends observed in all cases but minimum LOW temperatures.

Looking at seasonal samples, calculated trends in the first period are not homogeneous. Nevertheless it must be noticed a clear warming signal for Spring LOW (both in minimum and maximum) and for Spring HIGH maximum temperatures: all these cases show almost everywhere warming significant trends (up to 4.75 days/dec for 90th percentile of HIGH maximum temperatures, 53 %). Other seasons do not show clear tendencies for minimum temperatures extremes apart from Autumn in LOW sub-set, whose cooling trend is clear. Maximum temperatures instead appear to outline an increasing variance trend with positive fluxes (even if almost everywhere non-significant).

The results of minimum temperatures of second period (negative non-significant trends) suggest a decrease in variability, while a weak (non-significant) decrease of warm extreme events and increase of cold extreme events is observed for maximum temperatures (positive fluxes for cooler thresholds and negative fluxes for warmer thresholds).

At seasonal scale these general tendencies are observed for minimum temperatures where great of the trends are negative (but non-significant). At the same time seasonal trends for maximum temperatures are more heterogeneous and the only clear signal is the increasing of events below colder thresholds in Autumn, especially for HIGH series.

As expected, most clear evidences of warming trends and increasing of extreme warm events are observed over the last sub-period. Yearly trends are very strong, especially for number of events above the warmer thresholds, whose p-value is always lower than 0.01. These exceedance probabilities have similar values both for HIGH and LOW and reach their maximum value for 95th percentile of minimum LOW series (+10.6 days/dec, 58%). Fluxes through lowest thresholds are always negative, but less significant.

Seasonal trends reflect what expected, beginning from the non-significance of winter trends, coherently with results found for average trends (tables 4.2 and 4.3). This accordance is observed also for Autumn series, whose minimum counts trends outline a warming trend of extremes (with increasing of warmest events) and whose maximum counts trends are found to be non-significant. Nonetheless most important results are the ones about Spring and Summer, that show very high values with respect to the mean of corresponding percentile. In general the observed increase is higher for LOW sub-

set than HIGH. Furthermore increase of extreme spring values is larger for minimum temperatures, while in the summer case flux of events for minimum and maximum temperatures are coeherent.

MINIMUM		LOW		[days/dec]	HIGH		[days/dec]
	percentiles	1926-1950	1951-1979	1980-2013	1926-1950	1951-1979	1980-2013
Year	1	+	-	-	+2.38±0.69	-	-0.68±0.41
	5	-	-	-2.77±1.26	+	-	-
	10	-	-	-6.07±2.04	+	-	-
	90	-6.65±3.80	-	**+15.4±1.8**	-	-	**+15.1±1.9**
	95	-6.04±2.25	-	**+10.6±1.5**	+	-	**+10.0±1.4**
	99	-	-	**+3.18±0.53**	+	-	**+2.79±0.61**
Winter	1	-	-	-	+	-	-
	5	-	-	-	+	-	+
	10	-	-	-	+	-	-
	90	-3.82±1.63	+	+	-	+	+
	95	-	+	+	-	+	+
	99	-0.55±0.34	+	+	+0.00±0.15	-	+
Spring	1	-	-	-	+	-	-
	5	-1.21±1.13	-	-	+	-	-
	10	-	-	-	-	-	-
	90	+	-	**+4.22±1.16**	+	-	**+4.19±1.20**
	95	+	-	**+2.71±0.73**	+	-	**+2.63±0.89**
	99	+	-	+0.59±0.31	**+0.68±0.41**	-	+
Summer	1	+	-0.35±0.41	-	+0.85±0.31	-	-0.29±0.20
	5	-	+	-1.31±0.52	+	+	-1.05±0.51
	10	-	+	-2.14±0.67	+	+	-1.93±0.70
	90	+	+	**+6.30±1.45**	+	-	**+6.31±1.30**
	95	+	-	**+4.60±1.09**	+	-0.94±0.49	**+4.32±0.91**
	99	-	**-0.18±0.12**	**+1.36±0.36**	+	**-0.53±0.25**	**+1.01±0.30**
Autumn	1	-	-	-	+0.35±0.43	-	-
	5	-	-	-	+	-	+
	10	+	-	-1.11±0.93	+	-	+
	90	-5.98±2.15	-1.95±1.05	**+3.43±1.05**	-5.59±2.13	-	**+3.43±1.05**
	95	-4.47±1.49	-	**+2.44±0.90**	-	-	**+2.19±0.8**
	99	-1.59±0.65	-	**+0.85±0.29**	-	**-0.00±0.09**	**+0.76±0.32**

Table 4.7. *Calculated trends for number of days above and below the fixed thresholds over the three subperiods (minimum temperatures). Font code is the same as table 4.1. Values are expressed in days/dec.*

MAXIMUM		LOW		[days/dec]	HIGH		[days/dec]
	percentiles	1926-1950	1951-1979	1980-2013	1926-1950	1951-1979	1980-2013
Year	1	+	+	-	+	+	-
	5	+	+	-	+	+3.98±2.23	-
	10	+	+	-	+	+5.17±2.82	-5.23±2.05
	90	+	-	**+13.4±3.0**	+9.19±3.98	-	**+10.7±2.9**
	95	+	-	**+8.61±1.96**	+5.42±2.29	-	**+7.52±1.90**
	99	+	-	**+3.51±0.89**	+	-	**+3.33±0.84**
Winter	1	-	-	-	+	-	+
	5	+	-	-	+	-	+
	10	+	-	-	+	-	-
	90	-	-	+	+	-	+
	95	-	+	-	+	-0.77±0.72	-
	99	-0.11±0.27	+0.17±0.18	+	+	-	+
Spring	1	+	-	-	+	-	-
	5	-	-	-0.83±0.59	+	+	-1.43±0.68
	10	-	-	-1.79±0.93	-	+	**-3.04±0.94**
	90	+3.60±1.62	-	**+5.32±1.65**	**+4.75±1.46**	-	**+5.10±1.56**
	95	+2.94±1.19	-	+3.56±1.20	**+2.71±0.81**	-	+3.29±1.17
	99	**+1.04±0.41**	**-0.01±0.15**	**+1.40±0.40**	**+0.50±0.26**	-0.04±0.22	+1.46±0.44
Summer	1	**+0.38±0.19**	+	-	**-0.03±0.08**	+	-
	5	+	+	-	+	+2.18±0.95	-1.15±0.47
	10	+	+	**-2.11±99.13**	+	+	**-2.24±0.71**
	90	+	-	**+5.39±1.70**	+	-	**+4.82±1.55**
	95	+	-	**+4.64±1.22**	+	-	**+3.84±1.06**
	99	**+0.18±0.16**	**-0.36±0.20**	**+1.58±0.57**	**+0.44±0.23**	**-0.22±0.13**	+1.20±0.49
Autumn	1	+	+	-	**+0.08±0.34**	+0.92±0.39	-
	5	+	+	-	+	+2.35±1.27	+
	10	+	+3.00±1.81	-	+	+2.69±1.79	-
	90	+	-	+	+	+	+
	95	-	+	+	-	+	+
	99	+	+	+	+0.04±0.29	+	-

Table 4.8. *Same as table 4.7 but for maximum tempertures.*

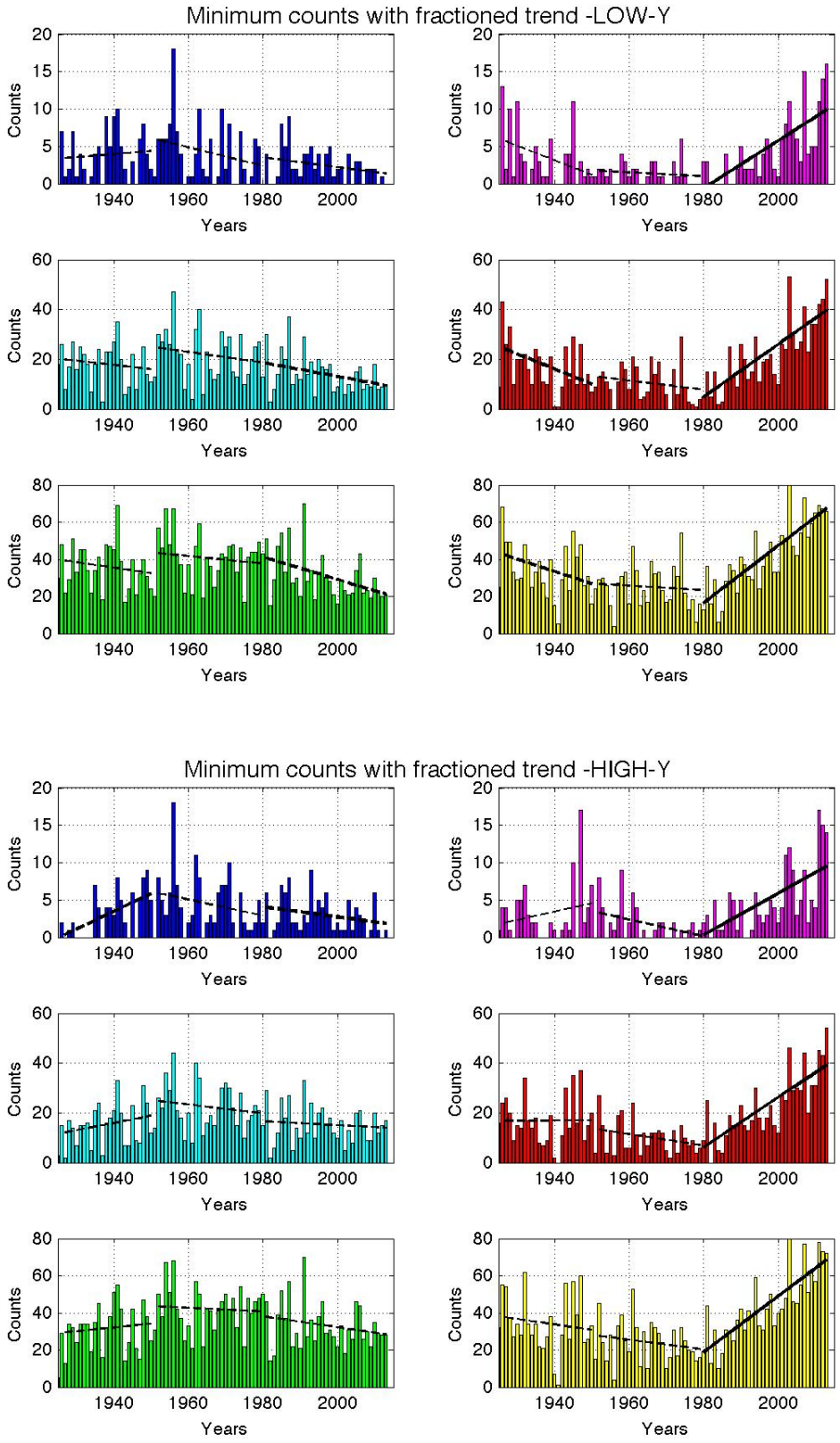

Figure 4.21. *Histograms representing number of events above or below the indicated thresholds for each year. Straight lines stand for calculated trends for the three sub-periods and follow the line-type code introduced above. These graphics deals with minimum temperatures. Group on the top (bottom) is for LOW(HIGH) data-set. Location and colors of plots related to each percentiles are the same as figure 4.19*

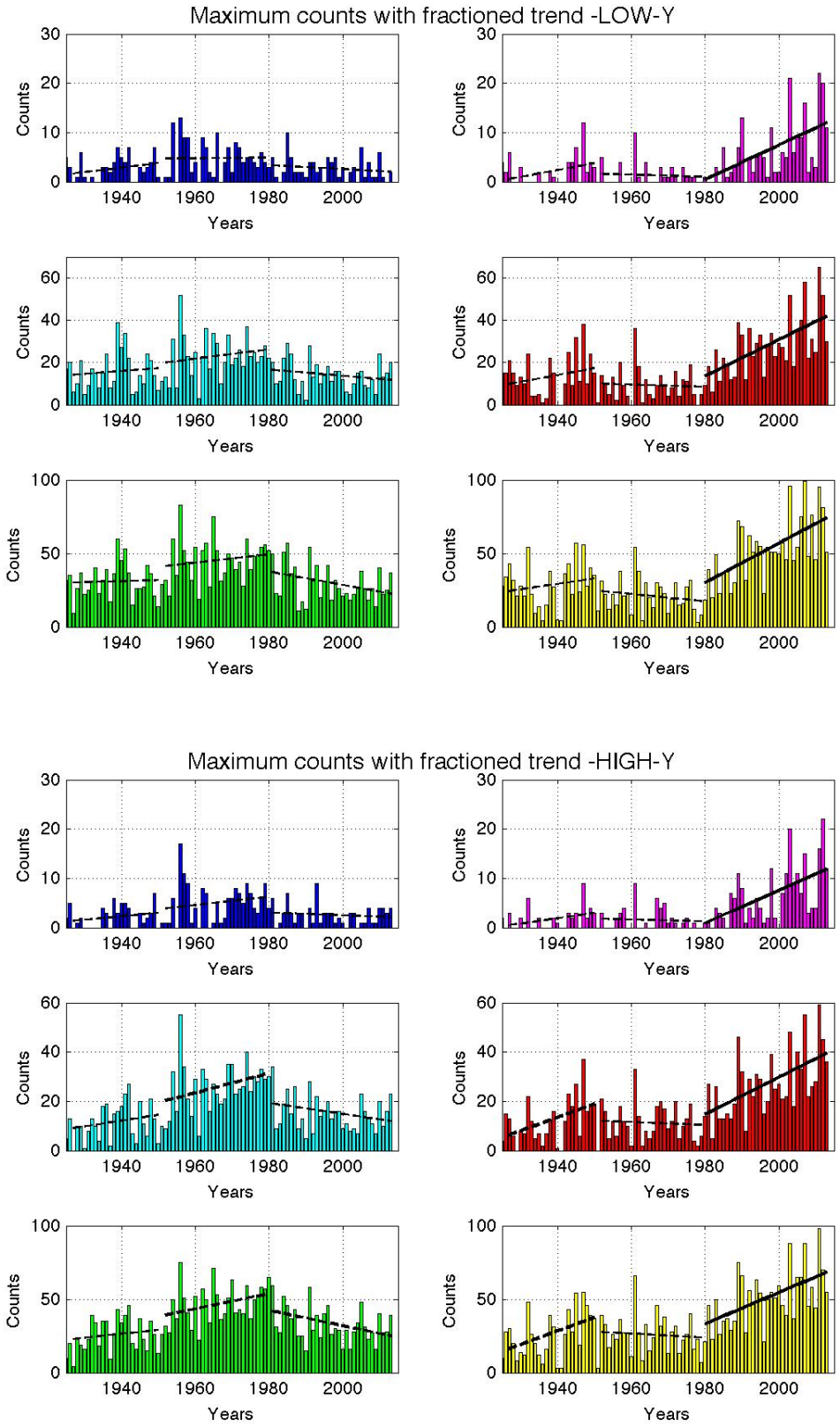

Figure 4.22. *Same as figure 4.21 but for maximum temperatures*

4.7 Trends in the moving percentiles

Asymmetric changes in cold and warm exceedance probabilities are strictly linked to the shape of the PDF and not necessary imply any changes in its higher moments. To highlight changes in the shape of the PDF, temporal changes in the percentile thresholds were analyzed. Anomaly temperatures recorded were separated in sub-samples, one per year. These data were sorted in increasing order determining, year by year, the thresholds of a set of percentiles of the distribution. Chosen thresholds in this study are 1st, 5th, 10th, 20th, 30th, 40th, 50th(median), 60th, 70th, 80th, 90th, 95th and 99th percentiles. The extracted annual series of the percentile thresholds underwent linear regressions with the aim of searching trends. Trends of this percentiles set allows to detect changes in shape of the temperature distribution, since in the case of a rigid distribution trend, all percentiles should present coherent values with respect to the median trend.

Generalized observed trend may be observed in table 4.9, which displays obtained tendencies for the entire period (1926-2013). Here it is found again a warming trend in both altitudinal bands, with slightly larger results for HIGH in minimum temperatures (as already found in the counts trends) and deeply stronger trends for maximum temperatures, coherent between the two regions.

Trends of the low percentiles are weaker than the highest ones, but for minimum LOW temperatures they appear to be stronger than corresponding high percentiles.

	MIN	[°C/dec]	MAX	[°C/dec]
percentiles	LOW	HIGH	LOW	HIGH
1	+0.13±0.06	-	+	+
5	+0.08±0.04	+	+	-
10	+0.07±0.03	+	+	-
20	+0.08±0.04	+	+0.08±0.03	+
30	+0.06±0.03	+0.07±0.03	**+0.09±0.03**	+
40	+0.06±0.02	+0.07±0.03	**+0.11±0.03**	+
50	+0.06±0.02	+0.08±0.02	**+0.13±0.03**	+0.10±0.03
60	+0.07±0.02	**+0.08±0.02**	**+0.14±0.03**	**+0.13±0.03**
70	**+0.06±0.02**	**+0.07±0.02**	**+0.14±0.03**	**+0.16±0.03**
80	+0.05±0.02	**+0.08±0.03**	**+0.18±0.03**	**+0.10±0.03**
90	+0.06±0.02	**+0.08±0.03**	**+0.21±0.03**	**+0.23±0.03**
95	+0.06±0.03	**+0.10±0.03**	**+0.25±0.04**	**+0.26±0.03**
99	+0.04±0.03	**+0.13±0.03**	**+0.27±0.05**	**+0.26±0.03**

Table 4.9. *Calculated trends and standard deviation for moving thresholds over the entire period (1926-2013).*

A better comparison between low and high percentiles with respect to the median may be better effectuated by looking at plots of figures 4.23 and 4.24. Minimum temperatures show in both altitudinal band coherent trend of every percentile with respect to the median, even if highest percentiles show slightly higher (lower) trends

for HIGH(LOW). A clear signal is given by maximum temperatures. Here trends of low and high percentiles are non consistent with the median trend. In both regions low percentiles are affected by a weaker (non-significant) trend and highest percentiles present very steep trend whose error bar (95% confidence interval, 1.96σ, where σ is the standard deviation) does not include values found for the median. These features imply that the distribution of maximum temperatures has enlarged and the variability has increased.

In this analysis, as previous ones, calculation of trends was performed on the three sub-periods, expecting, also here, to find non homogenous features in the first two periods and a very strong warming trend in the last one. Results of these calculations are displayed in the tables 4.10 and 4.11. Here it can be immediately noticed how in the last period almost every trend is significant and positive, while in the first two periods no significant generalized trends are observed. The only exceptions are the cooling of highest thresholds trends in minimum LOW temperatures over 1926-1950 and the warming of maximum HIGH temperatures in the same period (both coherent with found results in exceedance probabilities, tables 4.7 and 4.8). Nevertheless signs of non-significant trends outline, for the second period, a prevailing warming trend for minimum temperature percentiles and a cooling trend for maximum ones, suggesting again a decrease in DTR.

Coherence (or non-coherence) of these trends with their corresponding median trends are analyzed in figures 4.25, 4.26 and 4.27. First period doesn't show clear tendencies in variability except for a distribution widening for HIGH maximum temperatures and a decrease of right tails extremes for LOW minimum temperatures. In the second period trends appear to be in all cases coherent with median trends, with the already noticed increase of minimum temperatures and decrease of maximum ones. Third period's plots present, as expected, strong warming trends for almost all percentiles. Signals of enlargement of the distribution may be seen in these plot, but here error bars cover in nearly all case the median trend value. This is because over short periods it's not possible to detect highly significant changes in the shape of the distribution.

Therefore analyses over long period allow to decrease uncertainty and to assess with higher confidence that maximum distribution has undergone an enlargement that is mainly due to the last period.

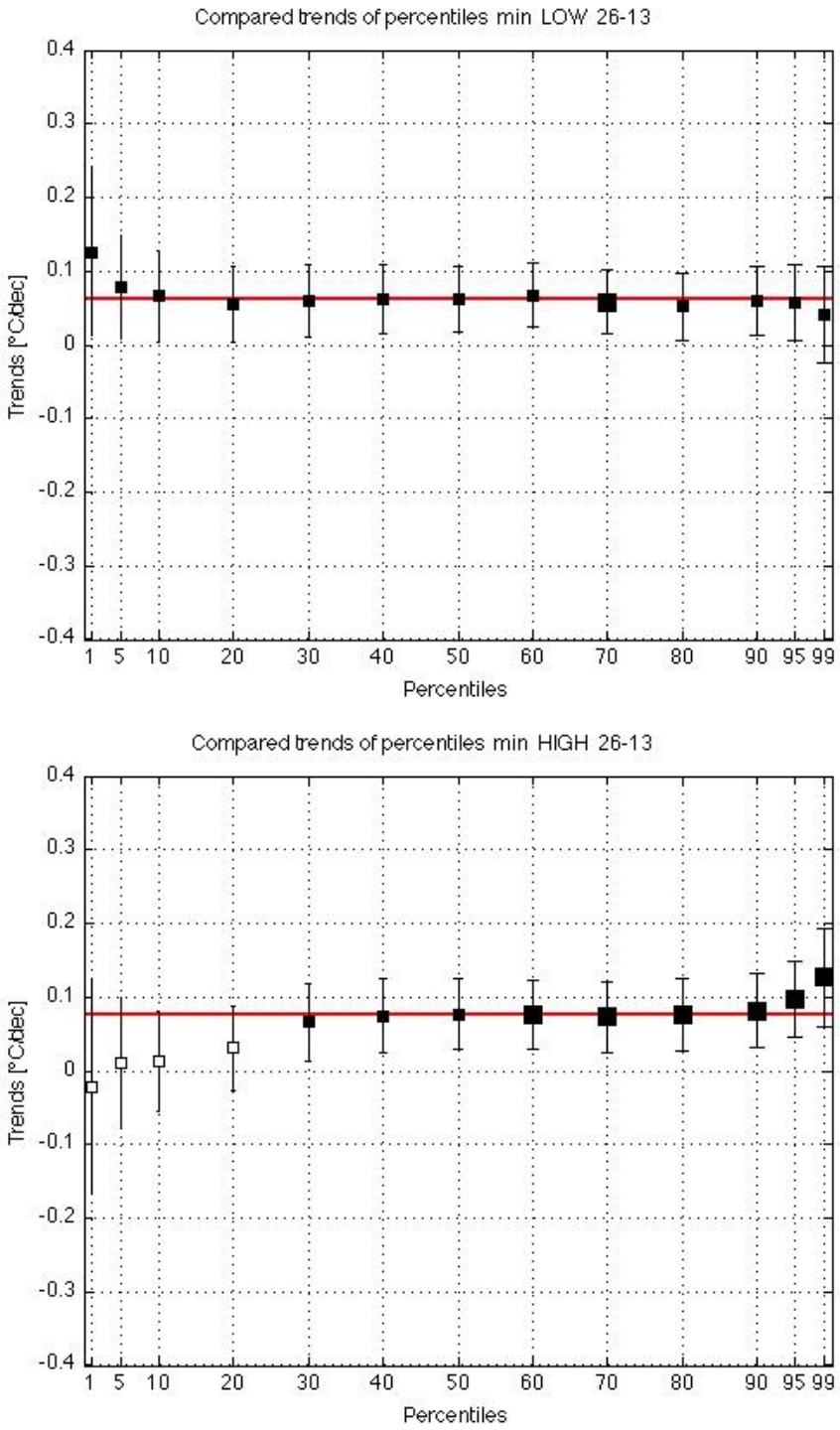

Figure 4.23. *Calculated trend for percentiles with 95% confidence (1.96σ) error bars (top: LOW, bottom: HIGH). Marker dimensions depend on the obtained significance: large black square stands for significance with p-value below 0.01, small black square stands for significance with p-value below 0.1, small white square stands for significance with p-value above 0.1. Horizontal line describes the median value, it is drawn in red if trend is positive and in blue when negative.*

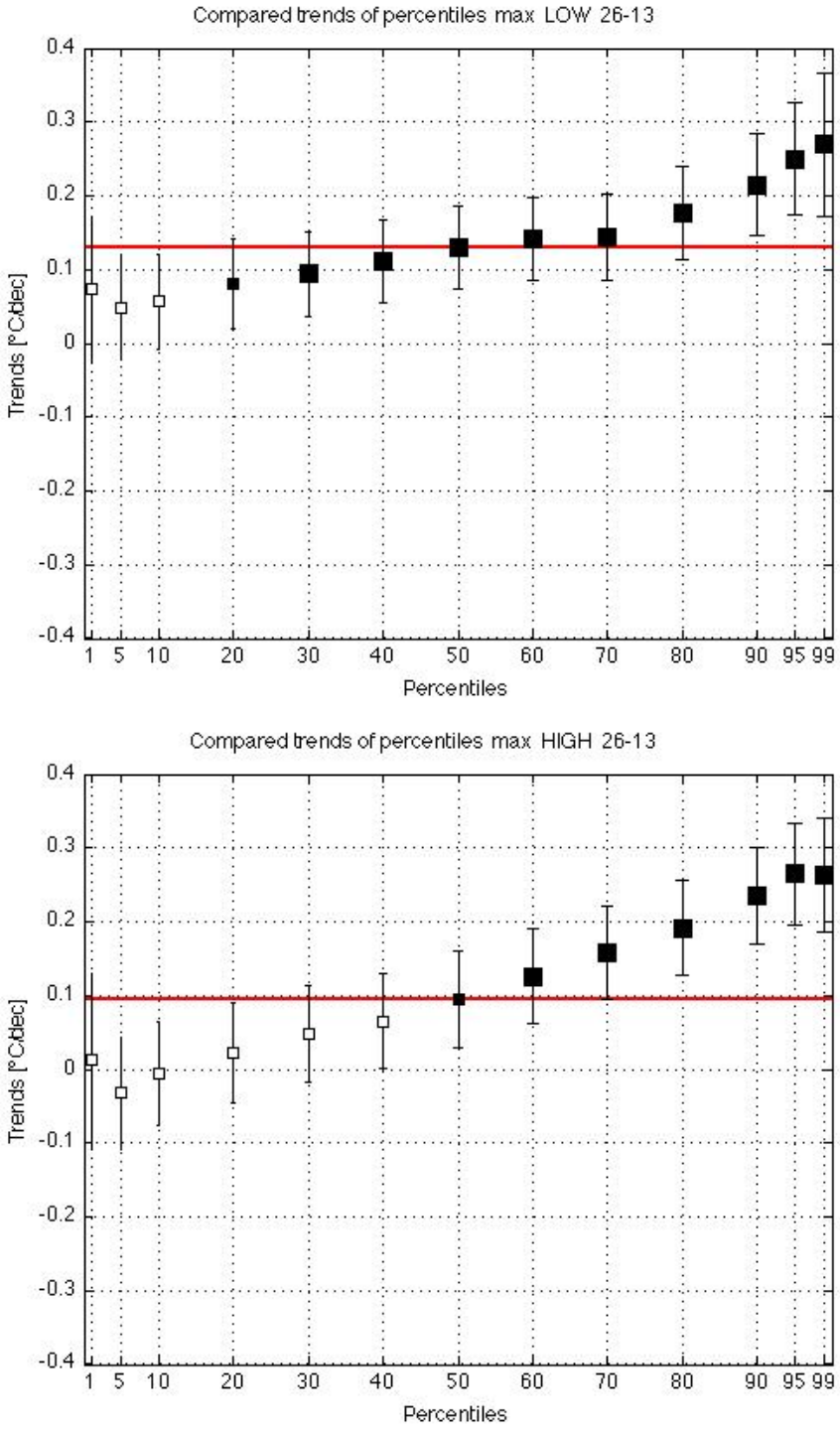

Figure 4.24. *Same as figure 4.23 but for maximum temperatures.*

MINIMUM		LOW	[°C/dec]		HIGH	[°C/dec]
percentiles	1926-1950	1951-1979	1980-2013	1926-1950	1951-1979	1980-2013
1	-	+	+	-1.21±0.52	+	-
5	-	+	+0.28±0.12	-	+	+
10	+	+	+0.29±0.10	-	+	+0.21±0.16
20	+	+	**+0.35±0.1**	-	+	**+0.35±0.11**
30	+	+	**+0.40±0.82**	-	+	**+0.45±0.10**
40	-	+	**+0.43±0.08**	-	+	**+0.45±0.09**
50	-	+	**+0.46±0.07**	-	+	**+0.42±0.09**
60	-	+	**+0.42±0.07**	-	+	**+0.44±0.08**
70	-	+	**+0.42±0.06**	-	-	**+0.46±0.07**
80	-0.21±0.14	+	**+0.45±0.06**	-	-	**+0.49±0.07**
90	-0.30±0.14	-	**+0.49±0.06**	-	-	**+0.48±0.08**
95	-0.44±0.15	-	**+0.52±0.07**	-	+	**+0.45±0.09**
99	-0.72±0.22	-0.22±0.14	**+0.47±0.10**	+	+	**+0.51±0.14**

Table 4.10. *Calculated trends with standard deviation for moving thresholds over the three sub-period (minimum temperatures).*

MAXIMUM		LOW	[°C/dec]		HIGH	[°C/dec]
percentiles	1926-1950	1951-1979	1980-2013	1926-1950	1951-1979	1980-2013
1	-	-	+	-0.91±0.37	-	+
5	-	-	+	-	-0.24±0.19	+
10	+	-	+0.27±0.13	-	-	+0.28±0.13
20	+	-	+0.33±0.13	-	-	+0.39±0.14
30	+	-	**+0.39±0.11**	-	-	**+0.41±0.13**
40	+	-	**+0.40±0.11**	+	-	**+0.45±0.12**
50	+	-	**+0.44±0.11**	+	-	**+0.49±0.12**
60	+	-	**+0.49±0.11**	+	-	**+0.49±0.12**
70	+	-	**+0.46±0.11**	+	+	**+0.45±0.11**
80	+	-	**+0.44±0.11**	+	+	**+0.45±0.12**
90	+	-	**+0.57±0.12**	+	-	**+0.47±0.12**
95	+	-	**+0.64±0.13**	+0.57±0.24	-	**+0.57±0.13**
99	+0.67±0.32	-	**+0.79±0.18**	+0.57±0.28	+	**+0.54±0.15**

Table 4.11. *Same as 4.10, but for maximum temperatures.*

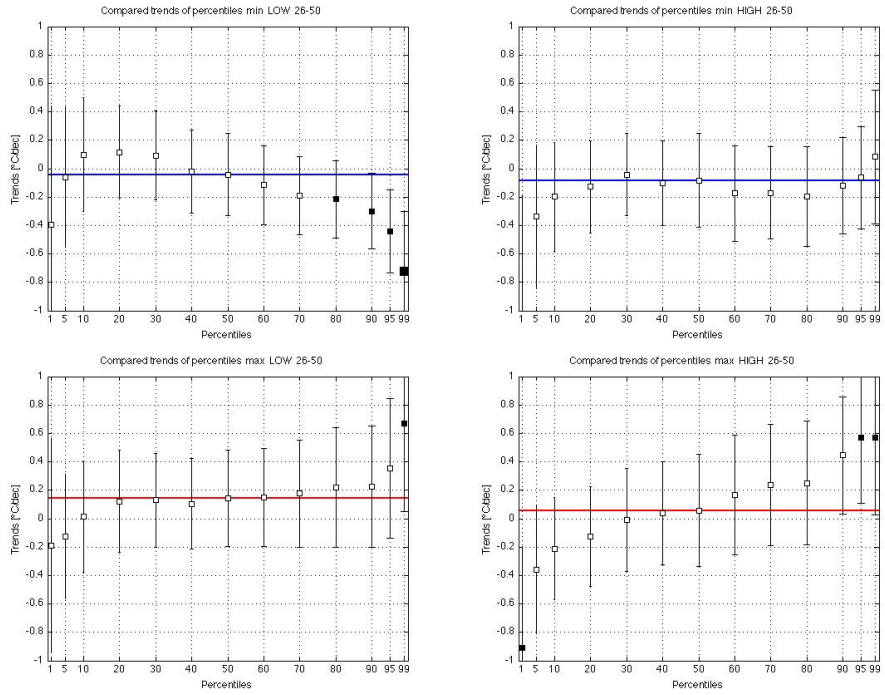

Figure 4.25. *Same as figures 4.23 and 4.24 but for 1926-1950 period. Please pay attention to the different y-axis range with respect to the previous figures.*

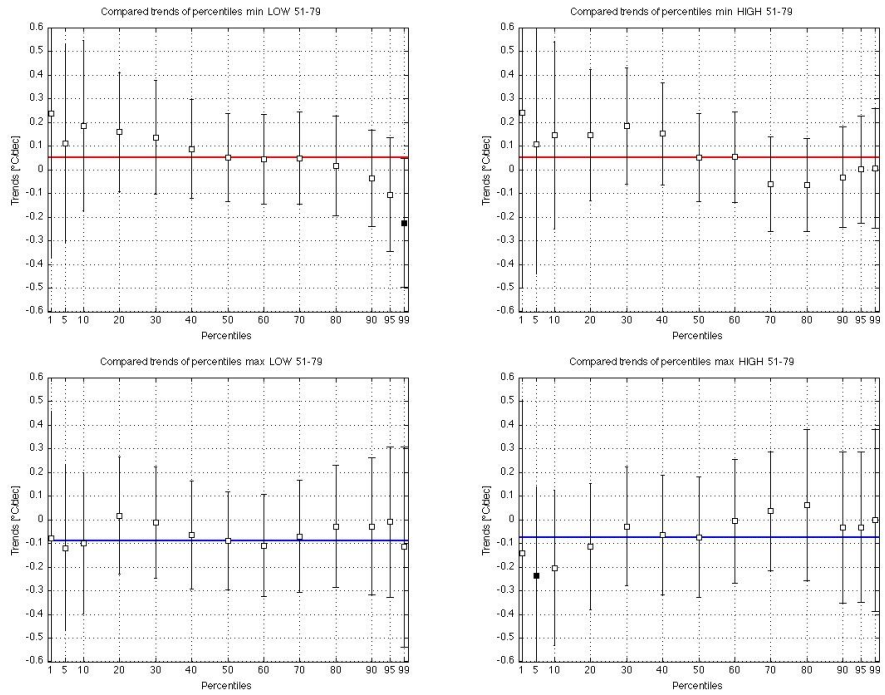

Figure 4.26. *Same as figures 4.23 and 4.24 but for 1951-1979 period. Please pay attention to the different y-axis range with respect to the previous figures.*

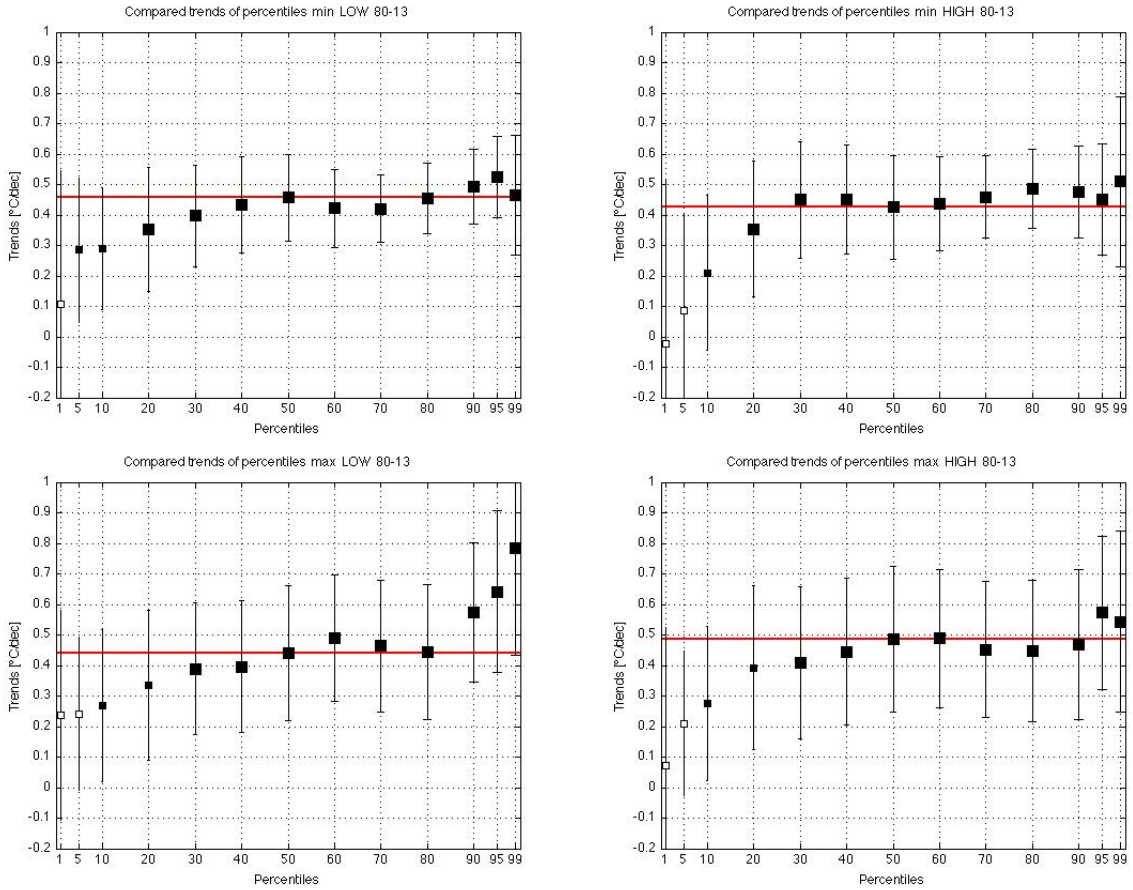

Figure 4.27. *Same as figures 4.23 and 4.24 but for 1980-2013 period. Please pay attention to the different y-axis range with respect to the previous figures.*

In order to allow a better comparison with literature, in particular with what shown in figure 1.19 [Simolo et al., 2010], percentile trend analysis was made also over the 1951-2013 period, results are shown in graphics of figure 4.28. Here it is possible to notice higher trends (with respect to those found over the 1926-2013 period) for every percentile but also large error bars, this last features allows to asses that percentile trends are always coherent with median trends, according to what found by Simolo et al. [2010]. Nevertheless for maximum temperatures there is a signal of a widening distribution (similar to what stated by Simolo et al. [2010]), even if reached significance is low.

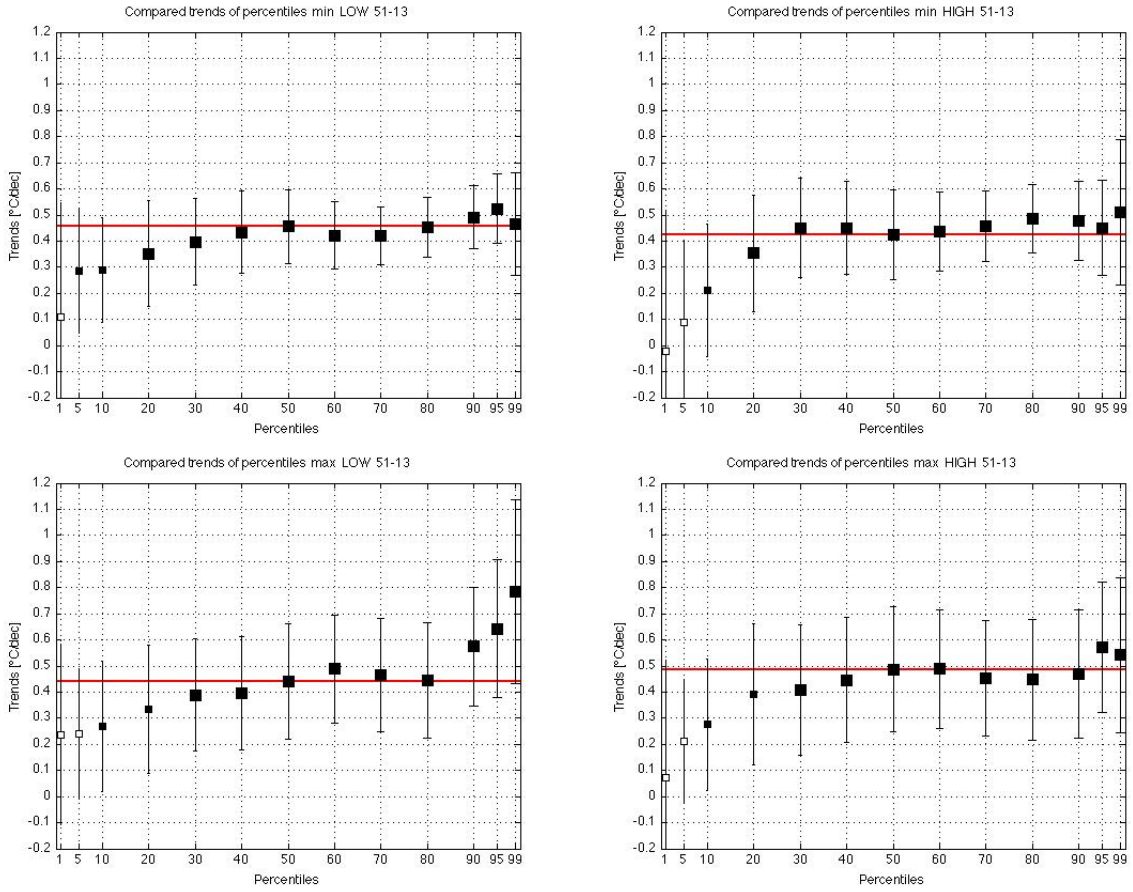

Figure 4.28. *Same as figures 4.23 and 4.24 but for 1951-2013 period.*

Chapter 5

Conclusions and Open Issues

5.1 Summary and conclusions

Daily temperatures series (maximum and minimum) of Trentino Alto Adige were collected, checked and homogenized. The data was clustered into two altitudinal bands that gathered stations with similar behaviours (HIGH and LOW).

Analyses allowed to find positive trends in the mean values on the 1926-2013 period, with stronger signals for maximum temperatures (0.11 ± 0.03 and 0.13 ± 0.03 °C/dec, for HIGH and LOW respectively) than for minimum ones (0.07 ± 0.02 for both elevation regions). Most intense warming trends are observed for Spring and Summer, especially at low elevations, while Winter and Autumn do not appear to be generally interested by significant trends.

Positive trends are found to be steeper in last decades. In fact, observed tendencies over the sub-periods previous to 1979 are weak and do not show general agreement, on the contrary, obtained trends for 1980-2013 period present highly significant trends (0.38 ± 0.06 and 0.38 ± 0.07 for minimum temperatures and 0.41 ± 0.11 and 0.42 ± 0.10 for maximum ones).

Together with an increase in average values, significant changes in extreme events are observed. In particular it is found that the number of days with temperature above 90th, 95th and 99th percentile threshold increased and, the same time, events below 1st, 5th and 10th percentiles decreased. These behaviors are observed especially for Spring and Summer maximum series. Also in this case signal have become more evident for last decades.

In order to understand whether these trends are due to rigid shift of the whole probability density function driven by the trend in the mean or if there are also changes in the shape (i.e. in the variability), percentile thresholds (for 1st, 5th, 10th, 20th... 80th, 90th, 95th, 99th percentiles) were estimated year by year and the obtained series analyzed for trend.

Trends of these percentile series revealed that for minimum temperature there is accordance with the trend in the median (50th percentile). On the contrary, for maximum

temperature coldest percentiles showed to have lower trends than the median, while warmer percentiles were found to have steeper trends.

These results lead to the conclusion that, at least for maximum temperatures, changes in exceedanc probabilities are partly to be attributed to a change in the shape of the pdf.

5.2 Is increased variability due to instrumental changes? An open issue

Homogenization process described above aimed at deleting non-climatic step-like changes in the mean of a series but didn't operate on variability. At this point it's right to wonder whether changes in instrumental features or in the number of stations may affect the results linked to variability of the sample (counts of events above or below the thresholds and trends in the percentiles). For these reasons some tests were performed in order to inspect the effects of these changes in the instrumental and sample characteristics.

First of all it was necessary to inspect whether changes in the number of available stations affected variability in the average regional series. Availability of data for each year may be observed in figure 5.1. In these plots it is clear that number of available series was not constant and there were some sudden increases and decreases of the number of stations. In particular it can be noticed the steep increase of number of available series in 1956 due to the fact that great part of Alto Adige stations began in that year. Another important increase may be noticed for years between1970 and 1980 and a significant decrease is observed after 2010, due to the high number of inhomogeneities in the last years and to the dismission of some stations.

For these reasons some reference series were created, selecting all series beginning before 1933 belonging to Trento province (FYLE33 series) and all series beginning before 1958 (FYLE1958) belonging to Bolzano province. With these sub-sets of stations, new HIGH and LOW average series were constructed, having an almost constant data availability. Their availability is shown in figure 5.2.

Annual variance of these series were then compared with variance of HIGH and LOW samples, displayed in figure 5.3 . It was then calculated the difference of the variance year by year. Results are shown in figure 5.4 with estimated trends. Here it is clear the negative trend of variance of maximum temperatures and minimum temperatures with respect to FYLE33 and FYLE58, apart from variance of minimum temperatures for LOW -FYLE58.

This signal is coherent with what expected. In fact increase in the number of available station is supposed to reduce variability.

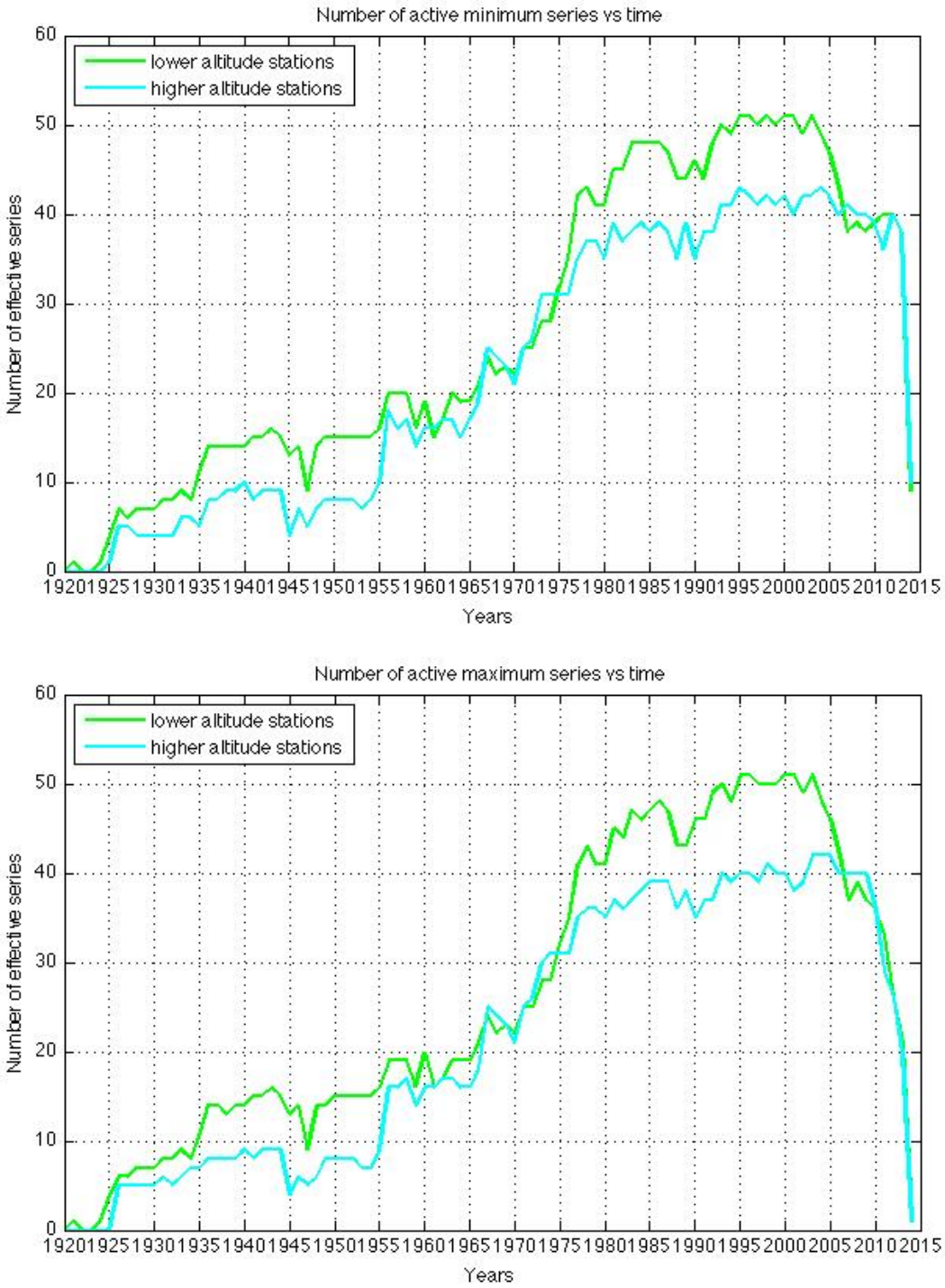

Figure 5.1. *Yearly availability for HIGH and LOW sub-samples for minimum (top) and maximum (bottom) temperatures. A series was labeled as available for the considered year if it had at least 182 days of data.*

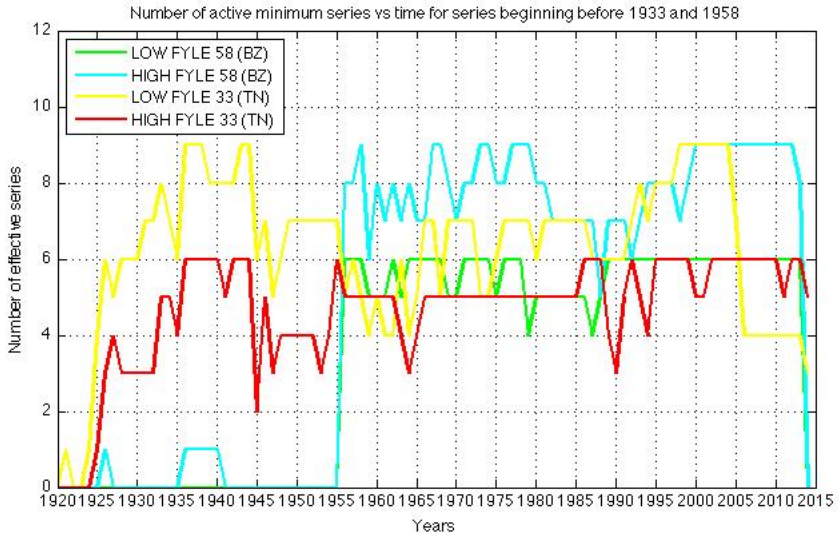

Figure 5.2. *Annual availability of FYLE series for HIGH e LOW altitudes.*

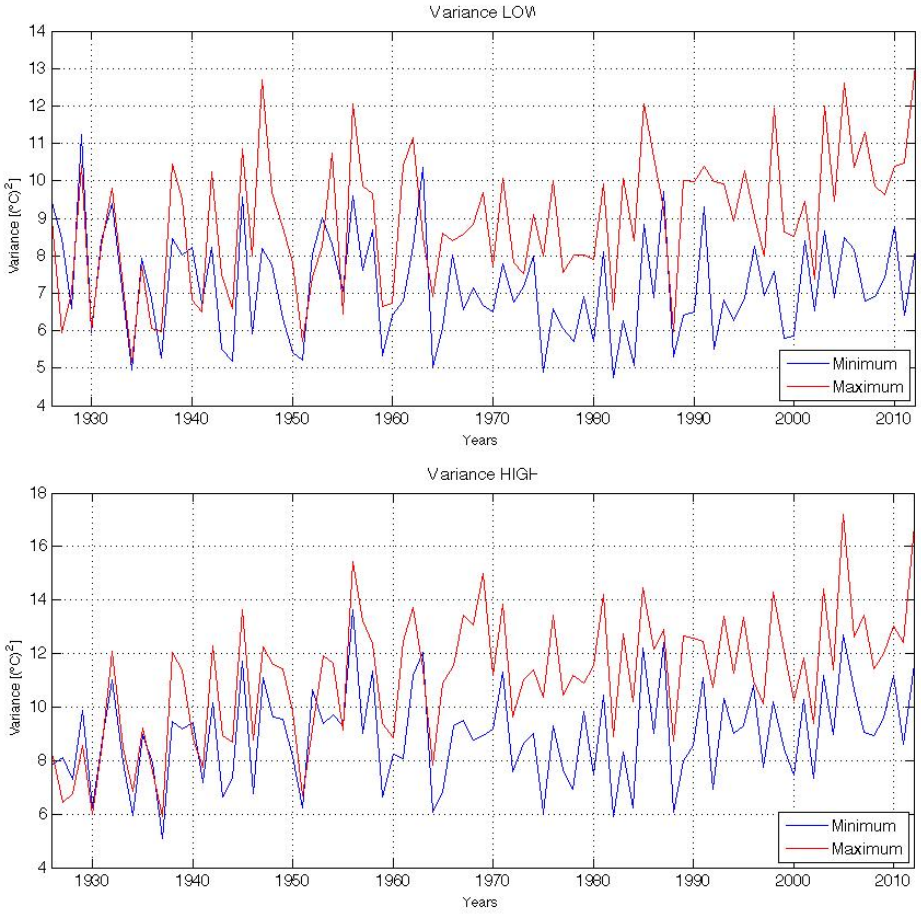

Figure 5.3. *Annual variance of minimum and maximum series for LOW (top) and HIGH (bottom).*

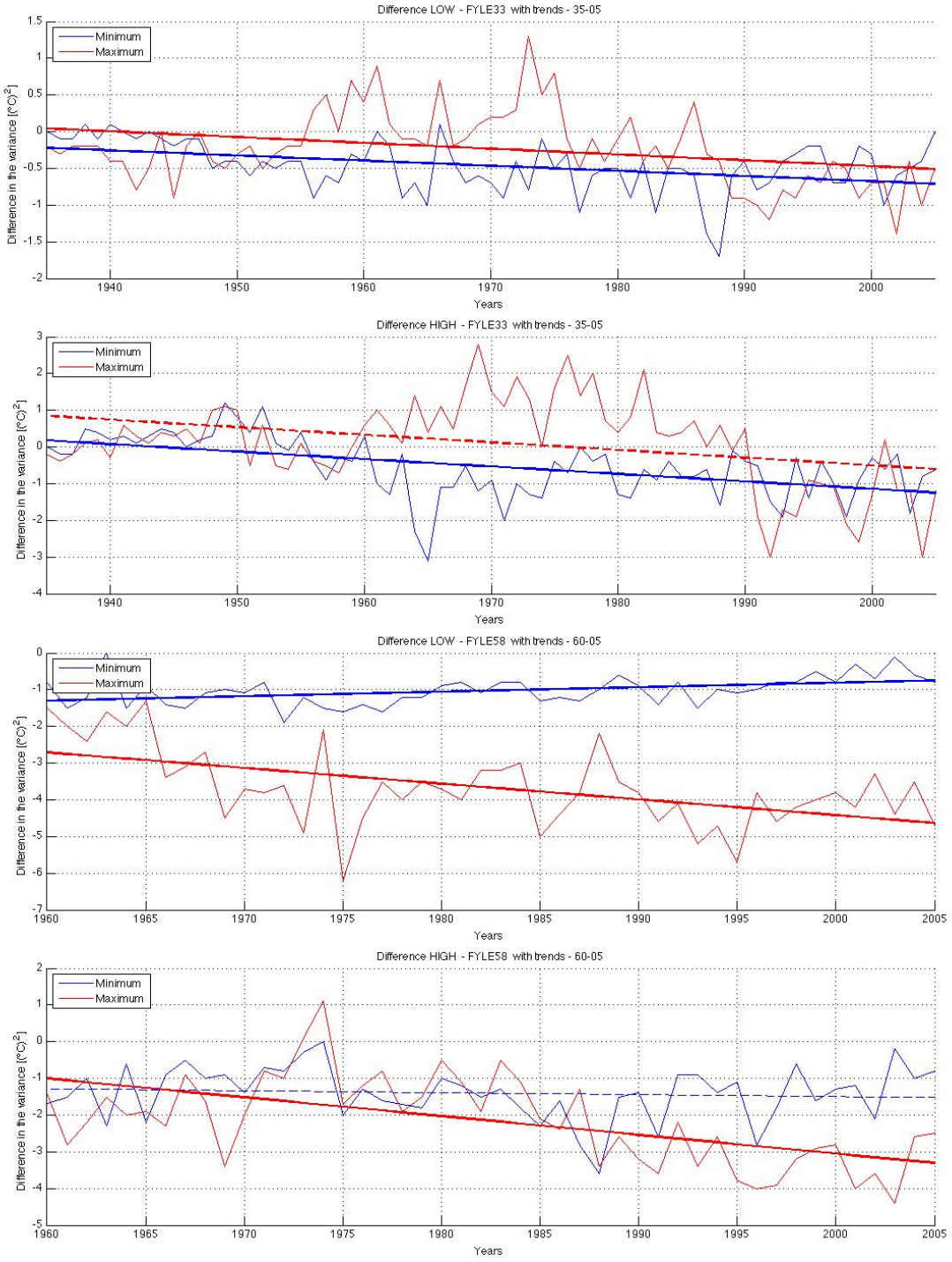

Figure 5.4. *Variance difference between LOW series and FYLE33-LOW series with trends (first plot). Second plot: difference between HIGH variance and FYLE33-HIGH with trends. Third plot: same as first one but for FYLE58-LOW. Fourth plot: same as second one but for FYLE58-HIGH.*

Another aspect that was necessary to inspect was the effect of the gradual conversion of series from mechanical to electronic on the variability of the average regional series. This was done because electronic instruments have a quick response to temperature changes due to a lower inertia. Consequently electronic series are expected to have higher variability.

This check was effectuated over two "ALL" average series (one for minimum temperatures and one for maximum temperatures). These series were obtained as daily averages of data coming from the entire sample without the separation between low and high stations. The ALL series were then compared, in their annual variance, with two series calculated as average of the parts of the Alto Adige series that were certainly recorded with electronic techniques and that begin before 1989 (in order to have a constant number of reference stations) (this reference sample was called BZ0024). Selection of the electronic series was possible thanks to the record-technique label provided by IdroBolzano.

This wasn't effectuated on Trentino sample since the series were provided as a merging between mechanical and electronic series and no informations about the merging period were available

Annual variance of the ALL series may be observed in figure 5.5 and its comparison with the electronic series of Bolzano Province is displayed in figure 5.6. The series of the difference between these series (ALL - BZ0024) underwent a trend analysis finding that there are positive trends (in the 1989-2009 period) both in minimum and maximum temperatures variances (even though trend for maximum temperature is non-significant). Values of this difference are negative, this means that the absolute value of the difference is decreasing. Therefore variance of ALL series increase, reducing its distance from BZ0024 series' variance. This evidence allows to state that the gradual migration towards electronic station affects variability of the sample, increasing it.

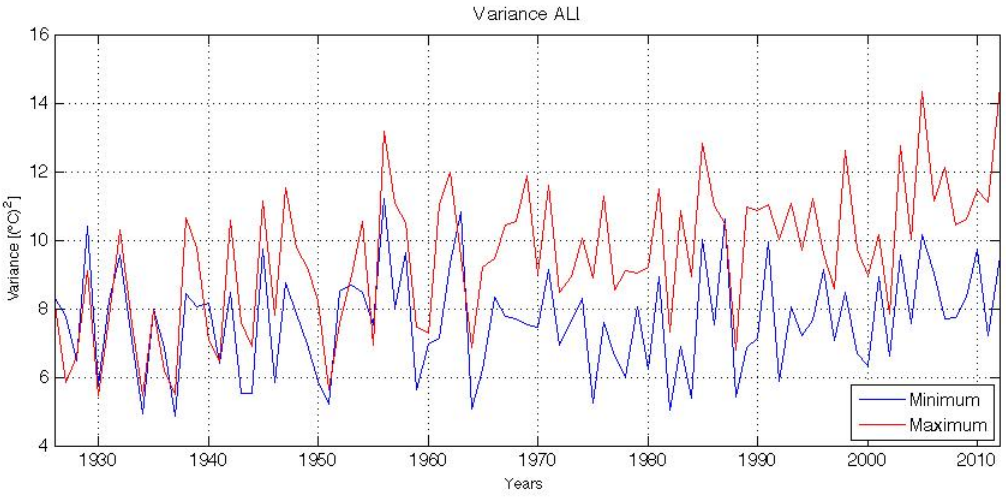

Figure 5.5. *Annual variance of minimum and maximum series for the ALL sample.*

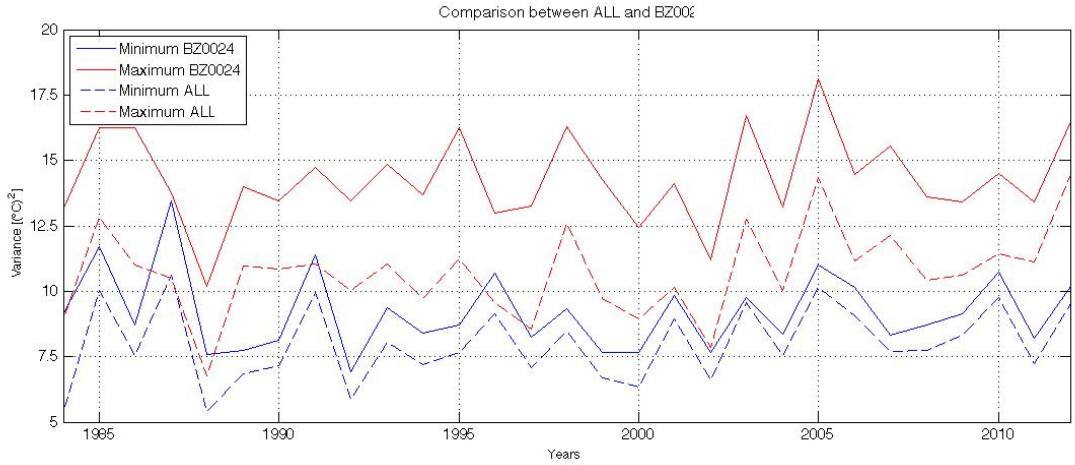

Figure 5.6. *Annual variance of minimum and maximum series for ALL stations limiting the sample at electronic series of Bolzano province (solid lines) compared to the entire sample's variance (dashed lines).*

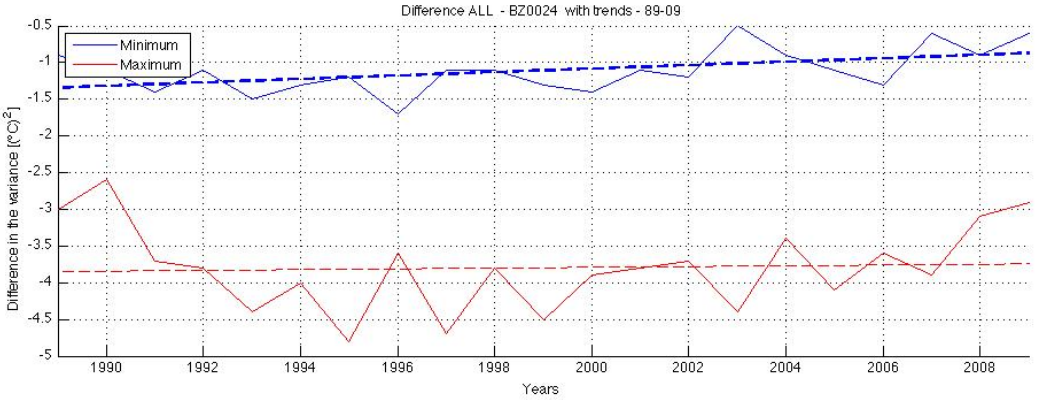

Figure 5.7. *Difference in the annual variance between ALL and BZ0024 with trends .*

Summarizing: decrease in the variance due to the increase of the number of station implies that trend in temperature variability could be larger than the one observed in this thesis. Consequently extreme events maybe are even more frequent and intense than observed here. At the same time it is to consider the fact that the increase of variance due to the gradual conversion of mechanical station could affect the pdf, widening it. Therefore the two observed effects act towards opposite directions. These results introduce now a right question: which part of the increase of variability is due to instrumental changes and which part is to confer to a climate signal? It would be necessary to perform parallel measurements of mechanical and electronic devices, however research is only at the beginning in these fields. Though, at the end, it is important to underline how these wonders do not cover the evidences of a warming climate and the certainty that this increase of temperatures has been stronger especially in last decades.

Acknowledgments:

This thesis work has been carried out in the framework of the HR-CIMA Project ("Hight Resolution Climate Information fo Mountain Areas"), Special Project P7 within the Project of Interest NEXTDATA (MIUR Ministero dell'Istruzione, dell'Università e della Ricerca). I sincerely thank Meteotrentino and the Ufficio Idrografico Provincia di Bolzano for providing the data.

Appendix A

Seasonal trends of exceedance probabilities: the plots

In this appendix one may see all plots for seasonal trends of exceedance probabilities of seasonal series. Here after the table 4.6.

		MIN	[day/dec]	MAX	[day/dec]
	percentiles	LOW	HIGH	LOW	HIGH
Year	1	-0.31±0.13	-	-	+
	5	**-1.00±0.37**	-	-	+
	10	**-1.39±0.55**	-	-	+
	90	+2.07±0.67	**+2.45±0.69**	**+4.77±0.76**	**+4.70±0.69**
	95	+1.36±0.47	**+1.58±0.45**	**+2.97±0.49**	**+2.94±0.43**
	99	+0.36±0.15	**+0.46±0.16**	**+0.91±0.18**	**+0.98±0.16**
Winter	1	-0.16±0.08	-	-0.07±0.06	-
	5	-0.55±0.23	-	**-0.48±0.21**	-
	10	-0.71±0.31	-	-0.66±0.29	-
	90	+	+0.64±0.24	**+0.90±0.32**	+0.63±0.30
	95	+	**+0.48±0.14**	+0.50±0.19	+
	99	+	**+0.21±0.06**	+0.19±0.06	**+0.18±0.07**
Spring	1	-0.10±0.05	-	-	-
	5	-0.28±0.18	-	-	-
	10	-0.41±0.26	-	-	+
	90	+0.71±0.27	**+0.81±0.28**	**+1.63±0.33**	**+1.69±0.31**
	95	**+0.50±0.17**	**+0.52±0.19**	**+0.93±0.24**	**+1.11±0.21**
	99	+0.13±0.06	+	**+0.27±0.08**	**+0.35±0.08**
Summer	1	-	+	+	+
	5	-0.36±0.17	-	+	+
	10	**-0.67±0.22**	-	-	+
	90	**+1.16±0.32**	+0.98±0.33	**+1.75±0.36**	**+1.74±0.30**
	95	**+0.74±0.23**	+0.50±0.23	**+1.14±0.24**	**+1.07±0.21**
	99	**+0.17±0.07**	**+0.06±0.08**	**+0.37±0.09**	**+0.28±0.08**
Autumn	1	+	+	+	+
	5	+0.18±0.19	+0.25±0.19	+0.27±0.18	**+0.43±0.19**
	10	+	+0.46±0.29	+0.50±0.28	**+0.75±0.27**
	90	-	+	+0.50±0.30	+0.60±0.27
	95	+	+	+0.39±0.20	+0.38±0.17
	99	+	+0.08±0.07	+	**0.13±0.07**

Table A.1. *Calculated trends for number of days above and below the fixed thresholds. Font code is the same as table 4.1. Values are expressed in day/dec.*

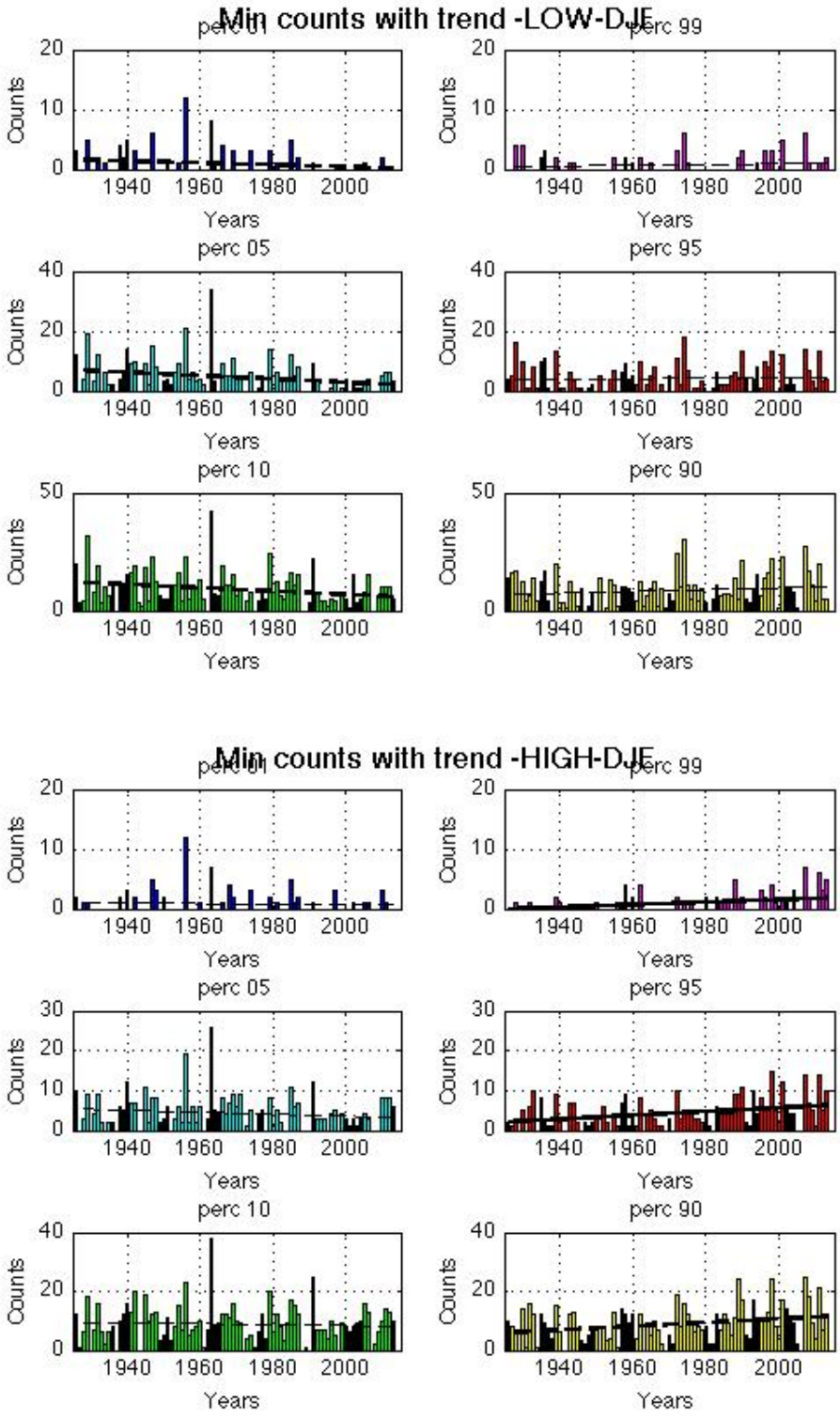

Figure A.1. *Same as figure* **??** *but for winter minimum temperatures.*

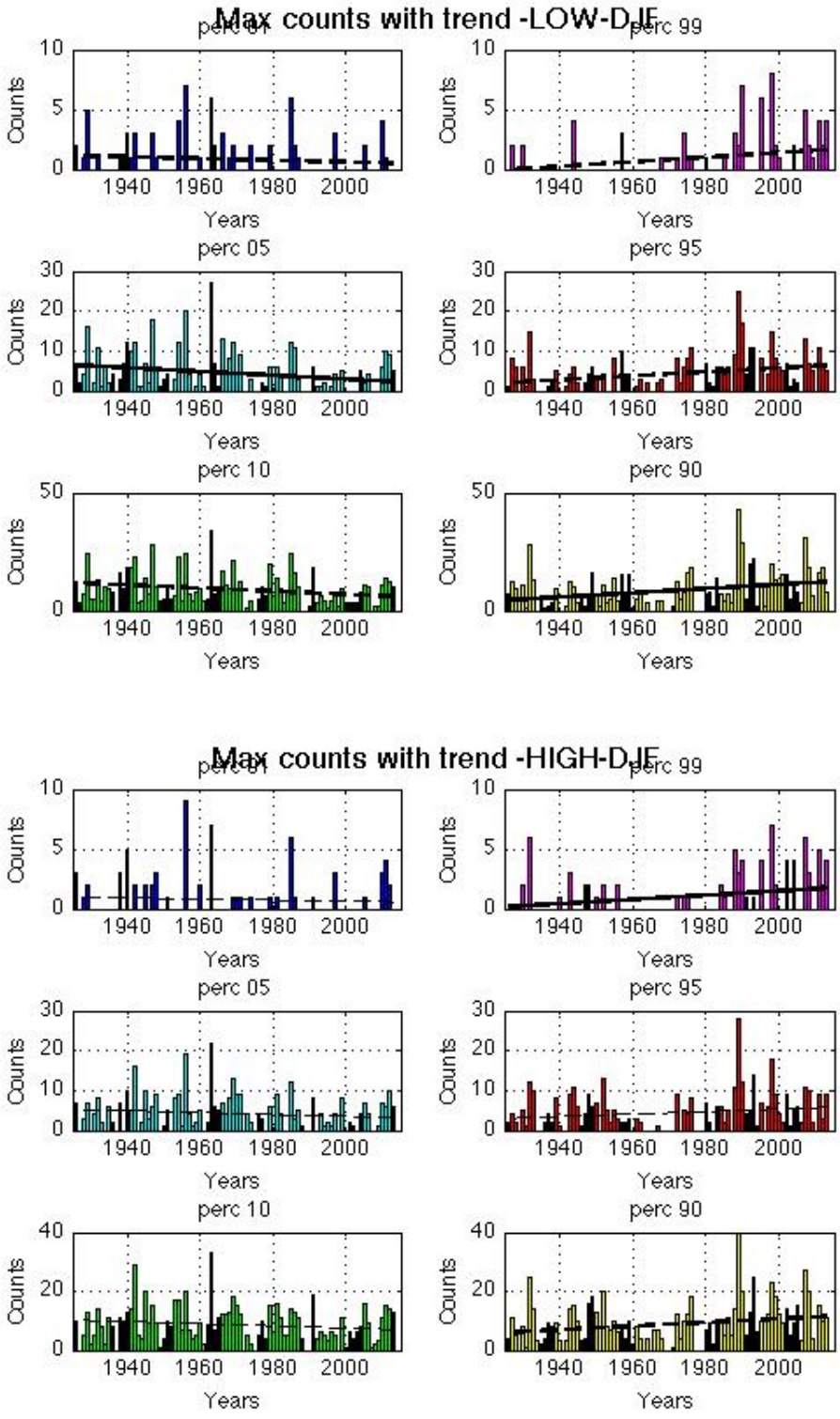

Figure A.2. *Same as figure 4.19 but for winter maximum temperatures.*

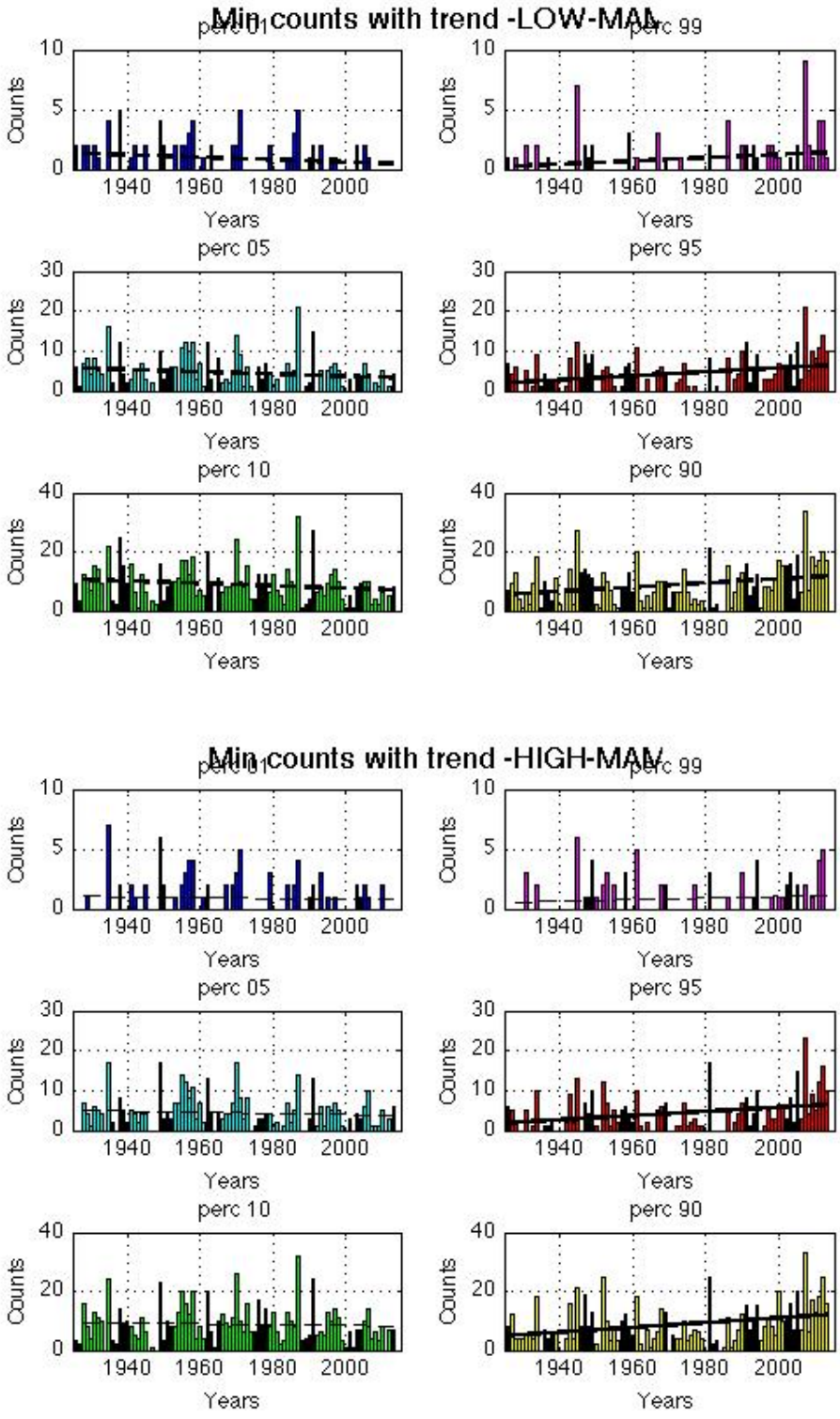

Figure A.3. *Same as figure 4.19 but for spring minimum temperatures.*

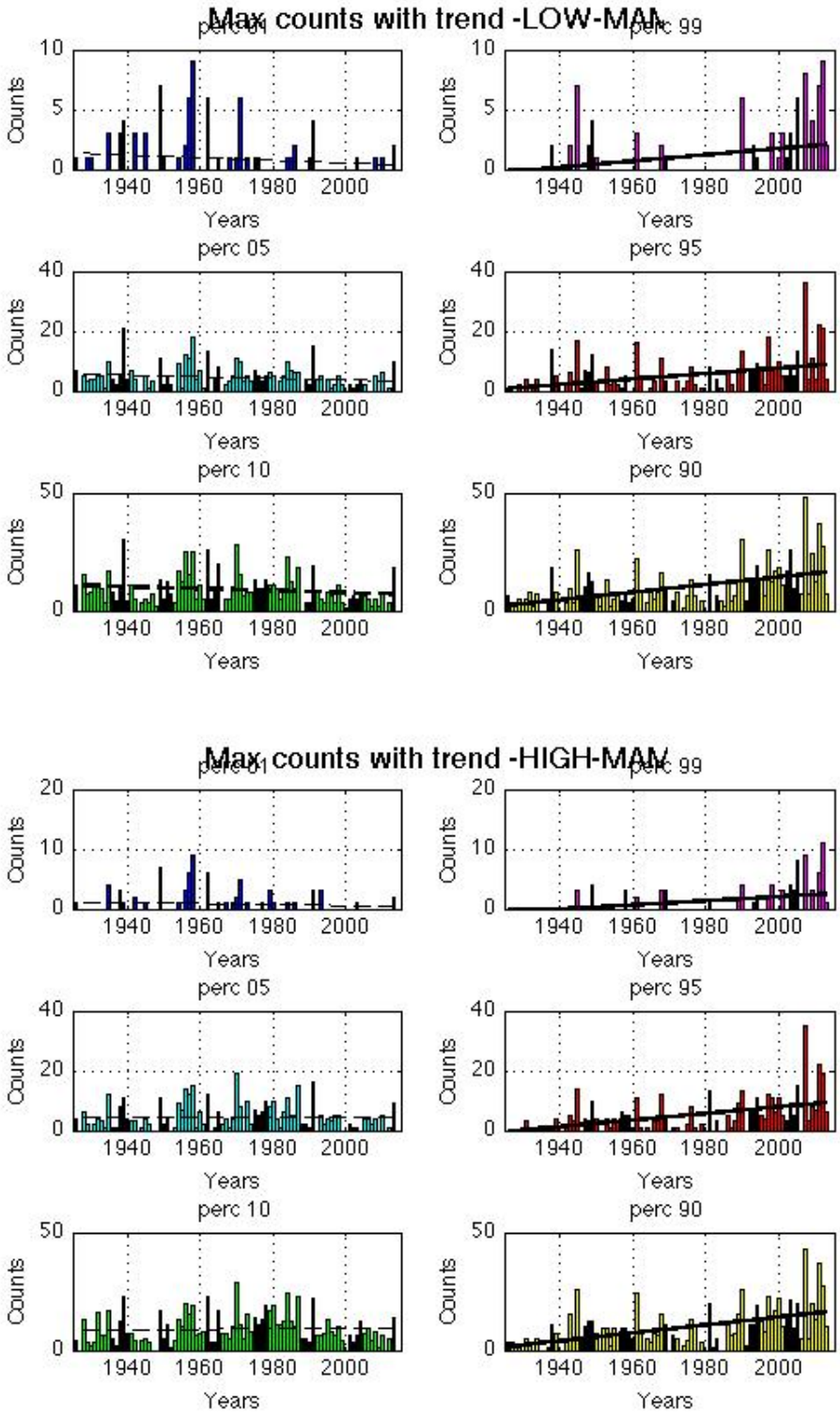

Figure A.4. *Same as figure 4.19 but for spring maximum temperatures.*

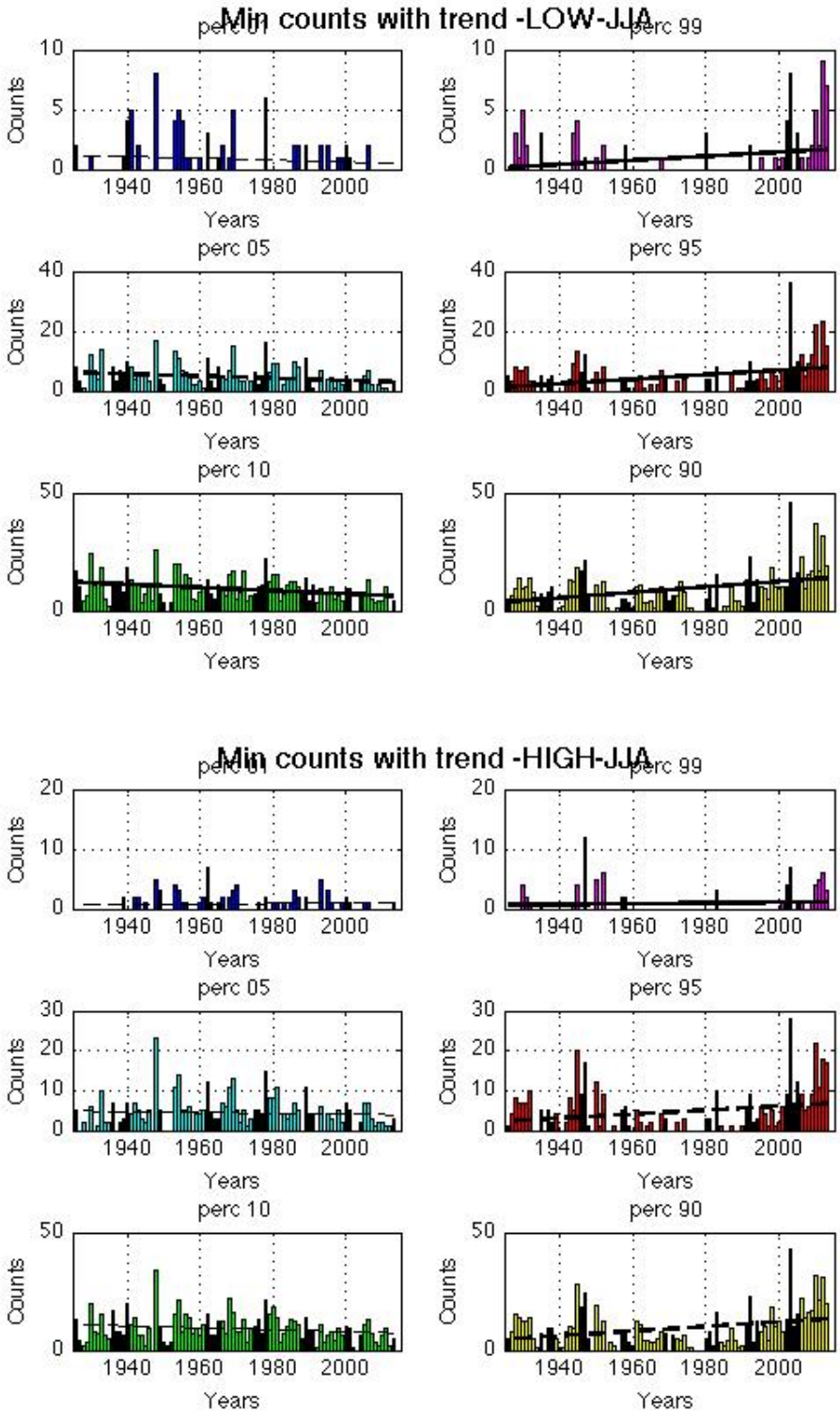

Figure A.5. *Same as figure 4.19 but for summer minimum temperatures.*

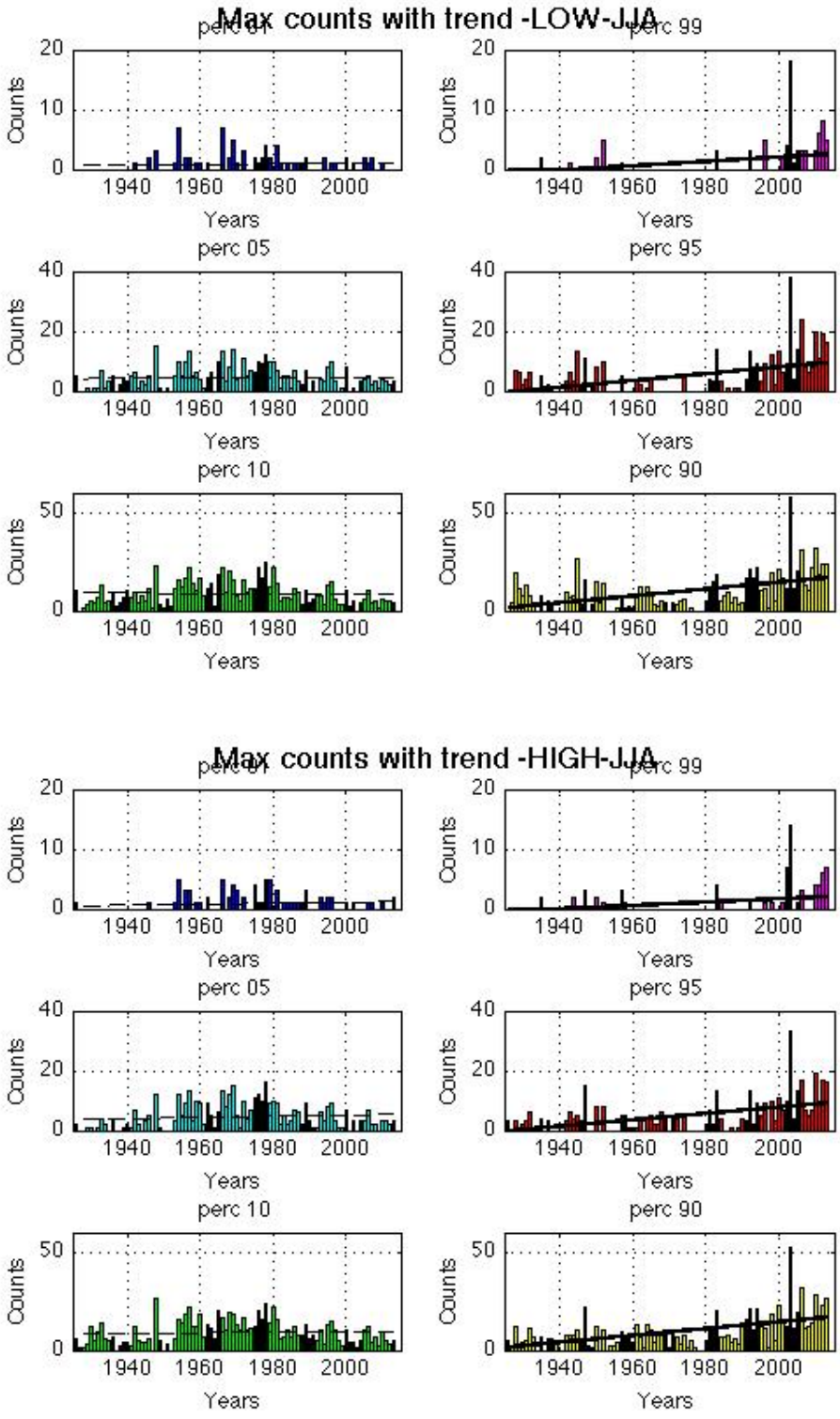

Figure A.6. *Same as figure 4.19 but for summer maximum temperatures.*

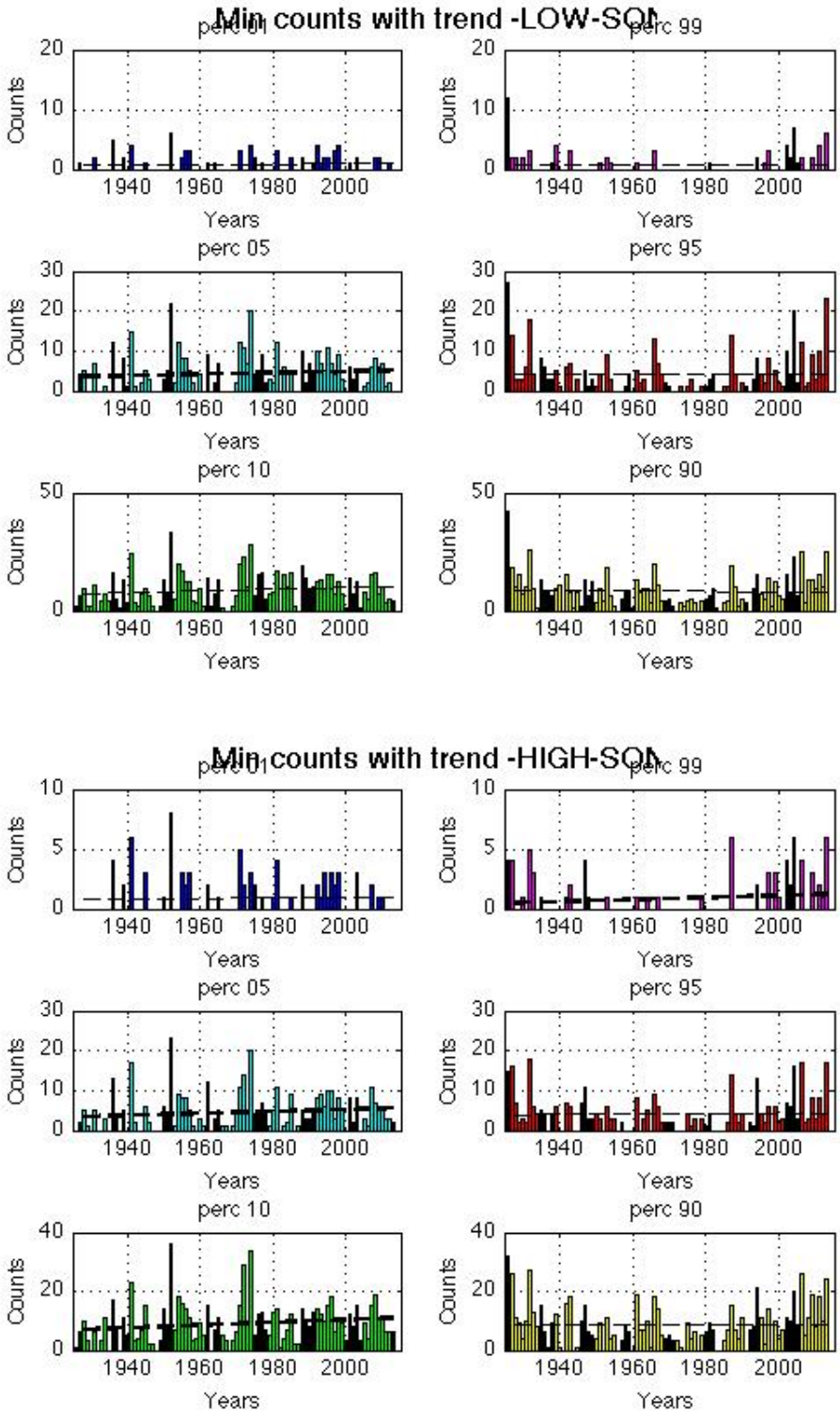

Figure A.7. *Same as figure 4.19 but for autmn minimum temperatures.*

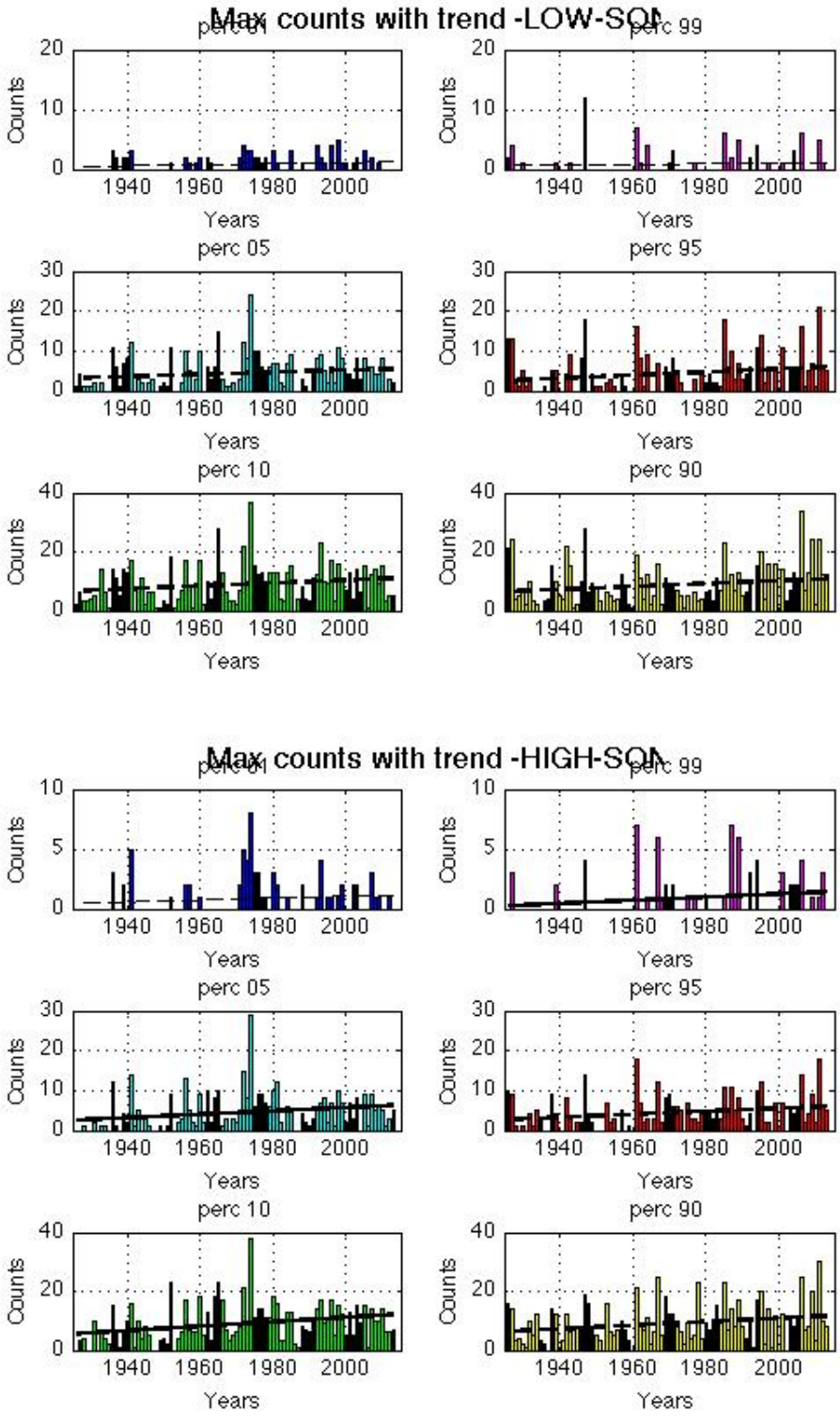

Figure A.8. *Same as figure 4.19 but for autumn maximum temperatures.*

Bibliography

Alexander, L., Zhang, X., Peterson, T., Caesar, J., Gleason, B., Klein Tank, A., Haylock, M., Collins, D., Trewin, B., Rahimzadeh, F., et al. (2006). Global observed changes in daily climate extremes of temperature and precipitation. *Journal of Geophysical Research: Atmospheres (1984–2012)*, 111(D5).

Ballester, J., Giorgi, F., and Rodó, X. (2010). Changes in european temperature extremes can be predicted from changes in pdf central statistics. *Climatic change*, 98(1-2):277–284.

Begert, M., Schlegel, T., and Kirchhofer, W. (2005). Homogeneous temperature and precipitation series of switzerland from 1864 to 2000. *International Journal of Climatology*, 25(1):65–80.

Böhm, R., Auer, I., Brunetti, M., Maugeri, M., Nanni, T., and Schöner, W. (2001). Regional temperature variability in the european alps: 1760–1998 from homogenized instrumental time series. *International Journal of Climatology*, 21(14):1779–1801.

Brown, S., Caesar, J., and Ferro, C. A. (2008). Global changes in extreme daily temperature since 1950. *Journal of Geophysical Research: Atmospheres (1984–2012)*, 113(D5).

Brunet, M., Jones, P. D., Sigró, J., Saladié, O., Aguilar, E., Moberg, A., Della-Marta, P. M., Lister, D., Walther, A., and López, D. (2007). Temporal and spatial temperature variability and change over spain during 1850–2005. *Journal of Geophysical Research: Atmospheres (1984–2012)*, 112(D12).

Brunet, M., Saladie, O., Jones, P., Sigro, J., Aguilar, E., Moberg, A., Lister, D., Walther, A., Lopez, D., and Almarza, C. (2006). The development of a new dataset of spanish daily adjusted temperature series (sdats)(1850–2003). *International Journal of Climatology*, 26(13):1777–1802.

Brunetti, M., Maugeri, M., Monti, F., and Nanni, T. (2006). Temperature and precipitation variability in italy in the last two centuries from homogenised instrumental time series. *International Journal of Climatology*, 26(3):345–381.

Della-Marta, P. M., Haylock, M. R., Luterbacher, J., and Wanner, H. (2007). Doubled length of western european summer heat waves since 1880. *Journal of Geophysical Research: Atmospheres (1984–2012)*, 112(D15).

Donat, M., Alexander, L., Yang, H., Durre, I., Vose, R., Dunn, R., Willett, K., Aguilar, E., Brunet, M., Caesar, J., et al. (2013). Updated analyses of temperature and precipitation extreme indices since the beginning of the twentieth century: The hadex2 dataset. *Journal of Geophysical Research: Atmospheres*, 118(5):2098–2118.

Donat, M. G. and Alexander, L. V. (2012). The shifting probability distribution of global daytime and night-time temperatures. *Geophysical Research Letters*, 39(14).

Frich, P., Alexander, L., Della-Marta, P., Gleason, B., Haylock, M., Klein Tank, A., and Peterson, T. (2002). Observed coherent changes in climatic extremes during the second half of the twentieth century. *Climate Research*, 19(3):193–212.

Giorgi, F. (2006). Climate change hot-spots. *Geophysical Research Letters*, 33(8).

IPCC (2013). *Climate Change 2013: The Physical Science Basis. Contribution of Working Group I to the Fifth Assessment Report of the Intergovern- mental Panel on Climate Change*. Cambridge University Press, Cambridge, United Kingdom and New York, NY, USA.

Katz, R. W. and Brown, B. G. (1992). Extreme events in a changing climate: variability is more important than averages. *Climatic change*, 21.3:289–302.

Klein Tank, A. and Können, G. (2003). Trends in indices of daily temperature and precipitation extremes in europe, 1946-99. *Journal of Climate*, 16(22):3665–3680.

Klein Tank, A., Wijngaard, J., Können, G., Böhm, R., Demarée, G., Gocheva, A., Mileta, M., Pashiardis, S., Hejkrlik, L., Kern-Hansen, C., et al. (2002). Daily dataset of 20th-century surface air temperature and precipitation series for the european climate assessment. *International Journal of Climatology*, 22(12):1441–1453.

Makowski, K., Wild, M., and Ohmura, A. (2008). Diurnal temperature range over europe between 1950 and 2005. *Atmospheric Chemistry and Physics*, 8(21):6483–6498.

Mearns, L. O., Katz, R. W., and Schneider, S. H. (1984). Extreme high-temperature events: changes in their probabilities with changes in mean temperature. *Journal of Climate and Applied Meteorology*, 23(12):1601–1613.

Moberg, A., Jones, P. D., Lister, D., Walther, A., Brunet, M., Jacobeit, J., Alexander, L. V., Della-Marta, P. M., Luterbacher, J., Yiou, P., et al. (2006). Indices for daily temperature and precipitation extremes in europe analyzed for the period 1901–2000. *Journal of Geophysical Research: Atmospheres (1984–2012)*, 111(D22).

Nogaj, M., Yiou, P., Parey, S., Malek, F., and Naveau, P. (2006). Amplitude and frequency of temperature extremes over the north atlantic region. *Geophysical Research Letters*, 33(10).

Rohde, M. et al. (2012). A new estimate of the average earth surface land temperature spanning 1753 to 2011. *Geoinformatics & Geostatistics: An Overview*.

Schär, C., Vidale, P. L., Lüthi, D., Frei, C., Häberli, C., Liniger, M. A., and Appenzeller, C. (2004). The role of increasing temperature variability in european summer heatwaves. *Nature*, 427(6972):332–336.

Scherrer, S. C., Appenzeller, C., Liniger, M. A., and Schär, C. (2005). European temperature distribution changes in observations and climate change scenarios. *Geophysical Research Letters*, 32(19).

Simolo, C., Brunetti, M., Maugeri, M., and Nanni, T. (2011). Evolution of extreme temperatures in a warming climate. *Geophysical research letters*, 38(16).

Simolo, C., Brunetti, M., Maugeri, M., Nanni, T., and Speranza, A. (2010). Understanding climate change–induced variations in daily temperature distributions over italy. *Journal of Geophysical Research: Atmospheres (1984–2012)*, 115(D22).

Toreti, A. and Desiato, F. (2008). Changes in temperature extremes over italy in the last 44 years. *International Journal of Climatology*, 28(6):733–745.

Vose, R. S., Easterling, D. R., and Gleason, B. (2005). Maximum and minimum temperature trends for the globe: An update through 2004. *Geophysical Research Letters*, 32(23).

Wilks, D. S. (2011). *Statistical methods in the atmospheric sciences*, volume 100. Academic press.

Yan, Z., Jones, P., Davies, T., Moberg, A., Bergström, H., Camuffo, D., Cocheo, C., Maugeri, M., Demarée, G., Verhoeve, T., et al. (2002). Trends of extreme temperatures in europe and china based on daily observations. In *Improved Understanding of Past Climatic Variability from Early Daily European Instrumental Sources*, pages 355–392. Springer.

Desidero ringraziare prima di tutto il Prof. Michele Brunetti per essere stato sempre presente, per l'illimitata disponibilità e per la professionalità con cui mi ha guidato nel corso di questo lavoro.

La mia gratitudine va a tutti coloro (parenti, amici e comparse) che mi hanno sostenuto e accompagnato in questo lungo percorso, chi più chi meno.
Elencare tutti risulterebbe poco sintetico ed oltremodo rischioso!

Intendo rivolgere un particolare pensiero a Diego. Vorrei ringraziarlo per la pazienza, per i momenti (molto alti e molto bassi) passati insieme e per essere stato un punto di riferimento sia professionale sia personale, oltre che un coinquilino prezioso (ma un po' impegnativo!).

Ultimi, ma solo per chiudere in bellezza, i miei genitori...
grazie per tutto, da 26 anni fa ad oggi
sempre qui, vicino a me.